

# Integration of Traffic and Structural Health Monitoring Systems Using A Novel Nothing-On-Road (NOR) Bridge-Weigh-In-Motion (BWIM) System

Amin Moghadam

Dissertation submitted to the Faculty of the  
Virginia Polytechnic Institute and State University  
in partial fulfillment of the requirements for the degree of

Doctor of Philosophy

in

Civil Engineering

Rodrigo Sarlo, Co-chair

Mohammad AlHamaydeh, Co-chair

Carin L. Roberts-Wollmann

Ioannis Koutromanos

July 01, 2022

Blacksburg, Virginia

Keywords: NOR BWIM systems, Traffic monitoring, Structural health monitoring (SHM),  
Multiple-presence event, Weight estimation, Integration of SHM and NOR BWIM systems

Copyright 2022, Amin Moghadam

# Integration of Traffic and Structural Health Monitoring Systems Using A Novel Nothing-On-Road (NOR) Bridge-Weigh-In-Motion (BWIM) System

Amin Moghadam

(ABSTRACT)

Bridges are vital components of the U.S. transportation network. However, every year, the transportation agencies report a large number of aging bridges that are structurally damaged. Also, evolving traffic, particularly the overloaded traversing traffic, can further threaten the bridges' integrity and safety. Bridge weight-in-motion (BWIM) is a system that takes the instrumented bridges as a scale and uses the structure response to compute the trucks' weights with no interruption in the traffic. In a particular type of BWIM, called nothing-on-road BWIM (NOR-BWIM), only a few weighing sensors should be installed under the bridge top slab. Since nothing will be installed on the road surface, NOR-BWIM addresses some of the main challenges of pavement-based WIM and traditional BWIM systems. These include lane closure, interruption to the traveling traffic, and sensitivity to daily tire impacts and harsh weather conditions. It also provides a portable solution with a less labor-intense installation process. Additionally, previous studies have shown that BWIM systems are versatile candidates for overcoming the critical challenges of structural health monitoring (SHM) across various types of bridges. Integrating the two systems is more cost-effective with improved performance; thus, it is more attractive to practitioners. However, the current BWIMs have serious shortcomings that make the integrated SHM-BWIM systems impractical in real-world long-span bridges. In the first two phases of this study, these shortcomings are addressed and a novel BWIM system is proposed. Then, the

novel BWIM system is used for SHM in the third phase of the study. These shortcomings are explained as follows. Most studies are performed on short/medium-span T-beam and slab-on-girder bridges. However, longer span lengths, construction methods, different slab properties (e.g., stiffness), etc., can affect the efficacy of the NOR-BWIM. Thus, there is a need to further evaluate this technique on other bridges, such as concrete-box-girder bridges with longer spans, to ascertain whether NOR-BWIM systems would still work effectively on such bridges. Thus, the first phase presents an experimental investigation conducted for a long-span concrete-box-girder bridge (144 m span) called the Smart Road bridge. A total of 18 experimental tests were performed on the bridge. Moreover, a cost-effective sensor placement was developed. It was found that the number of axles is detectable with an accuracy of 100%. Moreover, the estimated mean-absolute-error for axle spacing, vehicle speed, and gross vehicle weight were 4.6%, 2.6%, and 4.6%, respectively. Lastly, it was also demonstrated that the developed cost-effective NOR-BWIM system is capable of lane identification and truck position detection. The second main issue with the existing BWIM approaches is their limited suitability for simultaneous multiple-vehicle cases on multiple-lane bridges. To address this limitation, in the second phase of this study, a novel BWIM approach is proposed. The approach is built around removing the non-localized portion of the strain response. Keeping the localized portion of the strain response, which is not sensitive to nearby loads, allowing for enhanced detection. The superiority of this approach stems from its capability to handle multiple-vehicle cases. These may present with an arbitrary number of trucks and light-weight vehicles, simultaneously passing the bridge in any arbitrary pattern or configuration. To show the applicability of the approach, a finite element (FE) model of a long-span concrete-box-girder bridge was simulated. The model was validated against the experimental data collected under known large events. The FE model was then used to consider single-truck events (for proof-of-concept) and complex multiple-truck traffic cases. These included in-one-row trucks, zigzag patterns, side-by-side trucks, and a combination of

several trucks with several light-weight vehicles present. The results demonstrated that the proposed BWIM approach can detect the traversing trucks' axle weights and gross vehicle weight (GVW). Based on all complex multiple-truck cases, the overall mean absolute errors for GVW and axle weight estimations were 4.5% and 11.3%, respectively. In the last phase, a multiple-presence dual-purpose (MPDP) SHM approach was proposed to monitor the integrity of bridges using the BWIM system existing sensors. This approach centers on the influence line (IL) change and uses a developed multiple-presence IL (MP-IL) technique (in the second phase) for SHM application. This can effectively handle the multiple presence issue of the current integrated SHM-BWIM systems to make them more practical. Also, unlike many SHM-BWIM studies, noise and transverse position change (defined as false damage indicators) were included in the proposed procedure to provide a more realistic bridge health monitoring approach. A similar FE model simulated in the second phase was used to show the applicability of the approach. The model was then used to evaluate the MPDP approach under single and multiple truck events. Eleven damage scenarios were simulated, and three SHM trucks (a 3-axle, a 4-axle, and a 5-axle) were used to improve the SHM accuracy. Also, an updated sensor placement was proposed to work effectively for both BWIM and SHM applications in single and multiple-truck events. According to the results, the MPDP SHM procedure coupled with the novel MP-IL and the proposed sensor placement could effectively detect the damage scenarios in both single and multiple-truck events. Also, it was shown that using several independent SHM trucks can make the monitoring process more effective.

# Integration of Traffic and Structural Health Monitoring Systems Using A Novel Nothing-On-Road (NOR) Bridge-Weigh-In-Motion (BWIM) System

Amin Moghadam

## (GENERAL AUDIENCE ABSTRACT)

Every year, the transportation agencies report a large number of aging bridges that are structurally damaged. Also, evolving traffic and particularly overloaded traffic can threaten the bridges' integrity and safety further. Bridge weight-in-motion (BWIM) is a traffic system that takes the instrumented bridges as a scale and uses the structure response to compute the trucks' weights with no interruption in the traffic. In a particular type of BWIM, called nothing-on-road BWIM (NOR-BWIM), only a few weighing sensors should be installed under the road surface. Since nothing will be installed on the road surface, NOR-BWIM addresses some of the main challenges of pavement-based WIM and traditional BWIM systems. These include lane closure, interruption to the traveling traffic, and sensitivity to daily tire impacts and harsh weather conditions. It also provides a portable solution with a less labor-intense installation process. Additionally, previous studies have shown that BWIM systems are versatile candidates for overcoming the critical challenges of structural health monitoring (SHM) across various types of bridges. The integration of the two systems is more attractive to practitioners because it brings improved performance at a lower cost. However, the current BWIMs have serious shortcomings that make the integrated SHM-BWIM systems impractical in real-world long-span bridges. In the first two phases of this study, these shortcomings are addressed and a novel BWIM system is proposed. Then, the novel BWIM system is used for SHM in the third phase of the study. These shortcomings are explained

as follows. Most studies are performed on short/medium-span bridges with particular types of structures. However, longer span lengths, construction methods, different bridge components' properties, etc., can affect the efficacy of the NOR-BWIM. Thus, there is a need to further evaluate this technique on other bridges with longer spans and different structural systems to ascertain whether or not NOR-BWIM systems would still work effectively on such bridges. Thus, the first phase presents an experimental investigation conducted for a long-span concrete-box-girder bridge (a different structural system than the literature) with 144-m spans. A total of 18 experimental tests were performed on the bridge. Moreover, a cost-effective sensor placement was developed. It was found that the number of axles is detectable with no error. Moreover, the estimated error for axle spacing, vehicle speed, and gross vehicle weight were all low. Lastly, it was also demonstrated that the developed cost-effective NOR-BWIM system is capable of lane identification and truck position detection. The second main issue with the existing BWIM approaches is their limited suitability for simultaneous multiple vehicles on multiple-lane bridges. To address this limitation, in the second phase of this study, a novel BWIM approach is proposed. The superiority of this approach stems from its capability to handle multiple-vehicle cases. These may present with an arbitrary number of trucks and light-weight vehicles, simultaneously passing the bridge in any arbitrary pattern or configuration. To show the applicability of the approach, a model of the long-span bridge was simulated. The model was validated against the experimental data collected under known traffic events. The model was then used to consider single-truck events and complex multiple-truck traffic cases. The results demonstrated that the proposed BWIM approach can detect the axle weights and gross vehicle weight (GVW) of the traversing trucks. Based on all complex multiple-truck cases, the overall errors for GVW and axle weight estimations were 4.5% and 11.3%, respectively. In the last phase, a novel SHM approach was proposed to monitor the integrity of bridges using the existing sensors for BWIM. This approach uses the proposed BWIM system for SHM application. This can

effectively handle the multiple presence issue of the current integrated SHM-BWIM systems to make them more practical. Also, unlike many SHM-BWIM studies, noise and transverse position change were included in the proposed procedure to provide a more realistic bridge health monitoring approach. A similar model simulated in the second phase was used to show the applicability of the approach. The model was then used to evaluate the MPDP approach under single and multiple truck events. Eleven damage scenarios were simulated. Also, an updated sensor placement was proposed to work effectively for both BWIM and SHM applications in single and multiple-truck events. According to the results, the proposed SHM procedure coupled with the novel BWIM and the proposed sensor placement could effectively detect the damage scenarios in both single and multiple-truck events.

# Dedication

*To my wife, Mansoureh Sadat Jalali*

*AND*

*my parents, Reza Moghadam and Zahra Moghadam*



# Acknowledgments

I would like to thank my advisors gratefully, Drs. Rodrigo Sarlo and Mohammad AlHamaydeh, for their support, insightful comments and suggestions, guidance, tutelage, and help during my Ph.D. journey at Virginia Tech. My Ph.D. would not finish without my advisors' support. Gratitude is also extended to my supervisory committee: Dr. Carin L. Roberts-Wollmann and Dr. Ioannis Koutromanos. I would like to thank my wife, Mansoureh Sadat Jalali, who was always there through all my absences, travails, and impatience. She gave me love, encouragement, and support that helped me get to another achievement in my life. Finally, I would like to express my gratitude to my parents, Zahra Moghadam and Reza Moghadam, for their faith in me and allowing me to be as ambitious as I wanted in my entire life.

# Contents

- List of Figures xv
  
- List of Tables xviii
  
- 1 Introduction, Background, and Objectives 1**
  - 1.1 Introduction and Motivation . . . . . 1
  - 1.2 Background . . . . . 3
    - 1.2.1 Bridge-weigh-in-motion . . . . . 4
    - 1.2.2 Bridge health monitoring . . . . . 7
  - 1.3 Current Shortcomings . . . . . 10
    - 1.3.1 NOR-BWIM studies . . . . . 10
    - 1.3.2 SHM studies using IL . . . . . 13
  - 1.4 Research Phases, Objectives, and Scope . . . . . 13
    - 1.4.1 Phase 1: NOR-BWIM used for long-span Bridges . . . . . 14
    - 1.4.2 Phase 2: novel BWIM for multiple-vehicles events . . . . . 15
    - 1.4.3 Phase 3: novel SHM-BWIM for multiple-vehicle events . . . . . 16
  - 1.5 The Dissertation Structure . . . . . 17
  
- 2 Nothing-on-Road Bridge-Weigh-in-Motion Used for Long-Span, Concrete-**

<b>Box-Girder Bridges: An Experimental Case Study</b>	<b>19</b>
2.1 Introduction . . . . .	20
2.2 Experimental Setup . . . . .	25
2.2.1 Structure . . . . .	25
2.2.2 Monitoring system and sensor configuration alternatives . . . . .	25
2.2.3 Data collection and the vehicles used . . . . .	27
2.3 Methodology . . . . .	30
2.3.1 Prerequisite estimation approach . . . . .	30
2.3.2 Weight estimation method . . . . .	31
2.4 Results . . . . .	35
2.4.1 Strain gauge configuration selection . . . . .	35
2.4.2 Prerequisite estimation results . . . . .	36
2.4.3 Multiple-truck tests . . . . .	38
2.4.4 Truck lane position detection . . . . .	40
2.4.5 Weight estimation results . . . . .	42
2.5 Conclusions . . . . .	46
<b>3 A Novel Bridge-Weigh-in-Motion (BWIM) Approach for Simultaneous Multiple Vehicles on Concrete-Box-Girder Bridges</b>	<b>49</b>
3.1 Introduction . . . . .	50
3.2 Methodology . . . . .	54

3.2.1	Prerequisites' estimation approach . . . . .	55
3.2.2	Standard BWIM approach . . . . .	55
3.2.3	Proposed BWIM approach for multiple-truck presence . . . . .	56
3.3	Numerical Study and Experimental Validation . . . . .	64
3.3.1	Bridge description . . . . .	64
3.3.2	Finite element model . . . . .	65
3.3.3	Experimental validation . . . . .	67
3.4	Single and Multiple-truck Cases . . . . .	71
3.4.1	Sensor position for weight estimation . . . . .	72
3.4.2	Single-truck cases . . . . .	73
3.4.3	Multiple-truck traffic patterns . . . . .	74
3.5	Results . . . . .	75
3.5.1	Single-truck cases . . . . .	75
3.5.2	Multiple-truck cases . . . . .	79
3.6	Conclusions, Discussion, and Future Study . . . . .	84
<b>4</b>	<b>A Novel Dual-Purpose Procedure for Bridge Health Monitoring and Weigh-</b> <b>In-Motion Used for Multiple-Vehicle Events</b>	<b>87</b>
4.1	Introduction . . . . .	88
4.2	Methodology . . . . .	92
4.2.1	The multiple-presence dual-purpose (MPDP) SHM approach . . . . .	92

4.2.2	Prerequisites' estimation approach . . . . .	99
4.2.3	Standard influence line approach . . . . .	99
4.2.4	Multiple-presence influence line (MP-IL) approach . . . . .	100
4.3	Analysis . . . . .	101
4.3.1	Bridge description . . . . .	101
4.3.2	Validated finite element model . . . . .	102
4.3.3	Experimental procedure . . . . .	105
4.4	Discussion of Results . . . . .	113
4.4.1	Reference ILs and thresholds . . . . .	113
4.4.2	Single-truck and multiple-truck events . . . . .	115
4.4.3	Updated sensor placement . . . . .	118
4.4.4	Parametric study . . . . .	118
4.5	Conclusions and Future Study . . . . .	120
<b>5</b>	<b>Discussion and Future Work</b>	<b>124</b>
5.1	Phase 1: NOR-BWIM Used for Long-span Bridges . . . . .	124
5.2	Phase 2: Novel BWIM for Multiple-vehicles Events . . . . .	127
5.3	Phase 3: Novel SHM-BWIM for Multiple-vehicle Events . . . . .	129
	<b>Appendices</b>	<b>132</b>
	<b>Appendix A Bridge Bearings Stiffness Values</b>	<b>133</b>

A.1 Compressive stiffness . . . . .	134
A.2 Shear stiffness . . . . .	135
A.3 Rotational stiffness . . . . .	136
<b>Bibliography</b>	<b>138</b>

# List of Figures

2.1	The Smart Road (SR) bridge . . . . .	26
2.2	Strain gauge configuration alternatives (2d = the width of the slab inside the concrete box) . . . . .	27
2.3	The monitoring network . . . . .	28
2.4	The 5-axle truck and one of the 3-axle trucks . . . . .	29
2.5	Prerequisite estimation approach diagram . . . . .	31
2.6	The strain responses from strain gauge configuration alternatives . . . . .	36
2.7	5-axle truck strain response with sharp peaks . . . . .	38
2.8	Strain response for the multiple-truck case . . . . .	40
2.9	Strain response for the left-lane truck passage (should be compared with Figure 2.7) . . . . .	41
2.10	Reconstructed strain response vs. the original strain response (Run 6) . . . . .	43
3.1	A flowchart for the proposed BWIM approach steps . . . . .	57
3.2	The proposed BWIM approach . . . . .	59
3.3	A flowchart for the best envelope fit . . . . .	60
3.4	A flowchart for the adjacent truck effect removal . . . . .	63
3.5	The Varina-Enon bridge (VEB) . . . . .	65

3.6	An overview of the finite element model . . . . .	67
3.7	Trucks used for FE model validation (Table 3.2 shows the details of figures b and c) . . . . .	68
3.8	The FE model validation results . . . . .	71
3.9	Sensor positions for weight estimation . . . . .	73
3.10	Multiple-truck cases (the 3-axle and 5-axle trucks are Trucks 2 and 4 de- scribed in Table 3.3) . . . . .	75
3.11	Case 1: a 5-axle truck and a 3-axle truck on the lane one . . . . .	81
3.12	Case 3: a zigzag pattern with two 3-axle trucks on the first lane and a 3-axle truck on the second lane . . . . .	82
4.1	The cases occurred during bridge monitoring . . . . .	94
4.2	The MPDP SHM procedure . . . . .	97
4.3	The threshold computation procedure (TP=transverse position, NC=noise content, DI=damage indicator) . . . . .	98
4.4	MP-IL procedure . . . . .	101
4.5	The Varina-Enon bridge [74] . . . . .	102
4.6	The FE model validation results (Special permit) . . . . .	104
4.7	The FE model validation results (Superload) . . . . .	105
4.8	Finite element model overview and the mesh sizes . . . . .	106
4.9	Measurement points . . . . .	107



4.10	Region of interest and measurement points . . . . .	109
4.11	SHM trucks . . . . .	110
4.12	Comparison of the strain responses and ILs for the same trucks but with significantly different GVWs . . . . .	110
4.13	Reference IL vs. IL of the intact bridge subjected to test trucks . . . . .	114
4.14	The DI values for the damaged bridge under a single truck and the corre- sponding damage positions . . . . .	116
4.15	Reference IL vs. the IL of the damaged bridge with damage scenario 2 . . . .	117
4.16	The DI values for the damaged bridge under multiple trucks and the covered damage positions . . . . .	117
4.17	DI values for the cases specified in Table 4.1 . . . . .	119

# List of Tables

2.1	Summary of truck properties and test speeds . . . . .	29
2.2	Prerequisite estimation results . . . . .	39
2.3	Prerequisite estimation for multiple-truck tests . . . . .	40
2.4	Weight estimation results . . . . .	43
2.5	Axle weight estimates . . . . .	45
3.1	The bearings geometries . . . . .	66
3.2	Trucks' information for FE model validation in superload test (for Figures 3.7b and 3.7c) . . . . .	69
3.3	Trucks' information for weight estimation (single and multiple-truck cases) . . . . .	74
3.4	The results of the single-truck cases . . . . .	78
3.5	The results of multiple-truck cases . . . . .	80
4.1	Different configurations of the 3axle truck used for parametric study . . . . .	113
4.2	Thresholds and the DI values for different trucks on the intact bridge in different transverse positions and with different noise contents . . . . .	115

# List of Abbreviations

- $M^t$  The ideal strain response with no noise included
- $\Delta t_l^{x,x+1}$  The time-delay between the  $l^{th}$  peaks in the strain responses from  $x^{th}$  and  $(x + 1)^{th}$  successive strain gauges
- $\epsilon$  Added noise
- $A$  Toeplitz matrix created using the axles weights shifted vertically
- $B$  A matrix created using the influence line ordinates, shifted based on the truck axle spacings to adjust the time-instant when each truck axle enters and leaves the bridge structure
- $c_i$  The distance between the first axle and  $i$ th axle
- $d^{x,x+1}$  The physical distance between the  $x^{th}$  and  $(x + 1)^{th}$  successive strain gauges
- $f$  Sampling frequency
- $I$  The influence line vector consisting of the influence line ordinates
- $k$  The total number of scans in the strain response
- $L$  The likelihood function
- $M^m$  Measured strain vector
- $n$  The number of peaks (axles) in the strain response
- $n_p$  Peak separation factor

$P_n$  The  $n$ th critical point in non-localized strain removal procedure

$S$  Axle spacings vector

$v$  Truck speed

$W$  Axle weights vector

AS Axle weight

AW Axle weight

BDI Bridge diagnostics institute (the name of a company)

BWIM Bridge-weigh-in-motion

cBWIM Contactless bridge-weigh-in-motion

$d$  Half of the top width of the smart road bridge concrete box

DAQ Data acquisition system

DI Damage indicator

FAD Free of axle detector

FE Finite element

GVW Gross vehicle weight

IL Influence line

MAE Mean absolute error

MLE Mean absolute error

MP NOR BWIM Multiple-presence nothing-on-road bridge-weigh-in-motion

MP-IL Multiple-presence influence line

n Number of axles

NC Noise content

NOR BWIM Nothing-on-road bridge-weigh-in-motion

pdf The probability density function

ROI Region of interest

SHM Structural health monitoring

SP Secondary points in the non-localized strain response removal procedure

SR Smart road (bridge name)

ST Strain gauge

UL Upper limit

VEB Varina-Enon Bridge

# Chapter 1

## Introduction, Background, and Objectives

### 1.1 Introduction and Motivation

Civil infrastructure is susceptible to deterioration caused by aging, harsh weather conditions, and natural hazards [1]. This can seriously threaten bridges' structural safety and highways' pavement condition, causing issues such as fatigue, cracks, or even collapse [2, 3]. Also, the rapid growth of traffic volume and vehicle overweight enforcement on the degraded bridges imposes additional safety concerns and maintenance costs and challenges [4].

Intelligent transportation system (ITS) and structural health monitoring (SHM) systems have the potential to save highway infrastructure managers millions in traffic control and maintenance operations, respectively. However, implementation of these systems individually by industry has been slow [5]. The integration of the two systems is more attractive to practitioners because it brings improved value. On the one hand, ITS can make SHM estimates more accurate by providing load information. On the other hand, SHM can complement ITS data to help estimate vehicle weights more confidently and overcome deficiencies in camera measurements. By fusing system information, fewer sensors are required overall. Two main conditions should be met for the integrated system to be beneficial for the transportation agencies: first, detect the overloaded vehicles without disrupting the traffic, and

second, regularly monitor the bridge integrity without imposing much additional cost.

In this study, we have identified the use of a particular type of bridge-weigh-in-motion (BWIM) as a promising ITS candidate for integration with bridge SHM, due to commonalities in both instrumentation and extracted information. BWIM system uses the instrumented bridge and its responses as a tool for weight estimation. The first step in vehicle information computation using BWIM is always influence line (IL) calculation using experimental data. We define the influence line (IL) for a bridge as the variation of a structural response (strain in this study) at a certain point on the structure versus the position of a unit load on the bridge. Furthermore, suppose the stiffness of the indeterminate bridge changes due to a damage at a certain point. In that case, the structural response and, consequently, the IL of the bridge will change due to internal force redistribution. This concept can be used for bridge integrity monitoring applications. Thus, IL can be a connecting element to convert the SHM and BWIM systems to a single, multi-functional system. Also, in most cases, the BWIM system relies on strain measurements due to applicability to different types of bridges and simplicity in measurement and prerequisites calculation such as speed, number of axles. etc. Strain gauge is also a common type of sensor for SHM. Thus, the existing sensors for BWIM can also be appropriately adjusted for structural health monitoring (SHM). This can make the integrated system more affordable. However, one of the pressing challenges to integration is the estimation of influence lines during cases of multiple vehicles simultaneously on a bridge. This is particularly important for long-span bridges that needs lane closure. This imposes much additional costs and traffic concerns. This study proposes a novel methodology for multiple presence BWIM (MP-BWIM) and integrates it with a novel SHM methodology, forming the basis for dual-purpose (traffic and infrastructure) monitoring system.

In this study, a particular type of BWIM, called nothing-on-Road (NOR) BWIM, is used

[6]. In this system, only a few strain gauges should be mounted under the top slab and nothing need to be installed on the road surface. Thus, it does not need a traffic control or lane closure for system installation and maintenance. It also extends the durability of the monitoring system as they are not exposed to daily tire impacts. Thus, overall, it needs lower installation and maintenance costs. Additionally, the existing strain gauges can be used for SHM applications as well.

In this study, the influence line method is selected for SHM due to its inherent potentiality for BWIM systems' adjustment (due to commonalities in both instrumentation and extracted information) and great capability in SHM applications. IL-SHM is a nondestructive monitoring technique and does not damage the structure and is more cost-effective due to recent advances in electronic technologies such as transducers, data acquisition systems, cameras, computers, etc. This group is based on the static properties of the structures by measuring the static quantities. This method can be more advantageous over some dynamic methods that are usually insensitive to local damages in large-scale structures (such as bridges) and sensitive to environmental effects [7].

To explain the current challenges in more detail and define the structure of each study phase, a brief background is needed (provided in Section 1.2) for BWIM and SHM systems. The current restrictions are further explained in Section 1.3.

## 1.2 Background

This section first briefly introduces the BWIM system, available options, and available techniques in Subsection 1.2.1. Subsection 1.2.2 then explains the current SHM studies and the advantages of using IL in SHM in more detail.



## 1.2.1 Bridge-weigh-in-motion

### 1.2.1.1 BWIM introduction and initial studies

BWIM system uses the instrumented bridge and its responses as a tool for weight estimation. The concept of BWIM was first introduced by Moses [8]. In Moses approach, the truck speed, the number of axles, and the axle spacings should be obtained in advance. Moses suggested computing these parameters, called “Prerequisites” in this study, using switch tapes on the road surface. The switch tape is a device that alerts the computer to get the signals made by truck axle passage. Each tape consists of two metallic strips, and when the truck axle crosses over the device, the metallic strips get into contact with each other and create a signal [8]. Usually two switch tapes should be installed on the road surface to compute the speed and axle spacings of the traversing trucks using the generated signals.

Considering a predefined (theoretical) influence line (IL), weight was then suggested to be estimated by minimizing the error between the induced moment at the gauge location on the bridge girders and predicted static moments in terms of axle weights. Subsequent work then extended this concept to weighing side-by-side trucks by introducing the concept of influence surface [9]. This was calculated using the strain response of the bridge under a calibration truck moving alternatively in each lane. Unlike the previous study, two lanes were considered. Four switch tapes were placed on the highway (two in each lane) at certain distances for prerequisites’ estimation. The strain responses were obtained and recorded separately using the strain gauges clamped on each girder. This was needed to compute the effect of the truck loads in each lane on each of the supporting girders and to compute the influence line when the truck moves in the same lane and adjacent lanes. In this method, the error for each girder is the difference between the estimated moment and the measured one. It was shown that the weighing procedure for side-by-side vehicles is an extension of

the error minimization process developed for the single truck weighing in the previous study. The main difference is that the effect of the trucks on adjacent lanes should also be included in the minimization process. Thus, the multi-girder signals provide individual lane weighing when the influence of each truck on each girder is known.

#### 1.2.1.2 BWIM options

There are different types of BWIM in the literature for prerequisite estimation. These include 1) traditional BWIM [10] that uses additional devices (load cells, bending plates, etc.) on the road surface. 2) contactless BWIM (cBWIM) [11, 12] that unlike other techniques, uses a camera on the road surface, and 3) nothing-on-Road (NOR) BWIM [6, 13–15]. The latter one is called NOR since nothing is needed to be installed on the road surface, and only a few sensors should be mounted under the top slab. The advantages of NOR-BWIM include: 1) the sensors can be integrated with SHM systems using the existing sensors since regular strain gauges are the most common sensors used in this system, 2) it does not need a traffic control or lane closure for system installation and maintenance, 3) it has lower installation and maintenance costs 4) it does not need additional sensors/devices such as axle detectors [16], switch tapes, pneumatic tubes, etc. 5) it extends the durability of the monitoring system as they are not exposed to daily tire impacts. Due to NOR-BWIM inherent advantages, it is selected for this study.

#### 1.2.1.3 Prerequisites estimation techniques

Two main parameters in prerequisite estimation are the physical distances between the successive sensors and the time delay between the peaks in the strain response, which are usually equivalent to the number of traversing axles. The response peaks' clarity plays a key role

in the prerequisite estimation. This depends on two main factors. First, the bridge construction method that changes the structural behavior of the bridge and the load-transfer mechanism between different components when the truck gets close to the measurement locations. Second, the bridge geometrical characteristics, such as slab thickness. This influences the localized strain responses extracted from the vicinity of the tire path. Hence, placing the sensor close to the usual tire path can increase the sharpness of strain response peaks, particularly for closely spaced axles. Many studies obtained this information directly from the raw strain response measurements [6, 14, 15, 17]. However, some post-processing techniques accentuate the strain peaks in a case the peaks are not observable/sharp enough [18–21].

These techniques are either signal-processing-based or physics-based. In signal-processing-based techniques, tools such as continuous wavelet transform (CWT) are used [19] for feature generation; however, in physics-based techniques, either the internal forces (shear [20], moments [18], etc.) at certain points in the bridge and their combination are used or the truck axles' weights [21, 22]. An example for the latter case is the virtual axle method [21], in which the truck was initially assumed to have a large number of evenly distributed virtual axles. Then, using Moses algorithm, the weights of all axles were obtained to find the virtual/true axles knowing that the virtual axles have zero weights. The current shortcomings for prerequisite estimation techniques are later explained in Section 1.3.

#### 1.2.1.4 Weight estimation techniques

Once the prerequisites are obtained, they are used for weight estimation. In general, there are two main groups for weight estimation: 1) dynamic methods [23–27] and 2) static methods [28–31]. A common practice for satisfactory outcomes in dynamic methods is to use a detailed 3D model, which makes the process time-consuming [32]. On the other hand, static

methods directly use the recorded data, and no complex model is needed. This makes the static methods more suitable for real-time monitoring applications. In these methods, the influence line should always be obtained first through a procedure called “calibration”. This will then be used for axle weight, and gross vehicle weight (GVW) estimations of the future unknown trucks [33]. It was already explained that some studies have used a predefined theoretical IL [8] selected based on the bridge structure (simply-supported, etc.). However, some other studies directly compute the IL using the experimental measurements from the bridge subjected to a calibration truck with known weight, speed, axle spacings, and the number of axles. In this regard, in 2006, a novel method was proposed using strain measurements from a single passage of a single calibration truck [28]. In this study, IL was computed by minimizing the difference between the directly measured strain on the bridge and a theoretical strain response computed using an unknown IL. In 2009, Tikhonov regularization was used to improve the accuracy of the Moses algorithm [29]. In 2015, the Maximum Likelihood Estimation (MLE) method was introduced, taking the measurements from multiple calibration trucks with multiple passages for influence line estimation [34]. In this study, multiple trucks were used to take the effect of the trucks’ characteristics into account. Then, in 2018, the concept of probabilistic influence line seeking was introduced.[30]. However, in 2019, in a comparative study, it was shown that the MLE method provides the most accurate results [35], and this is why the MLE method is selected as a standards IL extraction method for this study for weight estimation. The current shortcomings for weight estimation techniques are later explained in Section 1.3.

### 1.2.2 Bridge health monitoring

Structural Health Monitoring (SHM) aims to monitor the state of the structure to detect the possible damages at the earliest stage. This will help reduce the life-cycle and maintenance

costs of the structure and improve its safety and reliability.

In general, there are two main SHM techniques, destructive and nondestructive [36]. However, for destructive techniques, one usually needs to test some samples extracted from the structure, which is not always possible. These techniques are not also suitable for online monitoring since the samples should be later tested in a laboratory. In contrast, nondestructive techniques do not damage the structure and are more cost-effective due to recent advances in electronic technologies such as transducers, data acquisition systems, cameras, computers, etc.

Nondestructive techniques can be used for local and global damage detection. The local damage detection methods are usually either visual or include some experimental methods to measure sound, light, displacements, electromagnetic field intensity, or temperature to detect the possible damage near or on the surface [37]. Some commonly used Non-destructive techniques are: concrete ultrasonic tester to measure crack depth [38]; Eddy current for welded joint crack detection [39]; Schmidt Hammer (or impact hammer) to determine the concrete strength [40]; and some more general methods such as digital coating thickness gauge for paint thickness measurement [41] and ground-penetrating radar for rebar detection [42].

There are also two groups of techniques that use different types of sensors, usually for global SHM purposes [7]. The first group is established based on either the structural dynamic characteristics such as damping ratio, natural frequencies, and mode shapes [43–49], or relevant properties (e.g., modal assurance criterion, modal strain energy, etc.) [50–53]. These methods have illustrated varying degrees of success in the previous studies. However, they are usually insensitive to local damages in large-scale structures (such as bridges) and sensitive to environmental effects [7].

The second group is based on the static properties of the structures. This group consists of

many different methods proposed in the last decades measuring the static quantities [54–56]. In this study, the unit influence line (UIL) method is selected due to its inherent potentiality for BWIM systems’ adjustment and great capability in SHM applications (discussed later in this section). As explained above, the first step in NOR-BWIM application is always calibration using a known vehicle and computing the influence line (IL) using experimental data. Furthermore, when any damage occurs, the stiffness of the bridge varies at a certain point. In that case, the structural response and, consequently, the IL of the bridge will change due to internal force redistribution. This obviously happens only for indeterminate bridges, but a truly determinate bridge does not usually exist in a real situation. This concept can be used for bridge integrity monitoring applications. Besides the BWIM existing strain gauges, IL can be the second tool (mathematical) to integrate the SHM and BWIM systems into a single, multi-functional system.

Bridge monitoring using IL calculation can employ different structural quantities. These include displacement influence line [57–59], rotation influence line [3, 60], strain/stress influence line [7, 22, 61]. The purpose of this study is to integrate the BWIM and SHM systems using the existing sensors for the BWIM. In most cases, BWIM uses some strain gauges and strain measurements due to measurement simplicity and its applicability to different types of bridges. It also provides a simpler way to compute the prerequisites such as speed, number of axles, and axle spacings.

Regarding the application of stress/strain IL in SHM, there are some studies that use the IL indirectly. Common examples are the BWIM-informed SHM systems. For instance, a WIM-based method was proposed for level I damage detection [61]. Two types of WIM systems were used, pavement-based and BWIM. IL was computed for the BWIM weight estimation. Then, a damage index was proposed that was the ratio of the computed weights using these two systems. This was based on the fact that the truck weight measured by the WIM systems

is constant while the truck weight computed using BWIM on the damaged bridge is different than on the intact bridge. In another study, called the “virtual axle” method, an additional weightless axle was assumed for the traversing vehicle to detect damage [22]. It was shown that any change in structural behavior caused by damage would lead to a non-zero estimate for the virtual axle. This was used as a damage indicator. In a more direct application of stress IL in SHM, a regularization method was proposed for the stress influence line based on a train passing over Tsing Ma Bridge in Hong Kong [7]. Three damage indexes were introduced and tested, the first-order and second-order IL change, showing satisfying results.

## 1.3 Current Shortcomings

### 1.3.1 NOR-BWIM studies

The techniques provided for prerequisite estimation are only tested on T-beam bridges, while other bridge types may reveal a different strain profile where the number of axles and their positions may directly be observable from the response such that no other methods are needed to be involved. Thus, other bridge types should be evaluated, particularly long-spans, where dynamic effects induced by vehicles may affect the difficulty of the process and accuracy. Also, in all these studies, the techniques were evaluated either using numerical or/and prototype models in a lab which are not usually representative of actual conditions.

Similar to the studies on prerequisites’ estimations, most of the current studies on weight estimations have been performed on short/medium-span bridges. This is because the common wisdom [16, 62] in the literature is that short-span or medium-span bridges and the ones with secondary elements are the most reliable choices for the NOR-BWIM application.

This is because the top slab of the long-spans is usually thicker, and thus, they might generate less sharp peaks associated with the traversing axles and are more likely to combine the peaks created by closely spaced axles. This makes the data analysis more challenging [62]. Additionally, the dynamics effect might be higher on the long-span bridges since they usually have lower natural frequencies. Therefore, they are more likely to match the vehicle frequencies [63].

Thus, like the studies discussed above, most of the NOR-BWIM applications in the literature have focused on either short-spans (span-length  $< 30\text{m}$ ) [20, 64, 65] or medium-spans ( $30\text{m} < \text{span-length} < 60\text{m}$ ) [16, 66]. There are also some cases in which medium-span composite box girder bridges with a span length of about 50m are tested [67, 68]. These tests are performed on a bridge with different materials (steel bridges and not concrete ones). To the author's best knowledge, only limited studies are somehow relevant to long-spans. However, even these studies have focused on SHM applications using NOR BWIM, not focused on the accuracy of the prerequisites and weight estimation [69].

Thus, this is still needed to consider the longer-span bridges (e.g., over 100 m). This is because, firstly, sensor placement is not carefully evaluated in the current studies and even the long-spans with deeper top slab thickness may still provide sharp peaks for prerequisite estimation depending on their structural systems and load transfer mechanism. Secondly, no clear study is currently available to understand how the dynamics effects can affect the BWIM system accuracy. Indeed, for long-span bridges with relatively smooth road surfaces, one may still obtain relatively accurate results with a reasonable error range. Thirdly, there are many long-span bridges throughout the world (such as Sutong bridge [70]) which are highly instrumented for SHM purposes, and their existing sensors can also be used to integrate the SHM systems with NOR-BWIM systems. This can make the existing monitoring systems more effective and cost-effective. Hence, further evaluation is needed for the



long-spans. This is going to be the topic of Phase 1 of this study.

Most of the current BWIM systems and IL extraction techniques are only capable of weighing a single truck on the bridge. This is because, for multiple-truck events, all trucks affect the measured strain response, and these methods cannot properly decompose the strain response associated with the desired truck. This can be considered a significant limitation for these current BWIMs on long-span bridges subjected to heavy traffic. Thus, other than what was discussed above, another reason why short-span bridges are recommended in the literature is to ensure that only one truck will be on the bridge during test and IL calibration. There are only limited studies about multiple-truck presence. However, these methods still require either time-consuming IL calibration [71] or are applicable to a small set of possible traffic combinations [72].

Also, the concept of influence surface instead of influence line is another solution introduced by some researchers for multiple-truck presence issue [9, 71]. However, in the influence surface calibration procedure, a series of transverse positions are needed to cover all possible truck transverse positions within two desired traffic lanes [73]. This makes it time-consuming and, thus, less applicable for commercial applications. Also, similar to the IL extraction techniques, during influence surface calibration, there should not be any unwanted vehicles on the bridge. This can only be possible for short-span bridges with limited traffic volume. For long-span bridges, a lane closure will be required that might impose traffic concerns and additional costs. Additionally, influence surface is computationally demanding since the system expands in both the number of equations and in complexity, and thus, linear methods cannot usually be used [73]. These disadvantages can be even worse for bridges with multiple lanes in each direction and heavier traffic conditions.

In another study, a weight estimation procedure was proposed and verified against a series of laboratory experiments on a slab-on-girder bridge [72]. This was performed using a load

distribution factor and considering how the truck weight is distributed between different lanes when it travels in a particular lane. However, it was shown that the method could work under the presence of only two vehicles in one row and side-by-side, and more complex traffic patterns were ignored. However, on a multiple-lane bridge with dense traffic, the presence of multiple trucks arbitrarily distributed in different lanes is very common.

The second phase of this study addresses this limitation in dealing with complex traffic patterns with arbitrary traffic patterns. If appropriately addressed, the multiple-presence events can help make the SHM more effective since multiple vehicles will make more deformation, and more useful SHM-related information will be obtained.

### 1.3.2 SHM studies using IL

The IL-SHM studies provided in Section 1.2 have two significant shortcomings. 1) They are not applicable for multiple-truck events. The current IL extraction techniques are not able to properly decompose the strain responses associated with each truck. However, it is not usually guaranteed to only have one truck at the monitoring step without lane closure on the long/medium-span bridges with dense traffic. Hence, these current IL techniques are not practical for long and medium-span bridges. 2) A challenging factor, i.e., transverse position change, is ignored while this can make a false damage indicator even for the intact bridge and need to be included in the process. These will be addressed in this study.

## 1.4 Research Phases, Objectives, and Scope

To address the shortcomings discussed in Section 1.3, three phases are selected for further evaluation.

### 1.4.1 Phase 1: NOR-BWIM used for long-span Bridges

To address the shortcomings associated with both prerequisites and weight estimation, a different but common type of bridge, a concrete-box-girder, was considered in a new experimental context. This is called the “Smart Road (SR)” bridge. In this construction method, the slabs (top and bottom) are integrated together. As discussed earlier, this causes a different global structural behavior and load-transfer mechanism compared to slab on girder and beam bridges. The SR bridge has significantly longer spans (144 m) that makes it a unique case study compared to the bridges in the literature. The main objective of this phase is to evaluate the accuracy of the NOR-BWIM systems on the long-span concrete box girder bridges. This will be performed in two main steps: prerequisite estimation and weight estimation using a standard BWIM method (MLE in this study). As discussed earlier, a suitable sensor placement can capture most of the localized strains under the tire paths, improving the accuracy of the prerequisite estimation. To find a suitable sensor placement, several strain gauge configurations were experimentally tested, and the most efficient one was selected. In fact, it was aimed to show if any additional techniques (discussed above) are needed to accentuate the peaks’ sharpness in the strain response extracted from a significantly long-span bridge when the proposed sensor placement is used. This is to understand if the long-spans can still produce clear peaks for closely spaced tandem axles, which are challenging in the BWIM area. This is because significantly longer-span bridges usually have thicker top slabs. Lastly, a few tests were conducted to understand if the NOR-BWIM system can also detect the truck lane position.

### 1.4.2 Phase 2: novel BWIM for multiple-vehicles events

As explained above, the second main issue with the current BWIM systems is their limitation in multiple-presence events. To address this shortcoming, in this phase, a novel BWIM approach is proposed. This approach successfully decomposes the strain responses of each vehicle in multiple-vehicle, complex events. These events can present with a combination of heavy and light-weight trucks on the bridge simultaneously. The idea centers on removing the non-localized portion of the response to only keep the localized response. The non-localized response will be made by the beam behaviour of the bridge while the localized response will be due to the plate behaviour. This is further explained in Chapter 3. The latter portion of the response is not usually sensitive to the nearby loads. This approach applies to more advanced BWIM systems such as NOR-BWIM as well. The influence line obtained from this technique is called multiple-presence IL (MP-IL) used in phase 3.

Another main advantage of this approach is that, unlike the standard BWIM techniques, no lane closure is needed even during the calibration process and if the calibration truck is surrounded by random vehicles. In fact, using the proposed BWIM, the IL can successfully be extracted despite the presence of unwanted trucks. This makes the system more cost-effective and safer and, as a result, more commercially feasible when no lane closure is needed.

To show the feasibility of the approach, a finite element (FE) model of a long-span concrete box girder bridge, called the “Varina-Enon” Bridge was simulated. The model was then validated against experimental data from the actual bridge under two large events. This bridge has three lanes in each direction. In general, in an actual situation on multiple-lane bridges with heavy traffic (such as the Varina-Enon), it is usually impossible to control the traffic with no lane closure to construct the desired traffic patterns. Thus, the FE model was

used to simplify the process and consider single-truck events (as a proof-of-concept) as well as complex multiple-truck traffic cases. These include in-one-row trucks, zigzag patterns, side-by-side trucks, and a combination of several trucks with several light-weight vehicles involved.

### 1.4.3 Phase 3: novel SHM-BWIM for multiple-vehicle events

In the last phase of the study, a multiple-presence dual-purpose (MPDP) structural health monitoring (SHM) approach is proposed to be used for both SHM and BWIM applications using the BWIM existing sensors. Using this approach, the transportation agencies can perform a level I damage detection on bridges. The structural damage detection includes four levels of identification: level 1 is for damage presence, level 2 is damage location identification, level 3 is damage intensity quantification, and level 4 is to determine the remaining service life to failure [45]. The proposed procedure computes the square error between the bridge IL experimentally extracted at the monitoring stage, and the initial IL obtained from the intact bridge.

This procedure has three clear contributions to the literature: 1) for the first time, the novel MP-IL extraction technique developed in the second phase, called Multiple-Presence IL (MP-IL), is used for SHM application. MP-IL can successfully handle multiple-truck events and obtain the IL [74] even if the calibration truck is surrounded by unwanted trucks. The MP-IL resolves the significant limitation of the standard IL extraction methods (such as MLE) and makes it a powerful tool for both SHM and BWIM. 2) Other important factors, such as transverse position and noise that can create false damage indicators, are also included in the proposed SHM procedure to provide a more realistic and reliable bridge health monitoring approach. 3) The proposed sensor placement proposed in the second phase was updated to

be effective for both the BWIM and SHM applications in single and multiple-truck events.

## 1.5 The Dissertation Structure

The three phases' results are reported in three chapters and organized in a manuscript-based format.

Chapter 2 reports the results of phase 1 (manuscript 1). In this manuscript, the monitoring system, the structure used, the strain gauge configuration alternatives, and the vehicles used are provided in Section 2.2. Section 2.3 explains the prerequisites and weight estimation methods in detail. The results for strain gauge configuration selection, prerequisites estimation of a single or multiple-truck passages, weight estimation (Gross Vehicle Weight and axle weights) of a single truck, and truck lane detection are discussed in Section 2.4. Finally, the main conclusions and future works are provided in Section 2.5.

Chapter 3 reports the results of phase 2 (manuscript 2). Details about standard BWIM and the proposed BWIM techniques are provided in Section 3.2. Section 3.3 introduces the finite element model of the bridge and how it is validated against experimental measurements of the actual bridge. Section 3.4 shows how the FE model is used for single and multiple-truck cases and with a general explanation of the suggested sensor placement. Also, the results are provided in Section 3.5. Finally, the main conclusions and future works are provided in Section 3.6.

Chapter 4 reports the results of phase 3 (manuscript 3). In this chapter, the proposed dual-purpose SHM procedure, standard IL, and the MP-IL techniques are presented in Section 4.2. Section 4.3 introduces the bridge structure, the validated finite element model against experimental data (similar model to the second phase model with some modification), mea-

surement points, and the monitoring approach. Section 4.4 discusses the results of single and multiple-truck events as well as a parametric study performed on the truck characteristics. Lastly, the main conclusions and future works are provided in Section 4.5.

Finally, Chapter 5 presents the conclusion of all phases along with the suggested future works.

# Chapter 2

## Nothing-on-Road

## Bridge-Weigh-in-Motion Used for

## Long-Span, Concrete-Box-Girder

## Bridges: An Experimental Case Study

Nothing-on-road bridge-weigh-in-motion (NOR-BWIM) leverages the response of an instrumented bridge to identify various aspects of traffic information. This system circumvents many of the current issues with traditional BWIM systems, such as lane closure, expensive installation, and extends the durability of the sensors. Most of the related available studies are performed on short-span (span-length  $< 30\text{m}$ )/medium-span ( $30\text{m} < \text{span-length} < 60\text{m}$ ) T-beam and slab-on-girder bridges. However, longer span lengths, construction method, different slab properties (e.g., stiffness), etc., can affect the efficacy of the NOR-BWIM. Thus, there is a need to further evaluate this technique on other bridges such as concrete-box-girder bridges with longer spans, in an effort to ascertain whether or not NOR-BWIM systems would still work effectively on such bridges. This work presents an experimental investigation conducted for a long-span concrete-box-girder bridge (144 m span). A total of 18 experimental tests were performed on the bridge. Moreover, a cost-effective sensor placement was developed for general use on similar long-span concrete-box-girder bridges.



It was found that the number of axles are detectable with an accuracy of 100%. Moreover, the estimated mean-absolute-error for axle spacing, vehicle speed, and gross vehicle weight, were 4.6%, 2.6%, and 4.6%, respectively. Lastly, it was also demonstrated that the developed cost-effective NOR-BWIM system is capable of lane identification and truck position detection.

## 2.1 Introduction

Overloaded trucks adversely affect highways' pavement condition and safety and can cause serious issues to bridges such as fatigue, cracks, or even collapse [75, 76]. To effectively manage financial resources for bridge maintenance, information about in-service conditions of bridges, such as the trucks' information, are needed [77]. Bridge-weigh-in-motion (BWIM) has the potential to provide valuable information for traffic monitoring and weight enforcement. The concept of BWIM was first introduced by Moses [8]. In Moses approach, the truck speed, the number of axles, and the axle spacings should be obtained in advance. These parameters, called "Prerequisites" in this study, were suggested to be calculated using switch tapes (already defined in Chapter 1) on the road surface. Considering a predefined (theoretical) influence line (IL), weight was then suggested to be estimated by minimizing the error between the induced moment at the gauge location on the bridge girders (using the measured strain response) and predicted static moments in terms of axle weights (by multiplying the axle weights in a matrix form and the IL). A subsequent work then extended this concept to weighing side-by-side trucks by introducing the concept of influence surface [9]. This was calculated using the strain response of the bridge under a calibration truck moving alternatively in each lane.

For prerequisite estimation, several BWIM types are proposed in the literature, including

traditional BWIM [10], contactless BWIM (cBWIM) [11, 12], and Nothing-on-Road (NOR) BWIM (sometimes referred to as Free of Axle Detectors or FAD), which was first introduced in the WAVE project [16] on medium-span bridges with an orthotropic deck. This technique was then used in other studies as well [6, 13, 20, 21].

This study focuses on the NOR-BWIM system, due to its inherent advantages. In this system, unlike other categories, all devices are easily installed under the bridge, and nothing is on the road surface; thus, this extends the durability of the monitoring system as they are not exposed to daily tire impacts and harsh weather conditions. Furthermore, no traffic control or lane closure is needed during installation and maintenance, reducing installation and maintenance costs. Additionally, strain gauges are the most common sensors used in this system, and no additional sensors, switch tapes, pneumatic tubes, etc. are needed; this makes the system even more affordable compared to other BWIM systems and pavement-based WIMs [78, 79].

Prerequisites estimation requires the time delay between the peaks in the strain response caused by traversing axles over the bridge. However, peak clarity/sharpness in the response depends on two main factors. First, the bridge construction method, which changes the global behavior of the bridge and load-transfer mechanism from the slab to other bridge components when the truck gets close to the sensors. Second, the properties of slab itself (such as slab stiffness and thickness), which influence the local strain right under the tire path due to a concentrated load; thus, right sensor placement which captures most of the local strains at the vicinity of the tires' concentrated loads can improve peak sharpness, particularly for closely spaced axles. Many studies obtained this information directly from the raw strain response measurements [6, 14, 15, 17]. However, there are some cases in which the peaks are not clearly observable in the recorded responses. Thus, they have proposed particular processing methods which result more observable and sharper peaks [18–

21]. Most of the studies in the literature focus on T-beam [18, 19] and slab-on-girder bridges [14]. There are, however, limited studies on NOR-BWIM system for concrete-box-girders [6], despite this being a common bridge type. However, these studies still demonstrate limitations in peak clarity for closely-spaced axles while devoting little attention to finding suitable sensor placement. Thus, more consideration is still needed for NOR-BWIM strategies for concrete-box-girders, particularly those which leverage significant traffic-induced local strain responses observed in these structures [80].

Once the prerequisites are obtained, they are used for weight estimation. In general, weight estimation methods can be classified into two different groups: 1) dynamic methods [23–27] and 2) static methods [28–31]. However, in dynamic methods, for satisfactory accuracy, a full 3D model is usually needed. This makes the computation very time-consuming such that it will not be suitable for real-time monitoring applications [32]. In contrast, static methods directly deal with measured data and no model is needed, and this makes the static methods adequate for real-time monitoring applications. In the static methods, the influence line is the main requirement for weighing the trucks in motion on bridges [33]. This is computed through a procedure known as “calibration” by minimizing the difference between the theoretical and measured responses. There are some studies in which the influence line is experimentally obtained using crossing vehicles with known weight and strain responses [28–30, 34]. However, a comparative study [35] showed that among all methods, maximum likelihood estimation (MLE) method provides the most accurate results, and this is why MLE method is the focus of this study for weight estimation, but in a different experimental context which is explained later in this section.

The main limitation with both studies on prerequisites and weight estimations is their short span-length while long-spans may show different behaviour. The common wisdom [16, 62] in the literature is that short-span (span-length < 30m) or medium-span (30m < span-length <

60m) bridges and the ones with secondary elements, such as bridges with orthotropic deck, are the best choices for NOR-BWIM system. The first reason is the simplicity of the data analysis since long-spans are more likely to combine the peaks created by closely spaced axles and to demonstrate only their combined contributions [62]. This can be due to the fact that longer-spans are usually deeper, and such elements (such as thicker top slab) will usually provide less sharp peaks. The second reason in the literature is that longer-span bridges have lower natural frequencies. Therefore, they are more likely to match the vehicle frequencies increasing the dynamics effect [63]. Thus, like the studies discussed above, most of the NOR-BWIM applications in the literature have focused on either short-spans (span-length  $< 30\text{m}$ ) [20, 64, 65] or medium-spans ( $30\text{m} < \text{span-length} < 60\text{m}$ ) [16, 66]. There are also some cases in which medium-span composite box girder bridges (consisting of a steel box and not concrete box) with a span length of about 50m are tested [67, 68]. To the author's best knowledge, only limited studies are relevant to using NOR BWIM on long-spans. However, even these studies have focused on SHM applications using NOR BWIM, not focused on the accuracy of the prerequisites and weight estimation [69]. Also, the bridge used is a steel bridge with orthotropic deck which can have very different structural and dynamic behavior compared to other bridge types. Thus, the longer-span bridges (e.g., over 100 m) should be considered further because of several reasons. Firstly, deeper elements, such as thicker top slabs, may still provide sharp peaks for prerequisite estimation depending on construction and sensor placement. Secondly, for bridges with relatively smooth road surfaces, the level of error due to dynamics effects can be still in a reasonable range and one may actually be able to still use the long-spans for NOR-BWIM as well. Thirdly, there are many long-span bridges throughout the world which are highly instrumented to be evaluated from the structural integrity point of view. Thus, the existing sensors for structural health monitoring (SHM) system can be used to integrate the SHM systems with NOR-BWIM systems to reduce the cost. Hence, further evaluation is needed for the long-spans to understand how the accuracy

of the results is and whether or not they can be chosen for NOR-BWIM systems at all.

To demonstrate the feasibility and limitations of the studies discussed above for both prerequisites and weight estimation, in a new experimental context, a different but common type of bridge, a concrete-box-girder, was considered. The construction method in this type of bridge makes the slab and webs integrated. As discussed earlier, this results in a different load-transfer mechanism from the spanning slabs to the webs compared to other bridge types. This bridge has significantly longer spans (144 m) compared to the bridges in the literature. The main objective of this study is to demonstrate a low-cost, NOR-BWIM system for long-span, concrete-box-girders and evaluating the accuracy of the results to understand if NOR-BWIM systems (for prerequisite estimation) and MLE method (for weight estimation) are still suitable for this particular bridge. In this study, to find a suitable sensor placement, several strain gauge configuration alternatives for prerequisites are considered, and the most effective one is analyzed. Secondly, the strain profile extracted from experimental measurements is evaluated to understand if the NOR-BWIM methods discussed above (to create more observable features) are actually needed for this particular long-span concrete-box-girder bridge. Also, it was aimed to understand if the long-spans with significantly longer spans, e.g., over 100 m, can provide clear peaks for closely spaced tandem axles. This is because significantly longer-span bridges usually have thicker top slabs. Lastly, it is shown if NOR-BWIM system can also be effectively used for truck lane detection.

This paper is organized as follows: Section 2.2 introduces the monitoring system, the structure used, the strain gauge configuration alternatives, and the vehicles used. Section 2.3 explains the prerequisites and weight estimation methods in detail. The results for strain gauge configuration selection, prerequisites estimation of a single or multiple-truck passages, weight estimation, i.e., Gross Vehicle Weight (GVW) and axle weights estimation of a single truck passage, and truck lane detection are discussed in Section 2.4. Finally, the main

conclusions and future works are provided in Section 2.5.

## 2.2 Experimental Setup

### 2.2.1 Structure

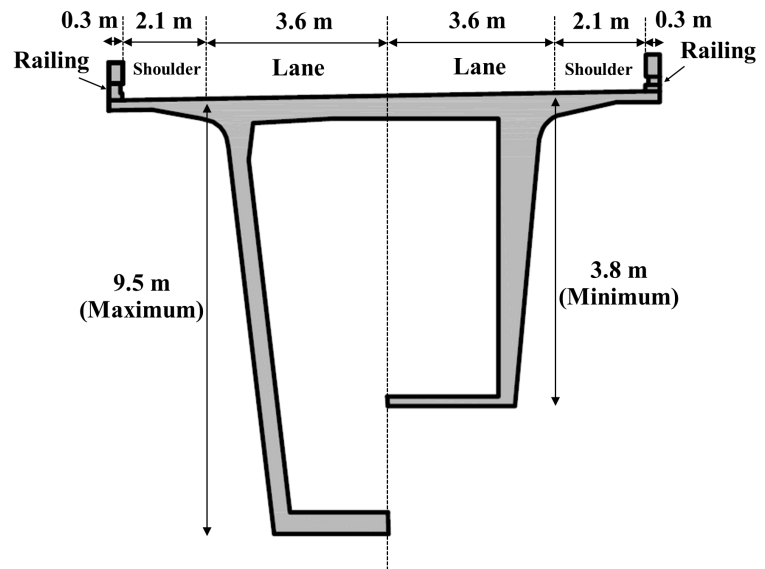
The Virginia Smart Road (SR) is a state-of-the-art, closed test-bed research facilities created and managed by the Virginia Tech Transportation Institute (VTTI). One of the bridges in the SR is a concrete-box-girder bridge called “SR bridge”. This is the second tallest state-maintained bridge in Virginia, shown in Figure 2.1. Figures 2.1a and 2.1b show the isometric-view of the bridge and the concrete box elevation, respectively. The SR bridge has two lanes and five spans in which the first and last spans are 86.5 m while other three are 144 m. In this study, the main focus is one of the longer spans (span 2). Also, as shown in Figure 2.1b, the total width of the slab is 12 m, including two lanes (3.6 m each), two shoulders (2.1 m each), and two railings (0.3 m each). The trapezoidal-shape concrete box has a variable height of about 3.8 to 9.5 m, with minimum depth in the mid-span.

### 2.2.2 Monitoring system and sensor configuration alternatives

In this study, only three strain gauges in the longitudinal direction of the bridge are needed for prerequisite estimation. Later, only one of the strain gauges will be used for weight estimation. However, in order to understand the effects of sensors position on the NOR-BWIM results, three different sensor configuration alternatives, Rows 1, 2, and 3, shown in Figure 2.2, were selected. The first two rows (Row 1 and Row 2) were on the internal surface of the slab, and the third one was on the internal side of the concrete wall. All rows were close to the mid-span of the second span (144/2 m from piers). The transverse distance between



(a) Isometric-view



(b) The concrete box elevation (variable height)

Figure 2.1: The Smart Road (SR) bridge

three rows was  $d/3$ , where  $d$  was half of the top width of the box ( $2d \approx 5.5$  m in this study). Row 1 was located approximately under the path of the left truck tires where maximum strain due to maximum local deflection was expected while Row 2 was located approximately mid-lane. The purpose for these two rows was testing to evaluate if maximum strain due to maximum local deflection will be an effective parameter on prerequisite estimation of the concrete-box-girder bridges. Also, Row 3 was in about 1.7 m from top. The purpose for Row 3 was to possibly reduce the cabling needed to connect the sensors to the data acquisition system (DAQ). Additionally, the distance between every two successive strain gauges were all chosen to be about 2 m. Lastly, the additional strain gauge (strain gauge 4) shown in Figure 2.2 is what should be used for truck lane position detection. This is discussed further in Subsection 2.4.4.

Figure 2.3 shows the monitoring network used. The strain gauges (BDI ST350) were 350  $\Omega$ , full Wheatstone, waterproof bridge strain transducers. Furthermore, the data acquisition

system (DAQ) was composed of a datalogger (the core of the network), integrating with all measurement modules. The datalogger's built-in GPS helped to time-synchronize all measurements with an accuracy of 0.001 s. Also, three measurement modules were connected to the datalogger to receive and transfer the strain data from the sensors to the datalogger. In this system, a cellular modem was also used to remotely transfer the data from the datalogger to a remote computer. Additionally, a charging regulator (a micro-controller-based smart charger with temperature compensation) was used. This optimizes battery charging and increases the battery's life. Two input terminals allow simultaneous connection of the system to a backup battery and AC power.

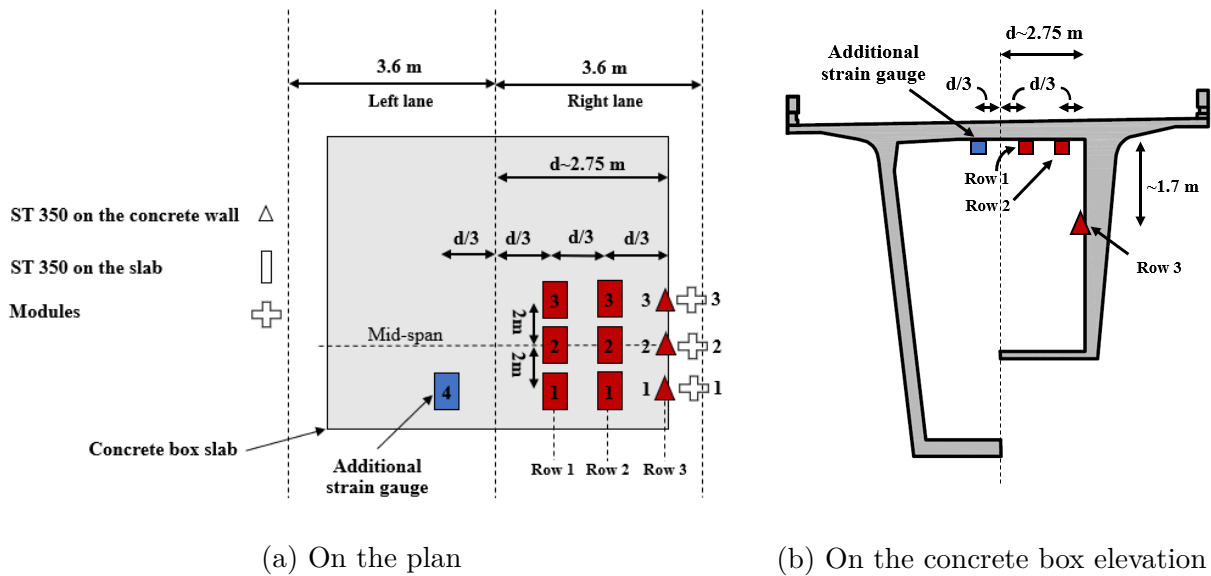


Figure 2.2: Strain gauge configuration alternatives ( $2d$  = the width of the slab inside the concrete box)

### 2.2.3 Data collection and the vehicles used

In this study, two truck groups were used: 1) three 3-axle trucks and 2) one 5-axle truck. One of the 3-axle trucks and the 5-axle truck are shown in Figure 2.4. All the trucks' information,



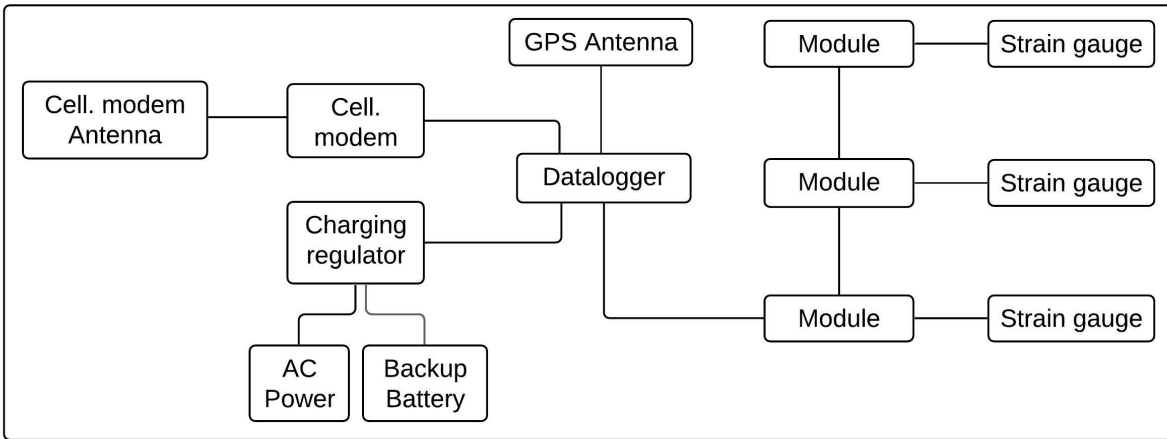


Figure 2.3: The monitoring network

including the number of runs, the number of axles, speeds, weights, and axle spacings are provided in Table 2.1. The axle spacings (center to center of tires) were measured using a tape measure on site. Additionally, the weights were measured using an off-road weigh station; however, due to some site restrictions, only the Gross Vehicle Weight (GVW) was reported for Trucks 1 and 2. Also, for Trucks 3 and 4, the weigh station was only able to measure the Gross Vehicle Weights (GVWs) and the tandem axle weights, not the individual axle weights in the tandem axles. For Truck 3, the front individual and rear tandem axles' weights were about 7.2 and 19.6 tonnes, respectively. Also, for the 5-axle truck (Truck 4), besides the GVW, three weights were reported, including one for the individual front axle (about 5.2 tonnes), one for the middle tandem (about 11.0 tonnes), and one for the rear tandem axles (about 9.7 tonnes). Table 2.1 shows a range for GVWs. This is because we were using the construction trucks and thus, GVWs were not necessarily constant for different truck passages. In total, 18 tests were performed, ten tests using Trucks 1 and 2 (five for each), and 8 tests using Trucks 3 and 4 (four for each). The weights for Trucks 1 and 2 were variable (shown in Tables 2.1 and 2.4) in different runs while it was constant for Trucks 3 and 4.



(a) 3-axle truck



(b) 5-axle truck

Figure 2.4: The 5-axle truck and one of the 3-axle trucks

Table 2.1: Summary of truck properties and test speeds

Truck no.	No. of runs	No. of axles	Speed (m/s)	GVW (ton)	AS* (m)			
					AS <sub>1</sub>	AS <sub>2</sub>	AS <sub>3</sub>	AS <sub>4</sub>
1	5	3	≈11	22.4-23.1	4.24	1.37	N/A	N/A
2	5	3	≈20	21.4-23.1	4.19	1.35	N/A	N/A
3	4	3	≈13 & 23	26.8	4.78	1.32	N/A	N/A
4	4	5	≈17 & 27	25.9	6.17	1.32	10.62	1.24

\*AS=Axle spacing

Also, the truck drivers were asked to run at a constant speed over the bridge. The speed for Trucks 1 and 2 was 11 and 20 m/s, respectively, while for Truck 3 and 4, the speed was 13 & 23 m/s and 17 & 27 m/s, respectively. The trucks' velocity versus time was recorded at a sampling rate of 100 Hz using a smartphone's internal GPS (iPhone XR) and stored on the cloud via the MATLAB Mobile application. However, this was only possible for Trucks 3 and 4 and not for Trucks 1 and 2 due to COVID-related restrictions for certain drivers.

Furthermore, the strain responses in the runs corresponding to Trucks 1 and 2 were recorded with a sampling rate of 100 Hz and for Trucks 3 and 4 with a sampling rate of 200 Hz. The data was then transferred remotely to a laboratory computer and stored properly.

## 2.3 Methodology

### 2.3.1 Prerequisite estimation approach

In the weight estimation procedure, prerequisites, i.e., number of axles, speed, and axle spacing, should always be computed first. Then, the results will be used for weight estimation. To calculate the prerequisites, assume that a  $n$ -axle truck moves over the right lane of SR bridge where Row 1 shown in Figure 2.2 is placed. It is shown later in Subsection 2.4.2 that the strain response for this particular bridge (concrete-box-girder), under a  $n$ -axle truck passage, consists of  $n$  clear peaks, which will be equal to the number of traversing axles. Knowing the time-delay between the corresponding peaks, i.e., between the first peaks, the second peaks, and etc., of the responses from successive strain gauges as well as the physical distances between the strain gauges, the truck speed can be computed using

$$v = \frac{1}{2n} \times \sum_{x=1}^2 \sum_{l=1}^n \frac{d^{x,x+1}}{\Delta t_l^{x,x+1}}, \quad (2.1)$$

where  $n$  is the number of peaks (axles) in the strain response, and  $d^{x,x+1}$  is the physical distance between the  $x^{th}$  and  $(x+1)^{th}$  successive strain gauges. Also,  $\Delta t_l^{x,x+1}$  is the time-delay between the  $l^{th}$  peaks in the strain responses from  $x^{th}$  and  $(x+1)^{th}$  successive strain gauges.

Once the truck speed is computed, the axle spacings should be calculated using

$$s_n = \frac{v}{3} (\Delta t_n^1 + \Delta t_n^2 + \Delta t_n^3), \quad (2.2)$$

where  $s_n$  is the  $n^{th}$  axle spacing and  $\Delta t_n^1$ ,  $\Delta t_n^2$ ,  $\Delta t_n^3$  are the  $n^{th}$  time-interval in strain responses obtained from strain gauges 1, 2, and 3, respectively. For clarity, these parameters, used in

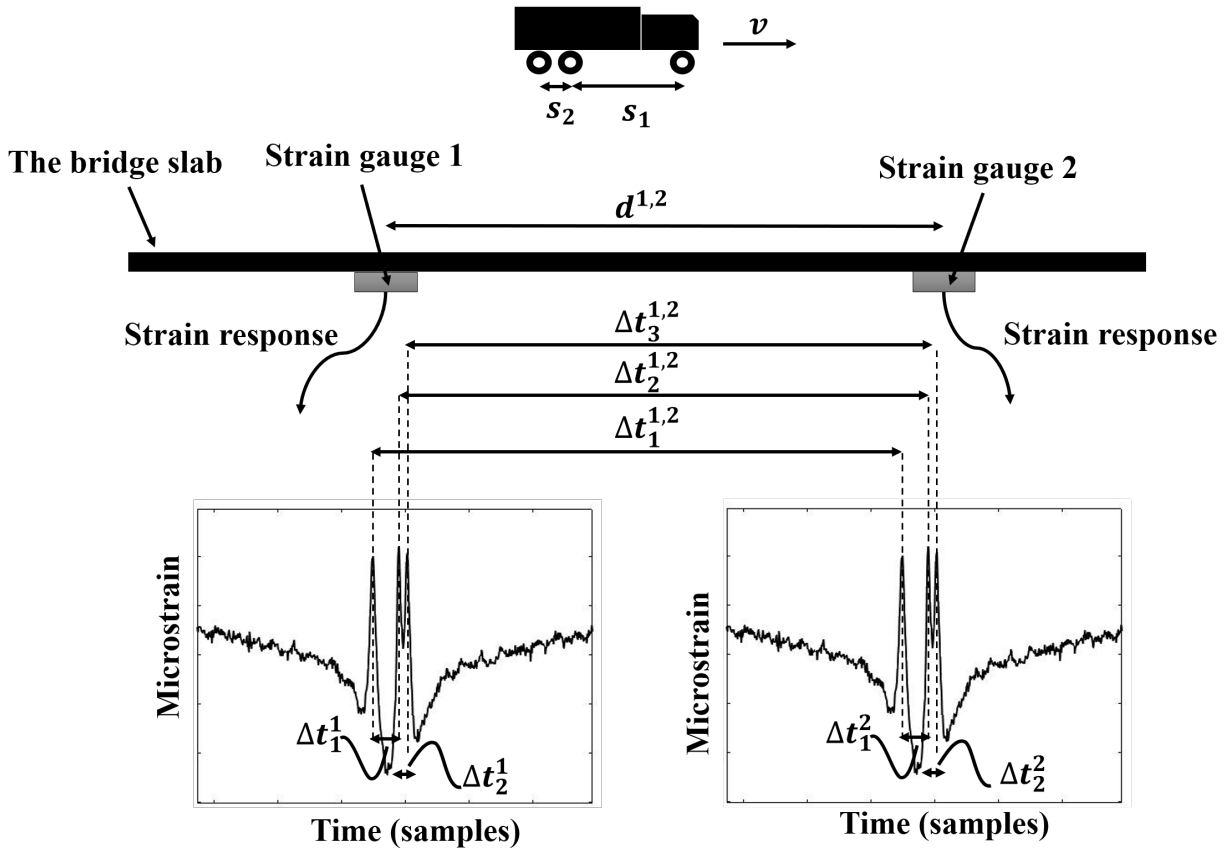


Figure 2.5: Prerequisite estimation approach diagram

Equations (2.1) and (2.2), are all also shown in Figure 2.5 for a 3-axle truck passage and only for two successive strain gauges.

### 2.3.2 Weight estimation method

Once the prerequisites are computed, the results should be used for weight estimation. As explained earlier, the first step is the influence line extraction from calibration data and using maximum likelihood estimation (MLE), first proposed by Ieng 2015. Unlike the method proposed by O'Brien et al. 2006, MLE method takes two (or more) trucks (with known weights and prerequisites) with multiple passages into account, considering the variability

of the effects of the calibration vehicle on the bridge. Then, the extracted influence line will be used to estimate the weight of unknown trucks. Most of the studies about MLE method have presented the derivations and required steps; however, since this method is relatively new (published in 2015), we have included further details here. This is to clarify the details which are not clearly explained in other studies. It is aimed to explain the steps in a way that one can practically implement them. As mentioned earlier, in this study, MLE is used in a different experimental context and on a long-span concrete-box-girder bridge to evaluate this approach further.

To explain the MLE method, assume that a  $n$ -axle calibration truck with axle weights of  $W = [p_1, p_2, \dots, p_n]$  and axle spacings of  $S = [s_1, s_2, \dots, s_n]$ , moves over a bridge at speed  $v$ , and  $M_{k \times 1}^m$  is the measured strain vector recorded with a sampling rate of  $f$  Hz. However, the strain measurement is always corrupted by noise,  $\epsilon$ . Thus,

$$M^m = M^t + \epsilon, \quad (2.3)$$

where  $M_{k \times 1}^t$  is the ideal strain response with no noise included such that

$$M^t = AI, \quad (2.4)$$

where  $I_{(k-d_n) \times 1}$  is the influence line vector consisting of the influence line ordinates. Also,  $A$  is a Toeplitz matrix with size  $k \times (k - d_n)$  in which  $k$  is the total number of scans in the strain response. Matrix  $A_{k \times (k-d_n)}$  defined as

$$A = \begin{pmatrix} p_1 & \cdots & 0 & \cdots & 0 \\ \vdots & \ddots & \vdots & \ddots & \vdots \\ p_i & \cdots & p_1 & \cdots & 0 \\ \vdots & \ddots & \vdots & \ddots & \vdots \\ p_n & \cdots & p_i & \cdots & p_1 \\ \vdots & \ddots & \vdots & \ddots & \vdots \\ 0 & \cdots & p_n & \cdots & p_i \\ \vdots & \ddots & \vdots & \ddots & \vdots \\ 0 & \cdots & 0 & \cdots & p_n \end{pmatrix} \begin{matrix} - > d_1 + 1 \\ \vdots \\ - > d_i + 1 \\ \vdots \\ - > d_n + 1 \\ \vdots \\ \vdots \\ \vdots \\ - > k \end{matrix}, \quad (2.5)$$

should be created using the axles weights shifted vertically with respect to vector  $D$  components, i.e.,  $d_1, d_2, \dots, d_i, \dots, d_n$ , in Toeplitz-matrix form. Each line in matrix  $A_{k \times (k-d_n)}$  relates to a time-step of the truck passing over the bridge. Matrix  $A_{k \times (k-d_n)}$  row numbers are shown in Equation (2.5) where

$$d_i = \frac{c_i f}{v}, \quad (2.6)$$

and  $c_i$  is the distance between the first axle and  $i^{th}$  axle. Note that  $d_1$  is always zero as the first axle is being compared with itself.

As discussed earlier, in MLE method,  $N$  truck runs will be considered. Thus, Equation (2.4) can be rewritten as

$$M_j^m = M_j^t + \epsilon_j, \quad (2.7)$$

where  $j$  varies from 1 to  $N$ . Assuming that all the measurements are independent and identically distributed, the likelihood function will be the product of the individual probabilities

$$L = \prod_{j=1}^N pdf(\epsilon_j | I), \quad (2.8)$$

where pdf is the probability density function of  $\epsilon$  and  $L$  is the likelihood function. According to MLE method, the  $L$  function should be maximized or instead, the negative of its natural logarithm should be minimized. By doing so, the final equation will be

$$\sum_{j=1}^N A_j^T A_j I = \sum_{j=1}^N A_j^T M_j^T. \quad (2.9)$$

In Equation (2.9), matrix  $A_{k \times (k-d_n)}$  and vector  $M_{k \times 1}$  are known, therefore, the unknown  $I_{(k-d_n) \times 1}$  vector can be computed. As explained earlier, the size of matrix  $A_{k \times (k-d_n)}$  generated for each calibration truck is a function of the axle spacings. This changes the number of columns in matrix A, and therefore, makes the matrix operation in Equation (2.9) impossible. In this case, to allow proper matrix operations, it is needed to adjust the number of scans to equalize the number of columns in A matrices for different trucks. For  $I_{(k-d_n) \times 1}$  verification, one of the original measured strain signals can be compared with reconstructed one using Equation (2.4). Once the  $I_{(k-d_n) \times 1}$  vector is obtained, as usual, Moses method,

$$W = (B^T B)^{-1} B^T M^m, \quad (2.10)$$

can be used for finding the unknown weights of an unknown truck passing over the bridge. In Equation (2.10),  $W_{n \times 1}$  is a vector consisting of the unknown axles weights, and  $B_{k \times n}$  is a matrix created using the influence line ordinates, shifted based on the truck axle spacings to adjust the time-instant when each truck axle enters and leaves the bridge structure.

## 2.4 Results

### 2.4.1 Strain gauge configuration selection

The first step is to determine which one of the alternatives, i.e., Rows 1, 2, and 3, shown in Figure 2.2, enables the most accurate prerequisite estimation. The reasons for considering these three alternatives were already explained in Subsection 2.2.2. Figure 2.6 shows the strain responses for the first strain gauges in Rows 1, 2, and 3 when Truck 1 crosses over the bridge. Row 1, located underneath the usual tire path, provides a reliable strain response such that one can easily observe three peaks which are related to the three axles of the truck. Similar results to what is shown in Figure 2.6a were observed in all 18 truck passages introduced in Table 2.1. Thus, Row 1, which is in an area where the maximum strain due to maximum local deflection happens, is a good candidate for the sensors placements. Figure 2.6b shows typical results from Row 2, located approximately mid-lane, and Figure 2.6c illustrates typical results from Row 3 on the concrete wall, and both of them do not provide three clear peaks. Thus, for this concrete-box-girder bridge, the strain gauges should be mounted close to the middle pavement marking (in about 0.8-0.9 m) where maximum strain due to maximum local deflection occurs to obtain a reliable strain response. This will be in an area where the concentrated tire loads will be usually present. Hence, in the rest of this paper, the focus will be only on the three strain gauges in Row 1. As mentioned earlier in Section 2.1, many current studies have difficulties in obtaining the observable peaks (particularly the closely-spaced ones) since they devote little attention to finding suitable sensor placement.



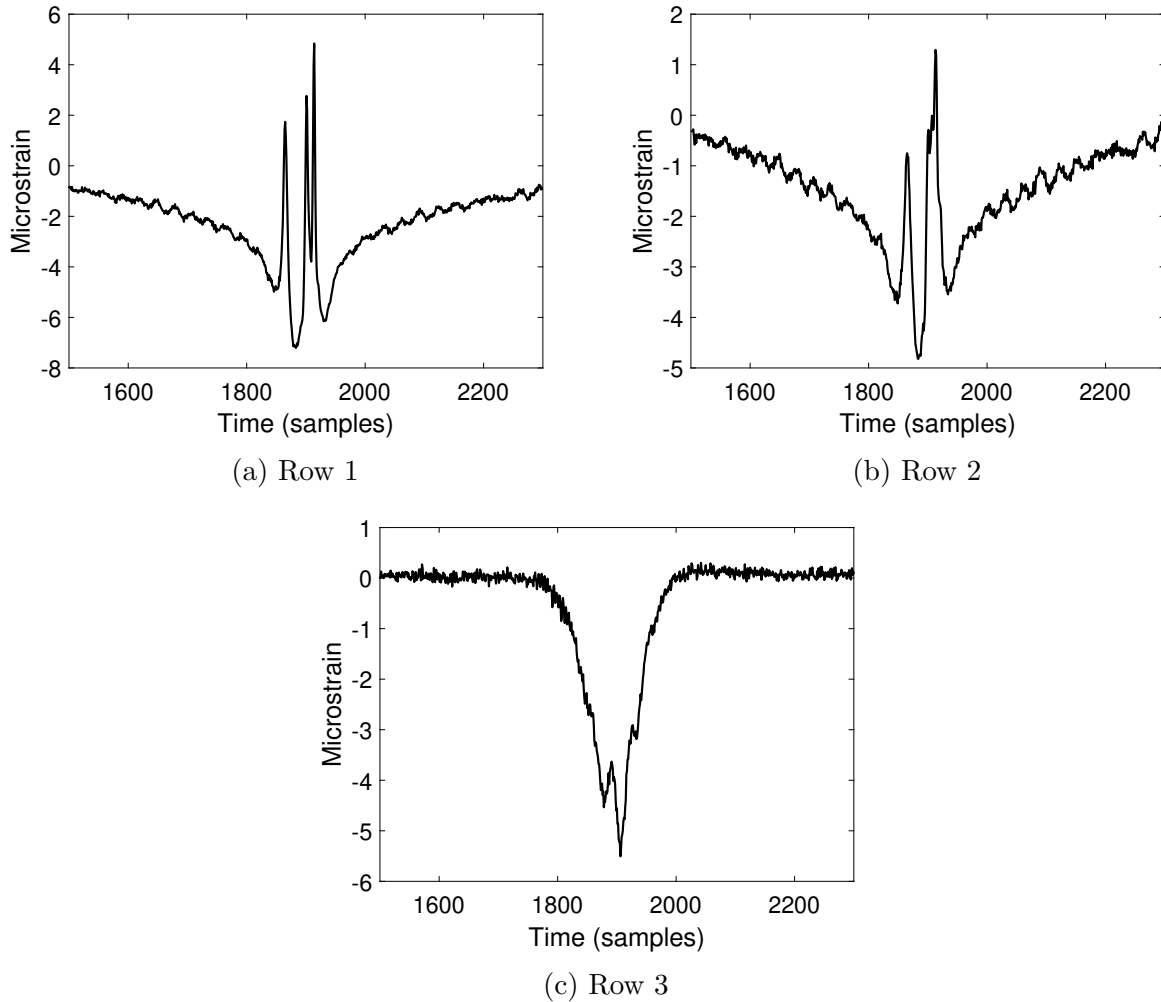


Figure 2.6: The strain responses from strain gauge configuration alternatives

### 2.4.2 Prerequisite estimation results

The strain responses from strain gauges in Row 1 were first extracted. Figures 2.6a and 2.7 show the strain responses for Truck 1 (3-axle) and Truck 4 (5-axle), respectively. In both figures, the number of axles are exactly matched with the number of peaks in the strain responses. To evaluate the repeatability of the process, for all 18 runs, the number of axles were obtained, and the results are shown in Table 2.2. According to this table, no error was observed in obtaining the number of axles. Also, as explained in Section 2.1, the NOR-

BWIM system has mostly been tested on T-beam and slab-on-girder bridges, while other bridge construction methods, such as concrete-box-girder, may reveal a different behavior (peak sharpness). However, here, for this particular sensor placement and for this concrete-box-girder bridge, it is shown in Figures 2.6a and 2.7 that the peaks are sharp enough, and unlike the studies discussed earlier, no additional method was needed for peak accentuation. This was the same for all 18 runs. This also shows that, unlike the general wisdom in the literature, the level of error due to dynamics effects is still in a reasonable range such that closely-spaced axles are easily detected for all cases (at least for this particular long-span bridge).

In the next step, the method explained in Subsection 2.3.1 was used to find the truck velocity and the axle spacing. All result errors for the speed and axle spacings are provided in Table 2.2. As explained in Subsection 2.2.3, due to the site COVID-related policies, the speed was only measured for Trucks 3 and 4 while for Trucks 1 and 2, only a rough estimation (using truck speedometer) was provided by the truck drivers. Thus, the average speed error in the last row of Table 2.2 is computed using Runs 11 to 18. According to this table, the mean-absolute-error (MAE) for speed is 2.56% and the margin of error is 1.14 (95% confidence), and thus, absolute speed error will be between 1.42% to 3.7% with 95% confidence. Additionally, for axle spacings error, all 18 runs were considered because, firstly, the ground-truth data was available for all, and, secondly, the estimated speed is what should be used in Equation (2.2) for speed calculation, not the measured speed. According to the last row of Table 2.2, the MAE for axle spacings 1, 2, 3, and 4 are 2.00%, 4.30%, 0.73%, and 1.15%, and the margins of errors for absolute errors are 0.79%, 1.62%, 0.52%, and 0.78%, respectively. This great agreement between the measured and estimated values shows that the NOR-BWIM system works with high accuracy in prerequisite estimation for this concrete-box-girder bridge, i.e., number of axles, speed, and axle spacing. In general, the errors vary from one truck to

another, likely due to a combination of the effect of transverse position of the trucks, noise level induced by different trucks, and etc. However, the main purpose of the prerequisite estimation is to provide required information for weight estimation. In Subsection 2.4.5, it is shown that when the correct prerequisites were used for test cases, the weight estimation error was only changed by a negligible amount (0.6%).

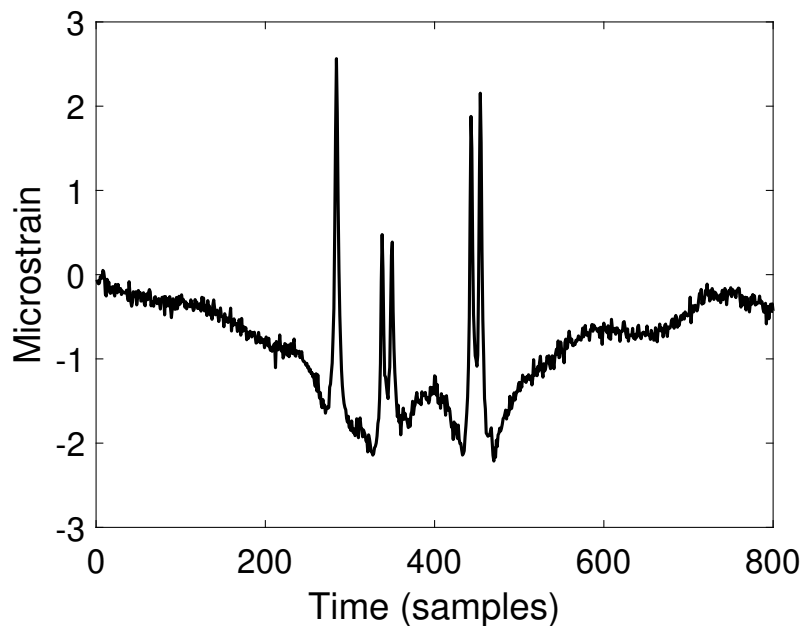


Figure 2.7: 5-axle truck strain response with sharp peaks

### 2.4.3 Multiple-truck tests

In this subsection, this is explained whether the prerequisite estimation for this long-span, concrete-box-girders is still valid if multiple trucks move over the bridge. Thus, the test was repeated two times for a case in which both the 5-axle (Truck 4) and 3-axle (Truck 3) trucks shown in Figure 2.4 crossed over the bridge with a low relative distance (about 10 m) and at 13.4 m/s (48.3 km/h). In both runs, five and three quite clear peaks were resulted for the 5-axle and 3-axle trucks, respectively. One of the strain responses is illustrated in

Table 2.2: Prerequisite estimation results

Run	Truck no. (Table 2.1)	No. of axles*	Speed error (%)	AS** (%)			
				AS <sub>1</sub>	AS <sub>2</sub>	AS <sub>3</sub>	AS <sub>4</sub>
1	1	3	-6.25	0.90	6.11	N/A	N/A
2	1	3	8.31	-3.67	4.65	N/A	N/A
3	1	3	0.89	-3.09	5.83	N/A	N/A
4	1	3	9.04	-3.01	5.36	N/A	N/A
5	1	3	8.43	-4.52	4.76	N/A	N/A
6	2	3	-1.09	3.25	1.68	N/A	N/A
7	2	3	-0.79	0.43	-2.87	N/A	N/A
8	2	3	-2.31	0.44	-4.35	N/A	N/A
9	2	3	-1.09	-1.44	1.68	N/A	N/A
10	2	3	-5.63	-1.49	-2.99	N/A	N/A
11	3	3	3.67	6.07	-15.43	N/A	N/A
12	3	3	5.64	3.11	-7.54	N/A	N/A
13	3	3	3.75	0.75	-0.70	N/A	N/A
14	3	3	-1.83	-2.41	-5.90	N/A	N/A
15	4	5	0.68	-0.31	4.84	0.63	-0.80
16	4	5	1.61	0.40	1.39	0.82	1.76
17	4	5	1.72	-0.44	-0.65	0.09	0.19
18	4	5	1.55	0.18	0.70	1.38	1.84
<b>AE***</b>	<b>N/A</b>	<b>N/A</b>	<b>2.56±1.14</b>	<b>2.00±0.79</b>	<b>4.30±1.62</b>	<b>0.73±0.52</b>	<b>1.15±0.78</b>

\*Estimated, \*\*AS=Axle spacing, \*\*\* Absolute error with 95% confidence

Note: Speed errors 1-10 are based on approximate truck speeds, not used in AE

Figure 2.8 for conciseness. Then, the speed and axle spacings were also computed for both runs and the results errors are shown in Table 2.3. According to this table, in both runs, the axle spacing estimation errors for the 5-axle truck were all less than 1% except for the last axle spacing in which the errors were 1.17% and 2.46% for Runs 1 and 2, respectively, but still very low. Additionally, the axle spacing estimation errors for the 3-axle truck were all between 1% and 2.18%. Furthermore, the speed estimation errors resulting from both runs were also very low for both trucks, which were 2.1% and 2.02% for the 3-axle truck and 1.04% and 0.39% for the 5-axle truck. This shows that, overall, using the sensor placements proposed, NOR-BWIM system still works accurately for this long-span, concrete-box-girder bridge even if more than one truck is simultaneously on the bridge. Also, although dynamics

effects can be observed at some points but the closely spaced axles are still detected.

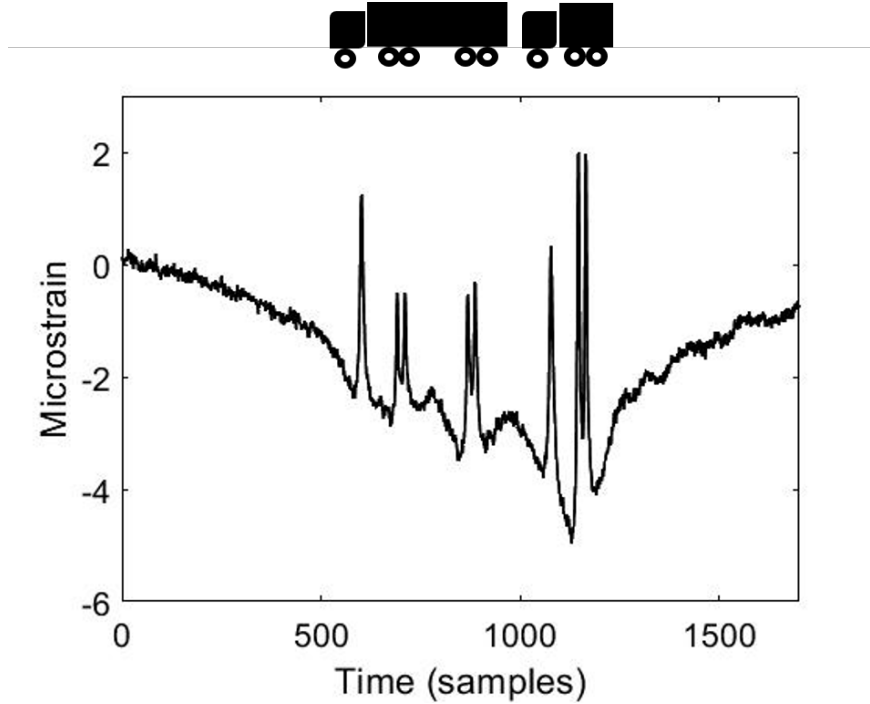


Figure 2.8: Strain response for the multiple-truck case

Table 2.3: Prerequisite estimation for multiple-truck tests

Run	Speed error (%) (3-axle)	Speed error (%) (5-axle)	AS* error (%)		AS error (%)			
			AS <sub>1</sub>	AS <sub>2</sub>	AS <sub>1</sub>	AS <sub>2</sub>	AS <sub>3</sub>	AS <sub>4</sub>
1	-2.10	1.04	-1.40	-1.44	-0.83	0.04	0.31	1.17
2	2.02	0.39	-1.12	-2.18	-0.35	-0.31	0.84	2.46

\*AS=Axle spacing

#### 2.4.4 Truck lane position detection

In this subsection, it is shown that adding only one more strain gauge under the left-lane slab (strain gauge 4 in Figure 2.2), truck lane position detection will also become possible for this long-span, concrete-box-girder bridge. Only two strain gauges will be needed for truck lane position detection, one of the strain gauges in Row 1 and the additional strain

gauge on the left lane. To show how the modified instrumentation plan can detect the truck lane position, five tests were performed, and in all, the 5-axle truck moved over the left lane where the additional strain gauge is installed and the strain response from strain gauge 1 shown in Figure 2.2 was recorded. One of these responses is shown in Figure 2.9. According to Figure 2.9, when the truck moved over the left lane and the strain was recorded on the right lane (over Row 1), only 3 peaks were captured for the 5-axle truck. This was the same for all five left-lane truck passages. On the other hand, as explained in Subsection 2.4.2, when the truck moved on the right lane and the strain response was recorded on the same lane, five sharp peaks (Figure 2.7) were observed. Thus, by comparing the strain response obtained from strain gauges 1 and 4, one can simply realize which lane the truck has moved through. In fact, if strain gauge 1 shows five clear peaks while strain gauge 4 shows less than that, the truck has moved through the right lane and vice versa.

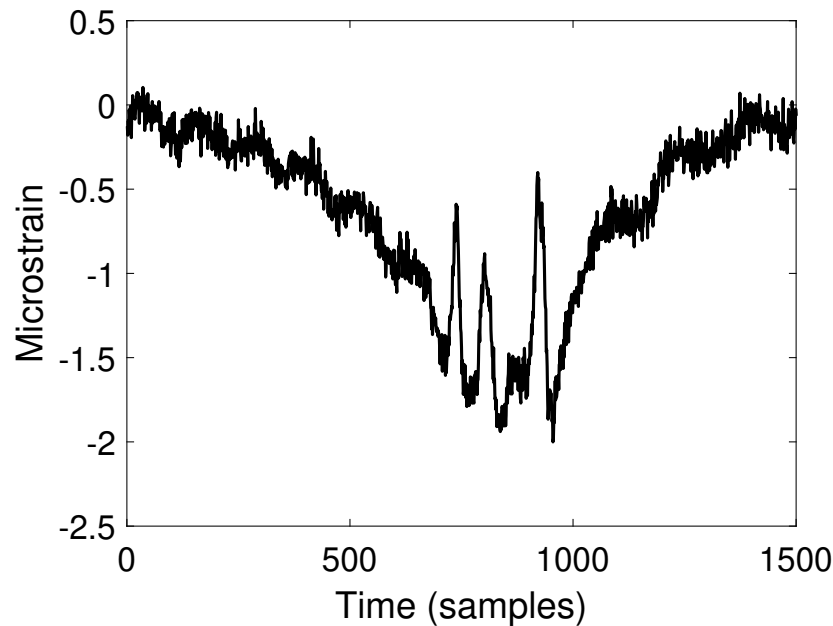


Figure 2.9: Strain response for the left-lane truck passage (should be compared with Figure 2.7)

### 2.4.5 Weight estimation results

Now that the prerequisites are successfully obtained with good accuracy, they can be used for weight estimation process. All strain responses were first denoised using “Symlets Wavelet” (sym4 with a level of wavelet decomposition of 5 in MATLAB). Also, as explained in Subsection 2.3.2, the first step in weight estimation using MLE method is calibration with several trucks with known individual axle weights and true prerequisites. However, it was explained in Subsection 2.2.3 that in this study, due to some site restrictions, only the Gross Vehicle Weights (GVWs) were reported for Trucks 1 and 2, and both GVW and the tandem axles’ weights (not the individual axle weights in the tandem axles) were measured for Trucks 3 and 4. Thus, Runs 11 through 14 shown in Table 2.2 were used for calibration, and it was assumed that the two rear closely spaced axles have the same weights; and therefore, the reported weight for the rear tandem axle was equally distributed between two individual axles. This simplifying assumption is in good agreement with real data in the literature [35]. To verify the IL, using the obtained influence line, one of the strain signals (Run 6) is reconstructed and compared with original response in Figure 2.10 showing a great agreement. The strain reconstruction is a circular process such that in the first step, the IL will be computed through the calibration process using a known truck with known axle weights. Then, the IL will be multiplied by the axle weights (in a matrix form) to reconstruct the strain response.

For weight estimation, only the runs that were not included in the calibration process were used: Runs 1 through 10 plus Runs 15 through 18 shown in Table 2.2 (14 runs in total). Table 2.4 shows the actual GVW, estimated GVW, and the weight estimation errors for all 14 runs. According to the last row in Table 2.4, the MAE for GVW estimation is 4.60%. Also, the absolute error, with 95% confidence, is between 2.54% to 6.66%. Additionally, out of 14 cases considered, 11 cases yielded an error less than 5.5%, and 2 cases had an error

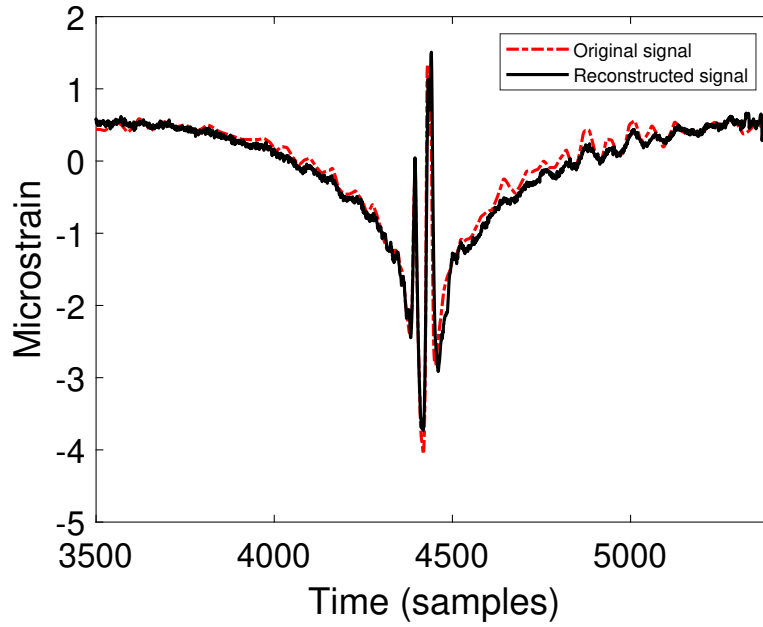


Figure 2.10: Reconstructed strain response vs. the original strain response (Run 6)

Table 2.4: Weight estimation results

Run	Actual weight (ton)	Estimated weight (ton)	Error (%)
1	22.82	20.87	-8.6
2	22.51	21.66	-3.8
3	22.45	22.25	-0.9
4	22.18	23.31	5.1
5	22.30	23.41	5.0
6	22.86	23.12	1.2
7	22.10	21.44	-3.0
8	21.17	20.52	-3.1
9	21.61	21.60	-0.1
10	22.00	23.19	5.4
15	25.90	23.40	-9.6
16	25.90	22.19	-14.3
17	25.90	25.22	-2.6
18	25.90	26.37	1.8
<b>Average</b>	<b>23.26</b>	<b>22.75</b>	<b>4.60± 2.06*</b>

\* Absolute error (AE) with 95% confidence



greater than 5.5% but still less than 10%, and only one case had an error greater than 10%.

In general, different factors can contribute in the weight estimation error in this particular long-span concrete-box-girder bridge: 1) inaccurate prerequisite estimations, 2) remaining noise level in the strain response, 3) different levels of dynamic effects, varying based on the truck velocity, weight, transverse position, road roughness. In this experimental study, most of these factors were simultaneously changing and this makes the parametric study difficult. Additionally, in real traffic monitoring cases, the first two factors are somewhat controllable by using more precise DAQ and sensors. However, here, a preliminary parametric study is conducted for the first two factors and further discussion is left for a future numerical study where these factors can be changed one by one. To evaluate the first factor, the test cases with known measured prerequisites (Runs 15 through 18) were considered, and instead of the estimated prerequisites, the true values for both calibration trucks and the test trucks were used. In all cases, the weight estimation error did not change by more than  $\pm 0.6\%$ . Additionally, to evaluate the second factor, for the same truck runs, noisy strain responses for both calibration and test were used. In all cases, a slight change (less than  $\pm 0.5\%$ ) in weight estimation error was observed. Also, in three cases, the error was increased, and in only one case, it was decreased.

On the other hand, the third factor, i.e., dynamic effects, cannot be controlled since unknown traversing trucks will move at different speeds, weights, and in different transverse positions and on roads with different roughness. But, according to Figure 2.6a, although some oscillations due to dynamics are present but it is unlikely to be the main source of error, and unlike the common wisdom in the literature, they do not result in significant weight estimation errors for this long-span bridge. Furthermore, there are many old, long-span bridges throughout the world which are highly instrumented to be evaluated from the structural integrity point of view. As a result of this study, these bridges can be used for

NOR-BWIM applications, and the existing sensors for SHM system can be used to integrate the SHM systems with NOR-BWIM systems to reduce the cost.

Table 2.5 shows the axle weight estimates to make some sense of axle weight estimations on long-spans. However, the associated errors are not reported. This is because, as discussed in Subsection 2.2.3, for the calibration truck (Truck 3) and the 5-axle truck (Truck 4), only the tandem axle weights (not the individual axle weights) were reported. Also, only GVW was reported for Trucks 1 and 2. Hence, estimation errors for the axle weights are left for a future study where the accurate axle weight are reported.

Table 2.5: Axle weight estimates

Run	Estimated axle weight (ton)				
	AW <sub>1</sub> *	AW <sub>2</sub>	AW <sub>3</sub>	AW <sub>4</sub>	AW <sub>5</sub>
1	7.15	7.13	6.59	N/A	N/A
2	7.83	6.14	7.69	N/A	N/A
3	7.12	7.97	7.16	N/A	N/A
4	6.70	7.99	8.62	N/A	N/A
5	5.81	7.96	9.63	N/A	N/A
6	7.06	9.05	7.01	N/A	N/A
7	7.41	7.59	6.44	N/A	N/A
8	6.74	8.80	4.97	N/A	N/A
9	7.43	7.76	6.41	N/A	N/A
10	7.46	9.05	6.67	N/A	N/A
15	4.87	2.64	2.78	6.35	6.76
16	5.75	2.83	2.18	5.86	5.57
17	6.99	3.35	3.13	5.47	6.28
18	7.69	3.24	2.87	6.19	6.37

\*AW=Axle weight

## 2.5 Conclusions

This study reports the results of an experimental investigation on a case study conducted in Blacksburg, VA, to evaluate how NOR-BWIM systems coupled with static weight estimation techniques perform. The novelty of this presented work is its applicability to non-typical bridge types, such as long-span concrete-box-girder bridges. This is to understand if long-span bridges (particularly with a span length of greater than 100m) that usually have deeper elements (e.g., thicker top slabs) can still provide sharp peaks for prerequisite estimation depending on construction and sensor placement. Also, it was aimed to understand that for bridges with relatively smooth road surfaces, the level of error due to dynamics effects can be still in a reasonable range and one may actually be able to still use the long-spans for NOR-BWIM as well. A key motivation for this study is that there are many long-span bridges throughout the world which are highly instrumented to be evaluated from the structural integrity point of view. Thus, the existing sensors for structural health monitoring (SHM) system can be used to integrate the SHM systems with NOR-BWIM systems to reduce the cost.

Moreover, in this study, an efficient and cost-effective sensor configuration was proposed to estimate the truck speed, number of axles, axle spacing, weight, and truck lane position. The following findings were reached:

According to the results, a key reason for the success of the system was careful selection of the sensor configuration. The clearest peaks in the strain response were obtained at the location where maximum strains due to maximum local deflections occurred, which was as close as possible to the wheel path. Results from the proposed sensor configuration showed that the strain response for this long-span, concrete-box-girder bridge consists of clear peaks which are equal to the number of passing truck axles, even for closely-spaced axles which is

usually a challenge in NOR-BWIM systems.

Also, no error was observed for the number of axles when the proposed sensor configuration was used. The mean-absolute-error (MAE) for speed was 2.56% and the margin of error was 1.14 (95% confidence), and thus, absolute speed error was between 1.42% to 3.7% with 95% confidence. Additionally, the mean-absolute-error for axle spacings 1, 2, 3, and 4 were 2.00%, 4.30%, 0.73%, and 1.15%, and the margins of errors were 0.79%, 1.62%, 0.52%, and 0.78%, respectively. Thus, in such a long-span bridge (144 m), the NOR-BWIM system still works accurately for prerequisite estimation and even closely-spaced axles were clearly observable.

In two other tests, both 5-axle and 3-axle trucks moved over the bridge with a low relative distance (about 10 m) and at the speed 13.4 m/s (48.3 km/h). In both runs, five and three quite clear peaks were resulted for the 5-axle and 3-axle trucks, respectively. According to the results, in both runs, the axle spacing estimation errors for the 5-axle truck were all less than 1% except for the last axle spacing in which the errors were 1.17% and 2.46% for two Runs, respectively, but still very low. Additionally, the axle spacing estimation errors for the 3-axle truck were all between 1% and 2.18%. Furthermore, the speed estimation errors resulted from both runs were also very low for both trucks, which were 2.1% and 2.02% for the 3-axle truck and 1.04% and 0.39% for the 5-axle truck. This shows that, overall, NOR-BWIM system works accurately for the considered long-span, concrete-box-girder bridge even if multiple trucks are concurrently on the bridge.

It was also demonstrated that the implemented NOR-BWIM system for this concrete-box-girder bridge was able to correctly identify the truck lane positions. For this, only two strain gauges, one under the right lane and one under the left lane, are typically needed. In the Gross Vehicle Weight (GVW) estimation, the mean absolute error was as low as 4.60%, and the absolute error, with 95% confidence, will be between 2.54% to 6.66%. Furthermore, in 11 cases out of 14, the error was less than 5.5%; however, in 2 cases, an error between

5.5% and 10% was observed. Only one case had an error greater than 10%. This shows that maximum likelihood estimation (MLE) can still be used for long-span bridges. Also, dynamics effects was in a reasonable range and did not make huge weight estimation errors. It should be noted that dynamic effects were not considered directly in this study. In fact, since the mean absolute error of GVW estimation was just slightly (about 1 percent) larger than other studies in literature on short-span bridges, one can say the dynamic effects did not have significant effect on the weight estimation accuracy (at least for this particular long-span bridge).

Other factors should also be considered in a future study. For instance, form of construction in the bridges can affect the peaks' sharpness in the strain response used for prerequisites' estimates. This is because various types of construction reveal different load-transfer mechanism from the slab to other components when the trucks get close to the sensors. In this study, concrete-box-girder bridge was considered, and other construction methods should be addressed in a future study.

It is true that no missed axles were observed in this study; however, in reality, variability in truck transverse position can be different than the cases tested, and even for row 1, missed axles can be still likely. However, using the suggested sensor placement, less missed axles are still expected. Also, if there are not clear peaks, the problem can still be solved using the best fit process for a number of different spacings and finding the minimum of the least squares minima.

# Chapter 3

## A Novel Bridge-Weigh-in-Motion (BWIM) Approach for Simultaneous Multiple Vehicles on Concrete-Box-Girder Bridges

Bridge-weigh-in-motion (BWIM) is a robust system that can accurately obtain traffic information to facilitate bridge design, maintenance, and management. However, the main issue with the existing BWIM approaches is their limited suitability for simultaneous multiple-vehicle cases on multiple-lane bridges. To address this limitation, in this study, a novel BWIM approach is proposed. The approach is built around the removal of the non-localized portion of the strain response. Keeping the localized portion of the strain response, which are not sensitive to nearby loads, allows for enhanced detection. The superiority of this approach stems from its capability to handle multiple-vehicle cases. These may present with an arbitrary number of trucks and light-weight vehicles, simultaneously passing the bridge in any arbitrary pattern or configuration. To show the applicability of the approach, a finite element (FE) model of a long-span concrete-box-girder bridge was simulated. The model was validated against the experimental data collected under known large events. The FE model was then used to consider single-truck events (for proof-of-concept) as well as complex

multiple-truck traffic cases. These included in-one-row trucks, zigzag patterns, side-by-side trucks, and a combination of several trucks with several light-weight vehicles present. The results demonstrated that the proposed BWIM approach is capable of detecting the axle weights and gross vehicle weight (GVW) of the traversing trucks. Based on all complex multiple-truck cases, the overall mean absolute errors for GVW and axle weight estimations were 4.5% and 11.3%, respectively.

### 3.1 Introduction

Deterioration by overloaded trucks can impose serious safety and structural issues and increase the risk of traffic accidents [75, 81]. Information about the traffic loads allows one to accurately evaluate the remaining service life [82]. In this regard, pavement-based weigh-in-motion (WIM) systems [78, 81, 83] have the potential to provide valuable information for traffic monitoring and weight enforcement [79]. This has been used in other areas as well. For instance, in a study conducted in 2017, a bridge health monitoring technique was proposed using interferometric radar sensors along with finite element modeling in conjunction with weight-in-motion (WIM) technology [84]. Merlynston Creek Bridge was used as a case study. While this study suggested an interesting technique, accurate interferometric radar sensors are usually expensive. Also, in general, pavement-based WIM systems use devices such as load cells, capacitance mats, bending plates, etc., which must be embedded in the pavement. This needs lane closure and causes traffic disruption during sensors' installation and maintenance and imposes some other issues such as sensors durability problem since they are exposed to tire impacts and harsh weather condition [63].

In contrast to previous techniques, bridge-weigh-in-motion (BWIM), first introduced by Moses [8], is a less intrusive solution which uses the bridge as a scale for weight estimation

using strain or acceleration measurements [11]. In BWIM approach, the truck speed, the number of axles, and the axle spacings should be obtained in advance to be later used for weight estimation. These parameters are called “Prerequisites” in this study. There are several prerequisite estimation methods in the literature, including traditional BWIM [10], contactless BWIM (cBWIM) [11, 12], and Nothing-on-Road (NOR) BWIM [13, 18–20]. In traditional BWIM, a set of axle detectors should be installed on the road surface, while in cBWIM, the axle detectors are replaced by one or two cameras. However, in NOR-BWIM (sometimes referred to as Free of Axle Detectors or FAD), nothing needs to be installed on the road surface; instead, a set of weighing sensors should be installed under the top slab. This resolves many issues associated with WIM and traditional BWIM systems such as lane closure and traffic disruption and provides a portable and even more affordable system.

In general, there are two categories for weight estimation methods: dynamic methods [23, 25, 27] and static methods [28–31]. Static methods are generally more suitable for real-time applications as, unlike the dynamic methods, they do not need a detailed finite element (FE) model; therefore, they are less computationally time-consuming. In static methods, by minimizing the error, which is the difference between the theoretical and measured responses, the influence line (IL) needs to be computed in advance using a truck with known prerequisites [33]. This procedure is known as “IL calibration”. Unlike the Moses method, which uses a theoretical influence line, there are some studies in which the influence line is experimentally obtained using crossing vehicles with known weight and strain responses [28–30, 34, 85]. In one of the recent studies, a novel regularization technique is proposed for IL extraction [85]. This novel regularization technique avoids filtering some important information and has a fast convergence speed.

Although BWIM is a powerful technique, weight estimation of multiple vehicles simultaneously on the bridge is still an active area of research. In fact, when multiple trucks are



simultaneously on the bridge, the standard BWIM methods are not able to properly decompose the strain responses associated with each truck. This causes overestimation of the trucks weights. There are only limited studies about multiple-truck presence. Current methods still require either time consuming IL calibration [71] or are applicable to a small set of possible traffic combinations [72]. The concept of influence surface instead of influence line was introduced for multiple-truck presence by Quilligan et al. [71] and was later used for other applications such as transverse position and others [82, 86]. Also, in a study conducted in 2021, an anti-noise regularization method was proposed for bridge influence surface extraction [87]. To evaluate the effectiveness of the method, a numerical model example and a laboratory experiment were provided. However, in the influence surface calibration procedure, series of transverse positions should be considered to cover all possible truck positions within two traffic lanes [73]. This makes it time-consuming and thus, less applicable for commercial applications. Also, during influence surface calibration, there should not be unwanted vehicles on the bridge. This can only be possible for short-span bridges with limited traffic volume. Additionally, it is computationally demanding since the system expands in both the number of equations and in complexity, and thus, linear methods cannot usually be used [73]. These disadvantages can become worse for bridges with multiple lanes in each direction.

In another study, a weight estimation procedure was proposed using a load distribution factor and considering how the truck weight is distributed between different lanes when it travels in a particular lane and on slab-on-girder bridges [72]. This was verified against a series of indoor experiments on only slab-on-girder bridges, showing that the method could work under the presence of only two vehicles in one row. Side-by-side and more complex traffic patterns were ignored. However, this can be a limitation for bridges with multiple lanes and dense traffic and leads to the selection of short-span bridges. For a multiple-lane bridge

with a large amount of traffic, the presence of multiple trucks combined with light-weight vehicles, arbitrarily distributed in different lanes, is very common.

Additionally, in the current literature about BWIM, most of the studies are performed on short-span bridges (span length < 20-30 m) [16, 62]. One of the reasons is to ensure that only one truck will be on the bridge during test and IL calibration. However, many long or medium-span bridges in the country are already instrumented for structural health monitoring (SHM) applications. Hence, the existing sensors can be used for traffic monitoring with no (or a little) additional cost if BWIM can quantify the weights of multiple trucks simultaneously on the bridge. This will also help to make the SHM more effective since multiple vehicles will make more deformation, and more useful SHM-related information will be obtained.

To address some of the limitations discussed above, in this study, a novel BWIM approach is proposed. The main advantage of this approach is that it successfully decomposes the strain responses of each vehicle in multiple-vehicle cases, with a combination of heavy and light-weight vehicles simultaneously on the bridge. The idea behind the approach is that it removes the non-localized portion of the strain response (later explained further), keeping only the localized peaks which are not sensitive to nearby loads. This approach only needs a single strain gauge per lane for weight estimation, thus making the system affordable significantly. This approach can also be used for more advanced BWIM systems such as NOR-BWIM.

Another main advantage of this approach is that even if the calibration truck (with known prerequisites) is surrounded by unwanted vehicles, unlike standard BWIM techniques discussed above, no lane-closure is needed for IL calibration, and the proposed approach can be used to successfully decompose the strain response associated with the calibration truck. This makes the system more cost-effective and safer and, as a result, more commercially

feasible.

To show the feasibility of the approach, a long-span bridge with three lanes in each direction was considered. Then, a finite element (FE) model of the bridge was made and validated against the experimental data (strain-time response) under known large events. In general, in heavy-traffic bridges, it is very difficult to control the traffic. Thus, the FE model was used to consider single-truck events (for proof-of-concept) as well as complex multiple-truck traffic cases, including in-one-row trucks, zigzag patterns, side-by-side trucks, and a combination of several trucks with several light-weight vehicles involved.

This paper is organized as follows: extensive details about standard BWIM and the proposed BWIM techniques are provided in Section 3.2. Section 3.3 introduces the finite element model of the bridge and how it is validated against experimental measurements of the actual bridge. Section 3.4 shows how the FE model is used for single and multiple-truck cases and with a general explanation about the suggested sensor placement. Also, the results are provided in Section 3.5. Finally, the main conclusions and future works are provided in Section 3.6.

## 3.2 Methodology

The weight estimation procedure has three steps. First, calculating the prerequisites, i.e., number of axles, speed, and axle spacing. This is explained in Subsection 3.2.1. Second, influence line extraction (IL calibration) using known trucks with known prerequisites. Three, using the extracted influence line and the computed prerequisites for weight estimation of unknown traversing trucks.

In this section, for steps two and three, two approaches are provided. 1) standard BWIM approach (explained in Subsection 3.2.2) which can be used for only one truck on the bridge.

2) the proposed BWIM approach for multiple-truck presence (explained in Subsection 3.2.3) which can handle multiple trucks simultaneously on the bridge.

### 3.2.1 Prerequisites' estimation approach

Prerequisites should be calculated using the physical distance between the successive sensors and the time delay between the peaks in the strain responses. The peaks are actually made due to a significant increase in the localized portion of the strains under the concentrated forces (axle weights). It is shown later in Subsection 3.5 that the strain response under a 5-axle truck passage, for instance, consists of five clear peaks when the sensors are placed in the right positions discussed in Section 3.4.1. This is equivalent to the number of traversing axles. In this study, the focus is weight estimation for multiple-truck cases, and it is assumed that the prerequisites were already computed properly. For further details on prerequisite computation, see two studies conducted by Deng et al. [20] and He et al. [18].

### 3.2.2 Standard BWIM approach

The first step in the weight estimation procedure is the influence line extraction from calibration data. In general, there are some studies that experimentally compute the influence line [28–30, 34]. Additionally, according to a comparative study conducted by Carraro et al. [35], maximum likelihood estimation (MLE) is the most accurate method, and this is why the MLE method is the one used as the standard weight estimation approach.

MLE method was first proposed by Ieng [34]. This method takes multiple truck passages into account, considering the variability of the effects of the calibration vehicle on the bridge. Then, the extracted influence line will be used to estimate the weight of unknown trucks using the Moses method [8] shown in Equation (3.1). In Equation (3.1),  $W$  is a vector

consisting of the unknown axles weights, and  $B$  is a matrix created using the influence line ordinates, shifted based on the truck axle spacings to adjust the time-instant when each truck axle enters and leaves the bridge structure. Also,  $M^m$  is the measured strain vector.

$$W = (B^T B)^{-1} B^T M^m, \quad (3.1)$$

As mentioned earlier, standard BWIM approaches (including MLE) are not able to properly decompose the strain responses associated with each truck. This causes overestimation of the trucks weights. Thus, they can be used for only one truck on the bridge.

### 3.2.3 Proposed BWIM approach for multiple-truck presence

The novel BWIM approach is proposed here to handle multiple-truck cases with arbitrary traffic patterns, consisting of multiple trucks and light-weight vehicles involved. When the bridge is subjected to a truck load that is right on top of the sensors, the strain response under the truck tires consists of two components that should be superposed together: 1) the strain of the entire bridge span (acting as a beam) due to the internal moments which appears as slowly changing compression in the top slab and 2) additional strain due to the top plate/slab bending (plate behavior) which appears as sharp peaks in tension corresponding to axle crossings. These two strain portions are called localized and non-localized strains. As long as the load is not significant (such as traffic load) to make the material nonlinear, both terms will be linear and thus, BWIM theory can be used.

In this study, the proposed approach first properly decomposes the strain responses associated with each truck in multiple-truck strain responses. To do this, a curve should be fitted to the non-localized portion of the response (later explained in detail). The non-localized

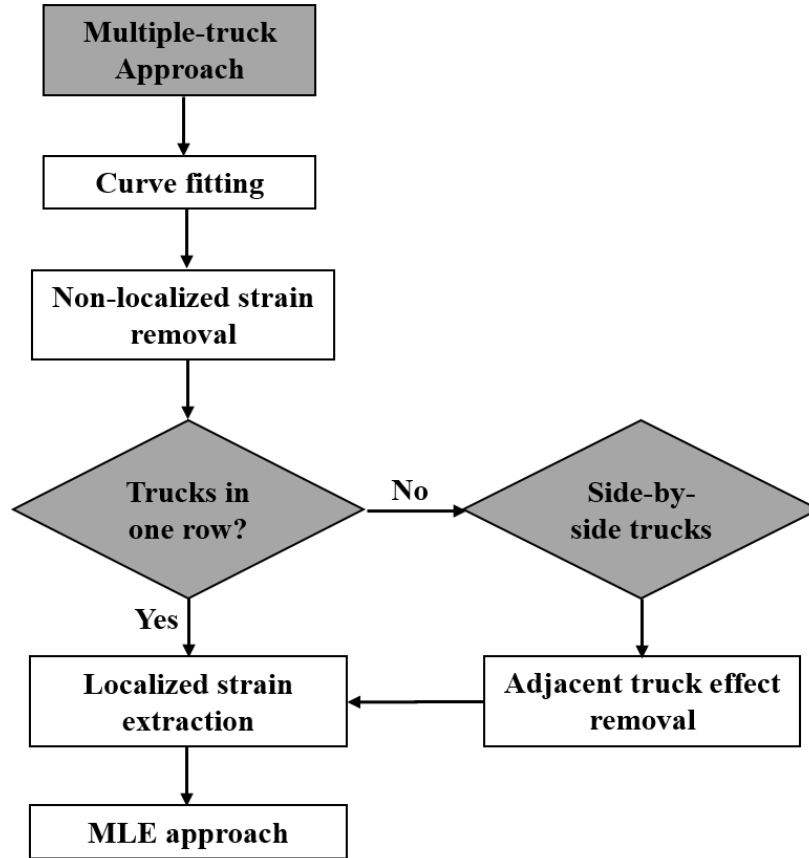


Figure 3.1: A flowchart for the proposed BWIM approach steps

portion will be removed by subtracting the fitted curve from the original strain response. Then, the strain response associated with each truck will be extracted and fed into the standard BWIM procedure. In fact, the proposed approach has one additional step (strain decomposition) before the steps explained in the original studies for standard BWIM methods [35]. It should be noted that if there is any side-by-side truck, its effect should properly be removed (later explained in detail) before the strain response extraction for each truck. These steps are shown in Figure 3.1.

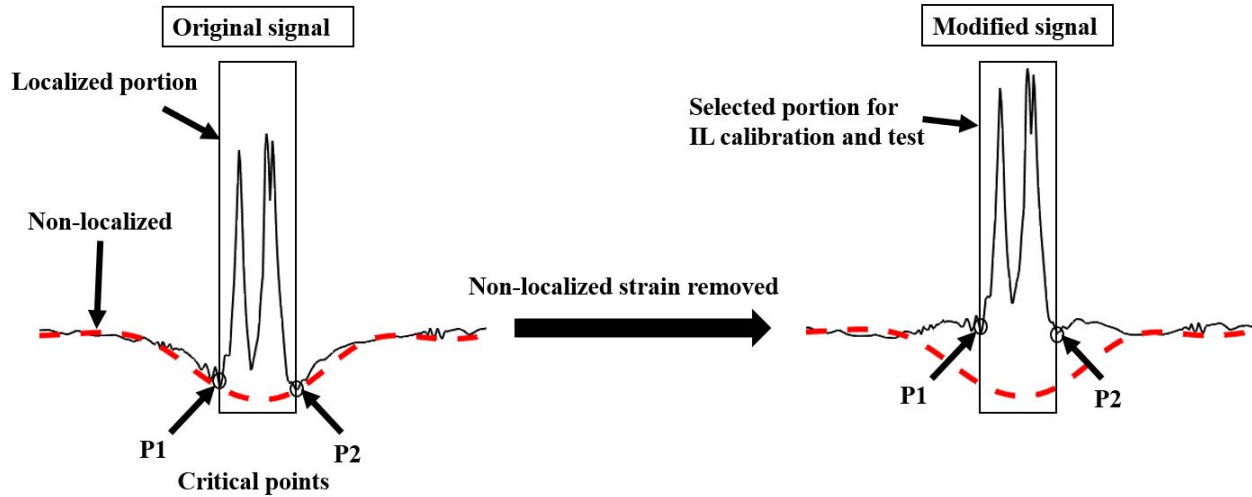
For one single-lane weight estimation, only one influence line is needed (similar to standard BWIM methods). However, for multiple-lane highways, multiple influence lines are needed (one for each). The advantage of this approach is that no lane closure is needed for IL

calibration to ensure that only one truck is on the bridge during calibration. This is because even if the calibration truck (with known prerequisites) is surrounded by unwanted vehicles, the proposed approach can still be used to decompose the localized strain response associated with the calibration truck. Then, the decomposed strain responses will be used for influence line extraction, similar to standard BWIM methods.

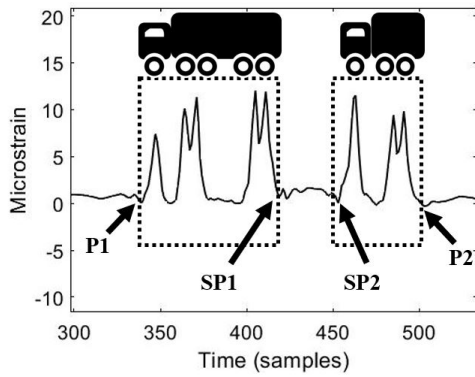
Here, the decomposition procedure is explained. According to Figure 3.2a (left side), a strain-time response extracted from a single-truck passage includes two portions: 1) localized portion under traversing axle weights, and 2) non-localized portion (dashed curve). The difficulties in processing strain-time responses for a multiple-truck case compared to a single-truck case are due mostly to distortions of the non-localized portion. In fact, a multiple-truck case will result in a deeper non-localized response than a single-truck case but with a similar localized strain portion. In the following, the proposed approach steps to decompose the strain responses under multiple trucks simultaneously on the bridge are explained.

In the first step to decompose the strain responses associated with each truck in a multiple-truck event, points  $P_1$  and  $P_2$ , called “critical points” in Figure 3.2a, should be calculated. These points should be selected approximately where the localized strain portion starts and ends. In this study,  $P_1$  and  $P_2$  were defined at 0.16 second before the first peak and 0.20 second after the last peak, respectively.

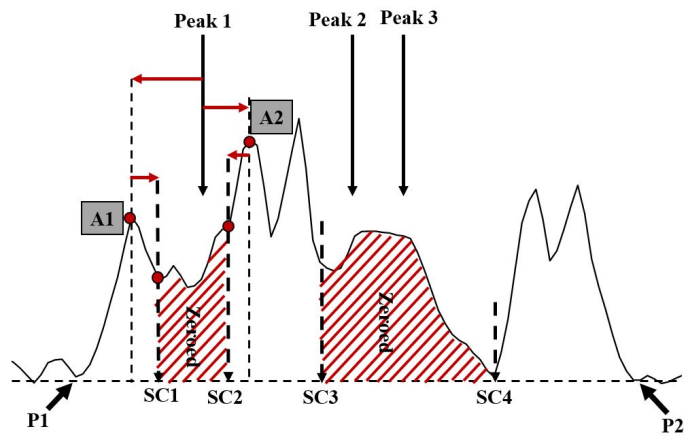
In the second step, a curve (dashed curve) should properly be fitted to the non-localized portion of the response. Then, the fitted curve should be subtracted from the original strain response to remove the non-localized portion to only keep the localized strain portion (modified response). This curve should meet a few requirements to provide satisfactory results: 1) for both single and multiple-truck cases, the curve should touch points  $P_1$  and  $P_2$  in Figure 3.2a such that when the non-localized portion of the strain is removed,  $P_1$  and  $P_2$  will be equal to a number close to zero (less than about 0.3 microstrain, for instance), 2)



(a) Single-truck cases



(b) In-one-row cases (non-localized strain removed)



(c) Side-by-side cases (non-localized strain removed)

Figure 3.2: The proposed BWIM approach



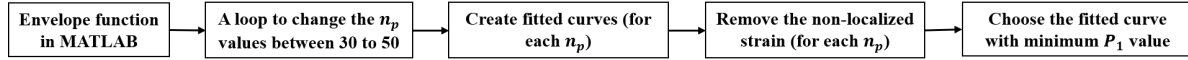


Figure 3.3: A flowchart for the best envelope fit

the curve should be a lower convex envelope between  $P_1$  and  $P_2$  such that for multiple-truck cases, majority of lower peaks between  $P_1$  and  $P_2$  should also be touched (see Figure 3.11a). An “envelope function” [88] can be used for this purpose. Envelope of a signal is a curve, smoothly connecting the maximum and minimums [88]. The outcome of an envelope function is two curves tangential to the input signal local minimums and maximums. However, only the lower envelope should be considered and the upper envelope should be discarded.

The envelope function can be used in any programming environment. In this study, it was found that the “Envelope” function in MATLAB can successfully satisfy these requirements when a proper “peak separation factor ( $n_p$ )” is selected. The envelopes are computed using spline interpolation over local minimums separated by at least  $n_p$  samples. The MATLAB code prepared for this study automatically checks different  $n_p$  values between 30-50 (found as the most effective range) and chooses the one that generates an envelope with smallest difference from  $P_1$ . To do this, a loop was programmed that changes the  $n_p$  value in each step and chooses the one with the lowest generated  $P_1$  in the modified strain response (the non-localized response removed). It was observed that, through this procedure, the generated lower convex envelope curve between the critical points will be automatically generated and satisfies other requirements explained above. A flowchart is presented in Figure 3.3 to show these steps clearly.

It should be noted that other than the envelope function, two other techniques were also considered in this study while they did not work as properly as the envelope function technique to flatten the strain response (to remove the non-localized strain). These techniques included: 1) Manual fitting process that needs the user to manually build the curve in a trial

and error process to find the best fit that generates  $P_1$  and  $P_2$  values close to zero when the non-localized response is removed. Thus, it can never be used for a large number of events. Also, the accuracy of the results can differ depending on the user's accuracy. 2) High-pass filter with a small cut-off frequency selected based on the Fast Fourier Transform (FFT) of the strain response. However, it was found that the high-pass filter technique can flatten the strain response but distorts the localized portion of the response.

The third step is localized strain extraction. In this step, a small portion of the modified response, shown on the right side of Figure 3.2a, should be selected to be used for IL calibration or test. For single-truck cases, this simply is the portion between  $P_1$  and  $P_2$  (already defined). However, the procedure is slightly different for multiple-truck cases. Multiple truck cases are either in one row, side-by-side, or a combination of these cases. For in-one-row multiple-truck cases (e.g., for a 5-axle and 3-axle truck shown in Figure 3.2b), some secondary points, e.g.,  $SP_1$  and  $SP_2$ , should be selected in a way similar to the critical points. For instance,  $SP_2$  is located in 0.16 s before the first peak in the response associated with the 3-axle truck and  $SP_1$  is in 0.20 s after the last peak of the 5-axle truck. This procedure helps to decompose the strain responses for even closely moving trucks in one row. To know when a truck ends and the other starts in Figure 3.2b, a proper threshold for the maximum axle spacing should be determined. When the distance between  $SP_1$  and  $SP_2$  exceeds from the threshold, the strain associated with the second truck starts. This threshold should statistically computed based on the traversing trucks (7 m in this study per Table 3.3).

For a case with two trucks moving side-by-side in two adjacent lanes, one additional step is needed between steps two and three explained above. This additional step is to remove the effect of the adjacent truck from the recorded strain-time response before feeding it into the proposed procedure. As it is later explained in Section 3.5, when a truck moves on a particular lane and the strain response is recorded on the same lane, sharp peaks will be

obtained if a proper sensor placement, explained in Subsection 3.4, is employed. However, the strain response from the other lane will be distorted. This is clearly shown in Figure 3.2c. This is the strain response for a 5-axle and 3-axle trucks moving side-by-side on lanes one and two, respectively, and the strain response is extracted from lane one. According to this figure, the strain response is a combination of clear and distorted peaks. However, only the clear peaks should be kept and the remaining should be properly removed for weight estimation.

To remove the adjacent truck effect, first the sample numbers of the peaks in the 3-axle truck strain response (from the second lane) should be manually obtained. Then, using the extracted sample numbers, the position of them should be found on the strain response extracted from the first lane. These are shown in Figure 3.2c (Peak 1, Peak 2, and Peak 3). Then, these peak points (Peak 1, Peak 2, and Peak 3) should be used as a reference to find four other points (e.g.,  $SC_1$ ,  $SC_2$ , etc.), which show the area that should be removed. For instance from Peak 1, one should move back and forward to find points  $A_1$  and  $A_2$ , which are the closest peaks of the 5-axle truck in its strain response. Then, moving from points  $A_1$  and  $A_2$  on the 5-axle truck strain response towards Peak 1,  $SC_1$   $SC_2$  will be obtained. These are where an abrupt change is made in the slope of the graph ( $>50\%$ ). The portion between these points should then be set to zero. The same procedure should be performed for Peaks 2 and 3 in Figure 3.2c to find the second portion that should be zeroed (between  $SC_3$  and  $SC_4$ ). A flowchart is presented in Figure 3.4 to show these steps clearly. The reason why this area should be set to zero is that when one of the axles is right on top of the place where the strain response is extracted (for in-one-row events with no side-by-side trucks), a clear peak appears; however, immediately after that, the strain response goes to zero. This is clearly shown later in Figure 3.11.

Now that the the adjacent truck effect (distorted responses) is removed, using the  $P_1$ ,  $P_2$

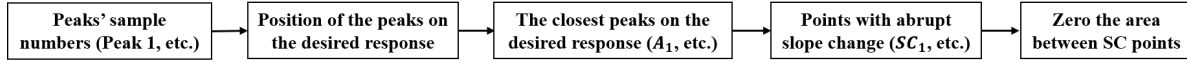


Figure 3.4: A flowchart for the adjacent truck effect removal

(already defined), the localized strain portion associated with the 5-axle truck should be selected. Other more complex traffic patterns. e.g., zigzag, etc., can also follow the same steps explained for in-one-row and side-by-side cases as they are a combination of these two cases.

The fourth step is to feed the decomposed strain responses to MLE. All steps of the proposed approach are shown in Figure 3.1 for clarity.

As a last point in the methodology, it should be mentioned that another advantage of the proposed BWIM method compared to the standard BWIM method is its capability of dealing with variable speeds. As explained above, the proposed method first decomposes the strains associated with each truck using the envelope function. This function is not dependent on the speed as it is just a mathematical operation. Once the strains are decomposed, they will be used for weight estimation using the standard BWIM and Moses method. The assumption of standard BWIM is that the speed of each individual truck is constant when it passes over the weighing sensor. In the standard BWIM method, this takes 3-4 s or even longer (depending on the truck length and speed) since this method takes the entire strain response (both localized and non-localized portions of the response) into consideration, while for the proposed method it takes only 0.5-0.9 s as the method considers only the localized portion of the response. Thus, it is quite reasonable for the proposed method to say that the truck speed will remain constant in 0.5-0.9 s. This can be considered another advantage compared to the standard BWIM that considers a longer strain response where the truck speed is not guaranteed to remain constant.

## 3.3 Numerical Study and Experimental Validation

### 3.3.1 Bridge description

The Varina-Enon bridge (VEB), shown in Figure 3.5, is a cable-stayed, post-tensioned, concrete-box-girder bridge, along Interstate 295 and over James River in Virginia with significant traffic flow. As shown in Figure 3.5a, the total length of the bridge is 1426.5 m with twenty-eight spans. The main span (cable-stayed portion) consists of seven spans (13 to 19) with a total length of about 466 m. Furthermore, the south end of the bridge (left side in Figure 3.5a) consists of two approach units (six 45.72-m spans each) while the north end (right side of the figure) includes two additional approach units, one with five and the other with four 45.72-m spans. Also, as shown in Figure 3.5b (taken using a lidar scanner), there are eight external, post-tensioning tendons in each span of the approach units (four on the right side and four on the left side). Each tendon consists of nineteen 0.6-in-diameter strands.

According to Figure 3.5c, the total width of the top slab is approximately 17.62 m, including three lanes (3.66 m each), and the two shoulders, which are 3.52 m and 3.12 m. The trapezoidal-shape concrete box has a total height of about 3.66 m, with top and bottom slabs' depths of about 0.25 m (plus 5 cm topping) and 0.2 m, respectively. Figure 3.5c shows the typical box dimensions for all spans; however, for two of the south spans (14 and 15) and two of the north spans (17 and 18), the boxes are tied together at each cable anchorage point by a delta frame. Since the focus of this study is span 6, the typical delta frame is not shown for conciseness.

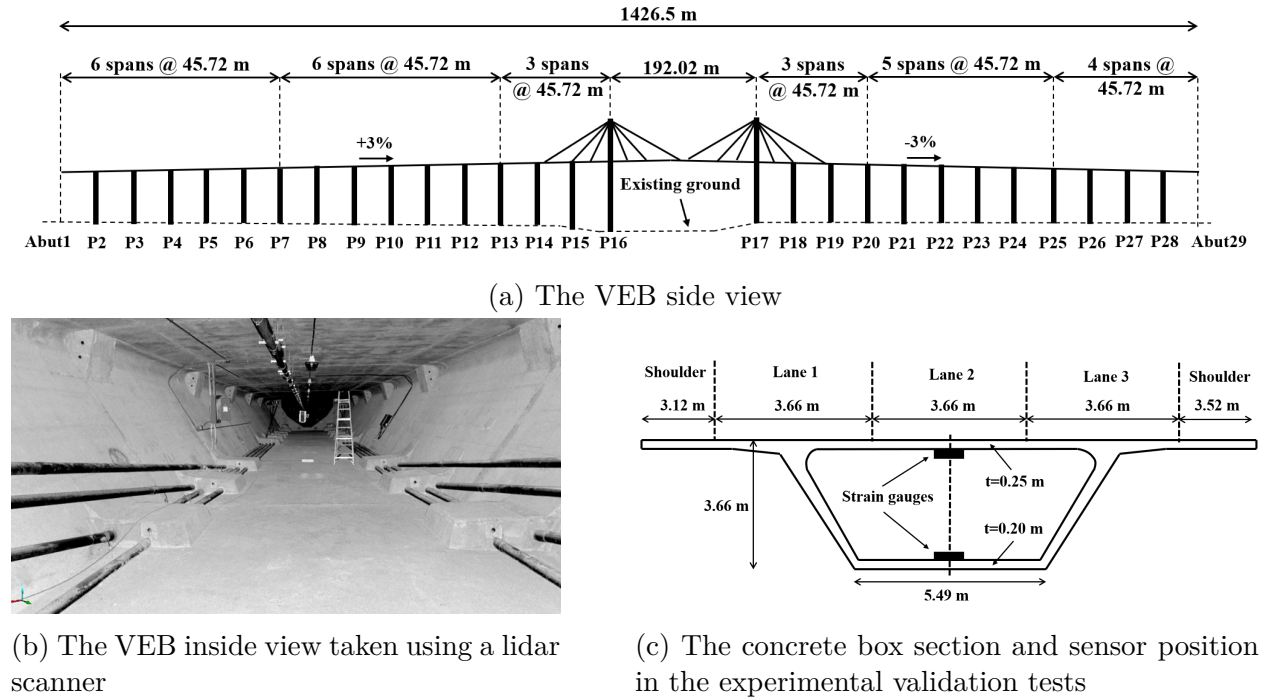


Figure 3.5: The Varina-Enon bridge (VEB)

### 3.3.2 Finite element model

In this study, CSI Bridge was used to create a 3-D finite element model of three spans (5 to 7) of the VEB. These spans are significantly far from the cable-stayed portion, and therefore, the cable stays were ignored and only the external tendons were modeled. As explained in Subsection 3.3.1, in each span, there are eight tendons (four on the right side and four on the left side). Each tendon consists of nineteen 0.6-in-diameter strands. These were explicitly modeled with two equivalent tendons (one on the right side and one on the left side) with equivalent areas. Other important bridge components such as bridge bearings should also be modeled [32]. According to the bridge shop drawings, the bearings for different piers are not the same. These bearings have different lengths, widths, and heights. In this model, we assumed that the bearings are all the same (for simplicity) and we assigned the bearing of Pier 6 to all other piers. This is because it was observed that changing the stiffness values

of the bearings does not significantly change the strain responses. In this model, each span is supported by two square-shaped (91 by 91 cm) elastomeric bearings whose geometries are shown in Table 1 (Pier 6 bearing). The bearings are modeled as elastic springs in vertical, horizontal, and rotational directions with stiffness values of 5456605 KN/m, 5010 KN/m, and 185776 KN.m/m, respectively. Appendix A shows the computation details.

Table 3.1: The bearings geometries

Length (cm)	Width (cm)	Total height (cm)	Total elastomer thickness (cm)	No. of layers	No. of plates	Steel plates thickness (mm)
91.4	91.4	13.5	11.4	10	9	1.6 (middle), 4.8 (other)

Because there was no evidence about the concrete strength and core test was not possible, the value 50 Mpa (7500 psi) was chosen through iteration to match the results of experimental measurements, explained further in Subsection 3.3.3. A general overview of this model is shown in Figure 3.6. In this model, eight-node solid elements were employed for the box girders and piers. Also, the piers, with a cross section of about 5.5 by 2.5 m and height of 34 m, were fixed to the ground. A general maximum mesh size of  $2.9 \times 1.2 \times 0.1$  m, in longitudinal, transverse, and depth directions, respectively, was selected. However, as shown in Figure 3.6, the mesh size was significantly refined around the sensor positions, i.e., throughout the concrete box and in a width of 3.6 m around the sensor positions, to a maximum size of  $0.2 \times 0.4 \times 0.1$  m. Then, the mesh sizes were evaluated through a mesh sensitivity analysis to ensure that the results are not dependent on the selected mesh sizes.

As shown in Figure 3.5c, two strain measurement points were selected, at the bottom of the top slab and on top of the bottom slab in 18.3 m from Pier 7 of the bridge (in span 6). To obtain the strain-time response under the traversing trucks, a time-history analysis was performed. Then, strain-time responses were simulated at desired points with a sampling rate of 33 Hz.

Additionally, the strain responses were extracted under two large truck crossing events. These events mirrored a set of experimental tests performed on the VEB in 2020. These are explained later in Subsection 3.3.3. To model the lanes (lanes 1,2, and 3), three centerlines (one for each lane) were defined with proper offsets from the longitudinal centerline of the bridge. Then, the lane width of 3.66 m was assigned to each lane centerline. The model dimensions match the actual structures.

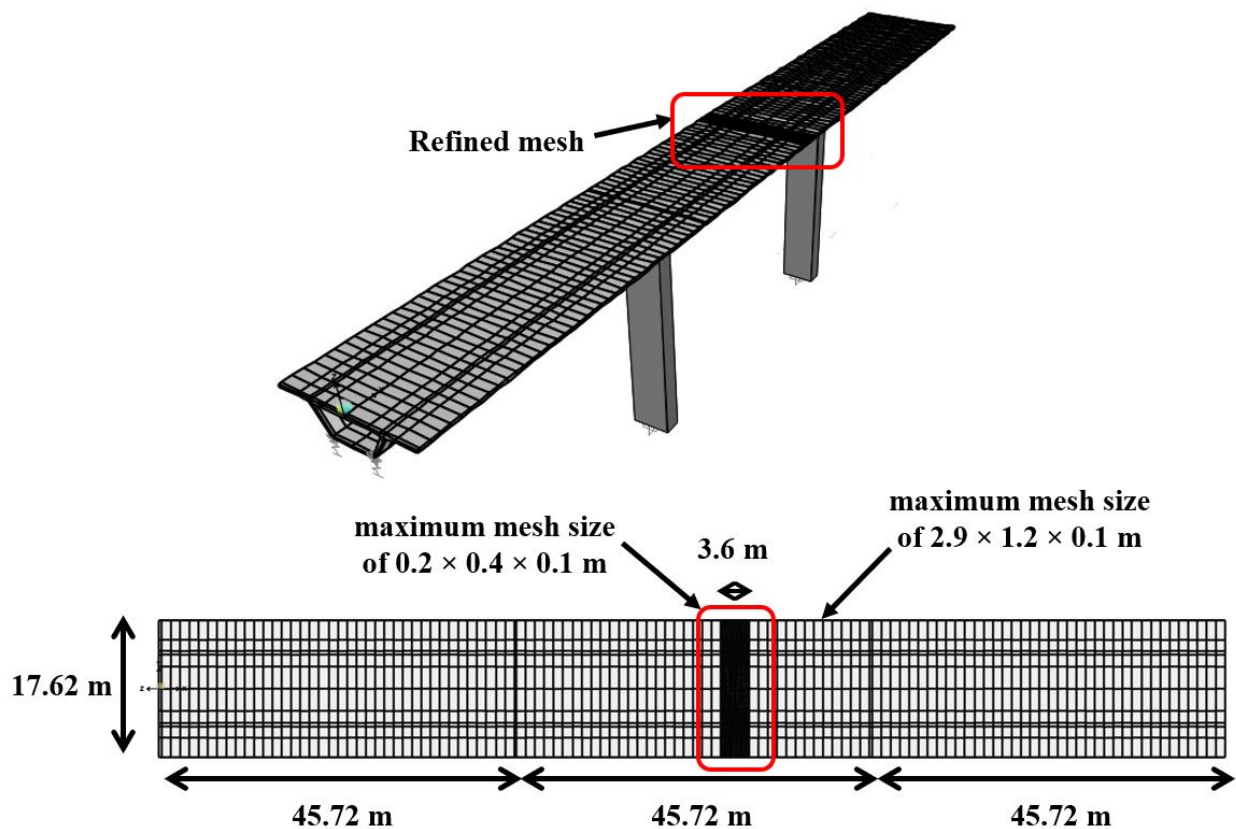


Figure 3.6: An overview of the finite element model

### 3.3.3 Experimental validation

To validate the FE model, experimental strain-time measurements, conducted on the VEB in 2020, were used. The responses (with a sampling rate of 33 Hz) were extracted at similar



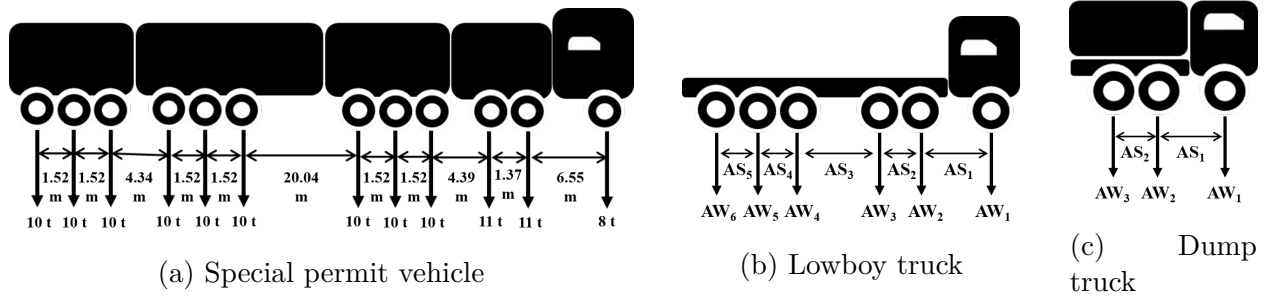


Figure 3.7: Trucks used for FE model validation (Table 3.2 shows the details of figures b and c)

locations shown in Figure 3.5c during large events' crossings. It should be noted that strain response is a very common response used for BWIM techniques. So, it was aimed to ensure that the strain response generated by the numerical model is fairly realistic and comparable with the strain response recorded on the actual bridge. That is why the strain response was the main factor for bridge model validation. It should be noted that the experimental data was only used to validate the FE model and for the rest of the process (weight estimation), the model is used to generate data.

There were two large events in the experimental tests. The first event was a special permit vehicle, crossing over the second travel lane. All axle weights and axle spacings are shown in Figure 3.7a. The second event was a superload test, with two lowboy trucks and two dump trucks, simultaneously crossing the VEB. Figures 3.7b and 3.7c show the general configurations for these truck types and more details are provided in Table 3.2. In this test, the two lowboys were on the third and second lanes and side-by-side to the two dump trucks traveled as close together as possible on the first lane.

Table 3.2: Trucks' information for FE model validation in superload test (for Figures 3.7b and 3.7c)

Truck label	Truck name	No. of axles	Axle weight (ton)						Axle spacing (m)				
			AW <sub>1</sub> <sup>a</sup>	AW <sub>2</sub>	AW <sub>3</sub>	AW <sub>4</sub>	AW <sub>5</sub>	AW <sub>6</sub>	AS <sub>1</sub> <sup>b</sup>	AS <sub>2</sub>	AS <sub>3</sub>	AS <sub>4</sub>	AS <sub>5</sub>
A	Lowboy 1	6	6.20	10.95	10.75	8.60	8.70	8.60	4.80	1.40	11.48	1.42	1.42
B	Lowboy 2	6	6.20	12.85	13.20	9.05	8.80	8.75	1.65	1.52	11.28	1.37	1.37
C	Dump 1	3	7.55	8.60	8.40	N/A	N/A	N/A	4.72	1.37	N/A	N/A	N/A
D	Dump 2	3	7.60	8.65	8.75	N/A	N/A	N/A	4.88	1.52	N/A	N/A	N/A

<sup>a</sup>AW=Axle weight, <sup>b</sup>AW=Axle spacing

The main purpose of this stage was to validate the FE model such that it provides similar general shapes for strain-time responses when it is under the same load, reasonable magnitudes (minimums and maximums), and captures the localized strains under the axles weights. According to Figure 3.8, these requirements are satisfied, and experimental and numerical strain-time responses are in good agreement.

Also, in the experimental tests, there was no clear evidence about the trucks' speeds. Different speeds in the FE model than the tests stretch or compress the numerical strain responses if the trucks' speeds are assigned smaller or larger than the tests, respectively. To avoid this, in the FE model, the speeds were gradually changed until the time interval between the first and last peaks in Figures 3.8a and 3.8c became the same. Then, other peaks were automatically matched together.

According to Figure 3.8, despite a great match between experimental and numerical results, there are some discrepancies between them. These can be due to several reasons, including the slight difference in material properties (reported in design plans vs. actual material), different actual topping thickness than the design plans, different bridge dimensions than the design plans. This can also be due to additional sources of error that are expected in an experimental setting, such as different trucks' transverse positions in the tests, different weights than the reported ones, different axles' configurations, etc. However, this model and the extracted strain-time responses were used for weight estimation. The discrepancies will not make any issue for it as long as the general shape and magnitudes are realistic. This is because both the IL calibration procedure (influence line extraction) and tests were done using the same model outputs.

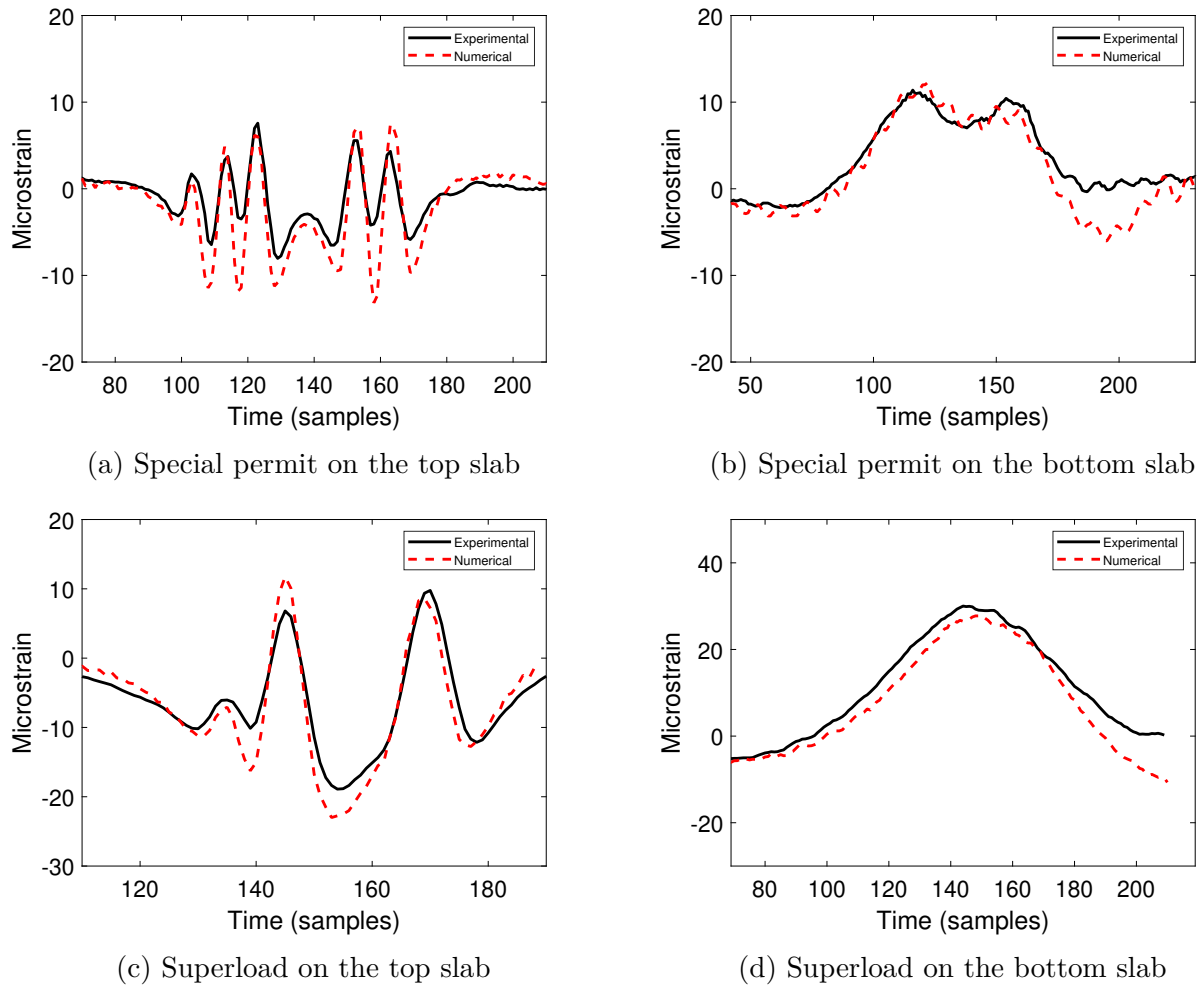


Figure 3.8: The FE model validation results

### 3.4 Single and Multiple-truck Cases

In an actual situation, it is usually very challenging to control the traffic (without lane closure) to consider desired traffic load patterns with multiple trucks involved. Thus, in the rest of this study, the validated FE model was used to resolve this issue. In fact, this model enabled the consideration of complex traffic patterns and provided realistic strain-time responses. However, for the remainder of the paper, sensor positions, sampling rate, and the vehicles used for weight estimation are different than model validation section. These are

described in the following subsections.

Also, before going through complex traffic patterns (Subsection 3.4.3), as a proof-of-concept, it was first needed to show that the proposed approach, explained in Section 3.2, works for single truck passages on lanes one or two. Subsection 3.4.2 is provided for this purpose.

### 3.4.1 Sensor position for weight estimation

To arrange a suitable sensor position for weight estimation, two assumptions were made. First, according to Virginia Code Title 46.2 (as defined in §46.2-341.4), when the posted speed limit is at least 65 miles per hour (104.6 km/h), no commercial motor vehicle should be driven on the left-most lane of any interstate highway with more than two lanes in each direction [89]. This includes the Varina-Enon bridge as well. Thus, only the rightmost two lanes were considered for IL calibration and testing.

Second, according to a survey conducted by Berard and Bourion [90], the average width of heavy trucks is 2.52 m, with 90% percent of them (approximately) within the range of 2.5 to 2.6 m. Also, according to the federal size regulations for commercial motor vehicles [91], the maximum width of commercial trucks is 2.6 m. Thus, as shown in Figure 3.9, for a standard lane width of 3.66 m (12 ft) and for a mean truck width of 2.52 m, the trucks' transverse position variability is going to be at most 57 cm if the strain gauges are placed in 57 cm from the pavement markings (at mid-span). This sensor placement (Figure 3.9) enables one to capture most of the localized portion of the strains under the trucks' tires. Thus, the strain response is expected to consist of clear peaks, and a slight change in trucks' transverse positions (within a range of  $\pm 57$  cm) should not damage the peaks' clarity. The results are shown later in Section 3.5. Also, for the rest of this paper, i.e., weight estimation for single and multiple-truck cases, the sampling rate is 100 Hz. This is different from the sampling

rate for model validation (33 Hz).

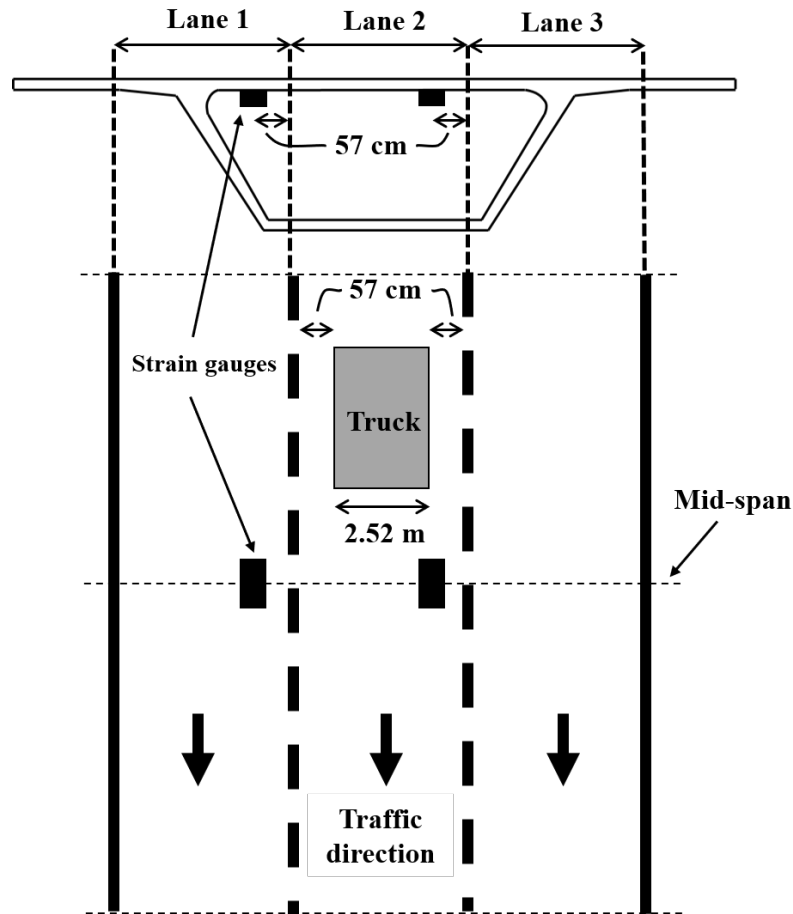


Figure 3.9: Sensor positions for weight estimation

### 3.4.2 Single-truck cases

As mentioned earlier, it was first needed to compare the weight estimation results from the proposed BWIM approach with standard BWIM methods (as a proof-of-concept) for single-truck cases. For both the standard and proposed approaches, two separate influence lines, i.e.,  $IL_1$  and  $IL_2$ , were extracted for lanes one and two. This was done using Truck 1 in Table 3.3 (different than the validation trucks) with multiple passages in different transverse positions. Once the influence lines were obtained, Trucks 2 through 6, introduced in Table

Table 3.3: Trucks' information for weight estimation (single and multiple-truck cases)

Truck no.	No. of axles	Axle weight (ton)					GVW (ton)	Axle spacing (m)			
		AW <sub>1</sub> <sup>a</sup>	AW <sub>2</sub>	AW <sub>3</sub>	AW <sub>4</sub>	AW <sub>5</sub>		AS <sub>1</sub> <sup>b</sup>	AS <sub>2</sub>	AS <sub>3</sub>	AS <sub>4</sub>
1	3	8.2	7.5	7.5	N/A	N/A	23.2	4.60	1.25	N/A	N/A
2	3	9.1	7.1	7.1	N/A	N/A	23.3	4.50	1.31	N/A	N/A
3	5	4.5	7.1	7.1	7.1	7.1	32.9	3.35	1.22	6.71	1.22
4	5	6.2	8.0	8.2	8.0	8.2	38.6	3.40	1.31	6.78	1.31
5	4	5.1	8.3	8.3	10.4	N/A	32.1	3.60	1.20	6.60	N/A
6	4	5.3	7.0	7.0	8.5	N/A	27.8	3.70	1.32	7.00	N/A

<sup>a</sup>AW=Axle weight, <sup>b</sup>AW=Axle spacing

3.3, were passed one by one on the first and second lanes, and ten strain-time responses (five for each lane) were obtained. In the last step, two different approaches (the standard BWIM and proposed BWIM), discussed in Section 3.2 were applied, and axle weights and GVWs were computed. Then, the results were compared together shown in Section 3.5.

### 3.4.3 Multiple-truck traffic patterns

Once it is proved that the proposed BWIM approach works for single-truck cases, more complex traffic patterns should also be tested. As shown in Figure 3.10, six different traffic patterns with multiple simultaneous vehicles' presence (trucks and light-weight vehicles) were considered for multiple-truck cases. These traffic patterns were including two in-one-row cases (Figures 3.10a and 3.10b) with a 5-axle and a 3-axle trucks, two zigzag cases with three 3-axle trucks (Figures 3.10c and 3.10d), a zigzag case with two 3-axle trucks and a 5-axle truck on the first two lanes and two light-weight vehicles on the third lane (Figure 3.10e), and a side-by-side case with a 5-axle and a 3-axle trucks on the first and second lanes, respectively. In all cases, the 3-axle and 5-axle trucks were Trucks 2 and 4, respectively, described in Table 3.3. Also, the light-weight vehicles were both a 2-axle vehicle

with axle spacing of about 4 m and equal axle weights of 0.6 ton (GVW=1.2 ton).

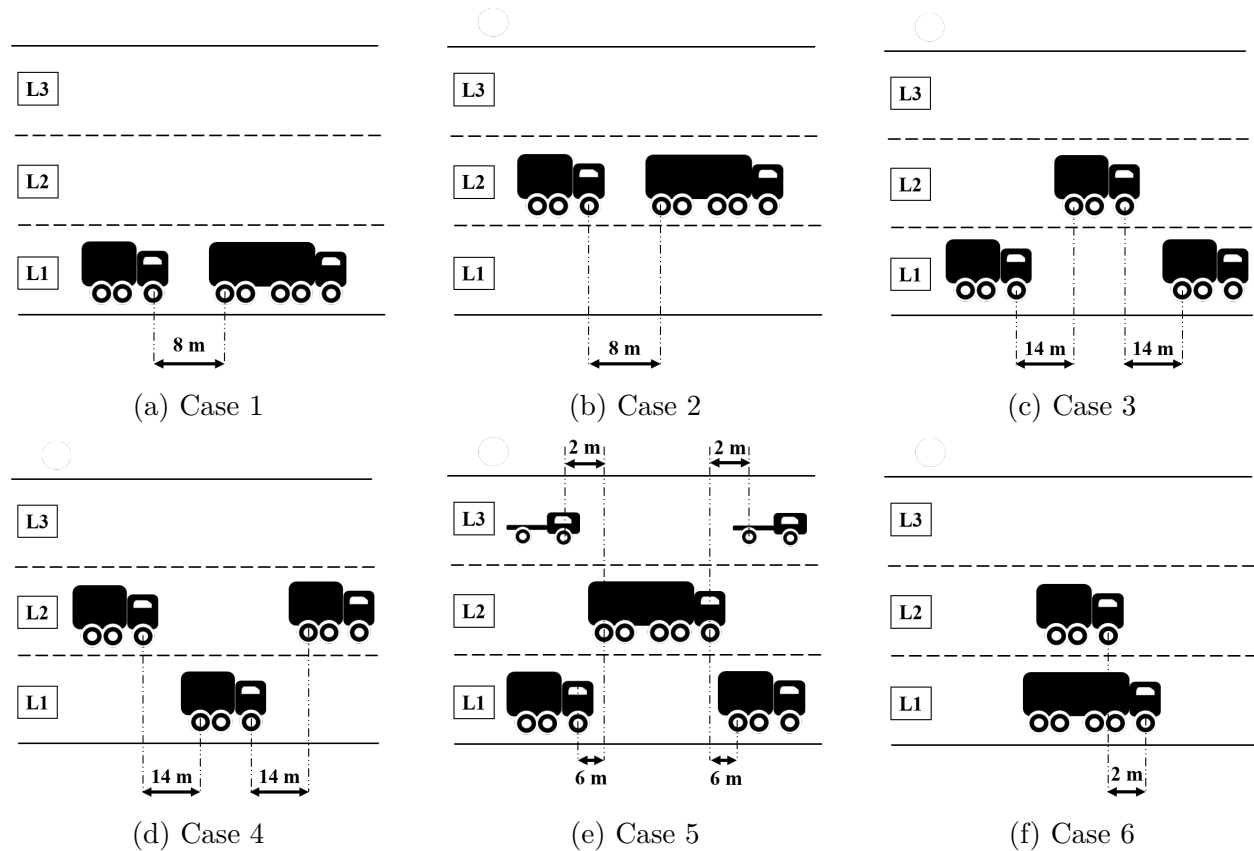


Figure 3.10: Multiple-truck cases (the 3-axle and 5-axle trucks are Trucks 2 and 4 described in Table 3.3)

## 3.5 Results

### 3.5.1 Single-truck cases

Before considering the multiple-truck cases, it was first needed to compare the performance of the proposed approach with the standard BWIM method in single-truck cases. This is to ensure that the non-localized strain removal does not sacrifice the accuracy of results much (the accuracy reduction is in a reasonable range). Hence, ten strain-time responses



were obtained for Trucks 2 through 6, introduced in Table 3.3 (for each truck two responses, one in lane one and another one in lane two). As mentioned earlier, Truck 1 was used for influence line extraction. Then, the standard BWIM and proposed BWIM, discussed in Section 3.2, were applied to the responses.

The estimated axle weights, estimated GVW, and their associated errors are shown in Table 3.4 for both approaches and lanes. According to this table, overall, the proposed approach improved the GVW estimation compared to the standard approach. The mean absolute errors (MAE) of the axle weights and GVW estimates for the standard approach were 4.1% and 4.8%, respectively, when the truck was on lane one. These errors were 2.2% and 7.4% for the same lane but the proposed approach. Additionally, MAEs of the axle weights and GVW estimates for lane two and the standard approach were 4.8% and 6.5% versus 2.4% and 10.6% for the same lane but the proposed approach. Hence, as mentioned above, the proposed approach improved the GVW estimation accuracy by 1.9% and 2.4%, respectively, for lanes one and two; however, it reduced the axle weight estimation accuracy by 2.6% and 4.1%. This increase in axle weight estimation error can be ignored since the GVW estimation accuracy is improved and multiple-truck weight estimation is enabled (discussed in Subsection 3.5.2). Also, axle weight errors are still in a reasonable range. Thus, one can conclude that removing the non-localized strain does not eliminate much important information.

Overall, for both standard and proposed approaches, the average absolute errors of GVW and axle weight estimates were greater for lane two than lane one. However, the errors' magnitudes are not consistently greater for all trucks in lane two than lane one. In this study, two main factors were detected for variability in errors. 1) Similarity of the characteristics of the test and calibration trucks: it was observed that the error is close to zero when the same truck is used for both IL calibration and test. However, when the test truck characteristics

(e.g., axle spacings, number of axles, etc.) are different from the calibration truck, both standard and proposed techniques are still capable of generating a strain response with great match with respect to the original one, but with more dispersion (compared to the case with the same test and calibration trucks). When the reconstructed strain is consistently above/under the original strain, a larger positive/negative error will result for both GVW and axle weight estimates. However, when at some points, it is above and at other points it is under the original response, the positive and negative GVW errors cancel out each other, and a small GVW error (close to zero) will result, but still, large axle weight errors are likely (depending on the level of dispersion). 2) The effect of smoothing technique for different strain responses: in this study, it was confirmed that the errors would be overall smaller when the strain responses are smoothed using “Symlets Wavelet” (sym4 with a level of wavelet decomposition of 2 in MATLAB). However, as mentioned earlier, its effect can still be variable for different responses.

In short, the errors due to these two factors can be cumulative (for the same error sign) or balancing (for opposite error signs). This is why different errors with different signs and values are observed from case to case and lane to lane.

Table 3.4: The results of the single-truck cases

App. <sup>a</sup>	L. <sup>b</sup> no.	Ax. <sup>c</sup> no.	Truck 1		Truck 2		Truck 3		Truck 4		Truck 5		Ave. err.* GVW <sup>f</sup> (%)	Ax. (%)
			Est. <sup>d</sup> (ton)	err. <sup>e</sup> (%)	Est. (ton)	err. (%)	Est. (ton)	err. (%)	Est. (ton)	err. (%)	Est. (ton)	err. (%)		
		1	8.98	-1.3	4.32	-4.0	6.01	-3.1	4.14	-18.8	4.89	-7.8		
		2	7.16	0.9	6.79	-4.3	8.08	1.0	8.56	3.1	6.77	-3.2		
Std. <sup>g</sup>	1	3	6.63	-6.6	6.85	-3.6	8.02	-2.3	6.67	-19.6	6.53	-6.7	4.1	4.8
		4	N/A	N/A	7.11	0.1	7.84	-2.0	9.52	-8.5	8.44	-0.7		
		5	N/A	N/A	6.90	-2.8	8.14	-0.7	N/A	N/A	N/A	N/A		
		GVW	22.77	-2.3	31.96	-2.8	38.09	-1.3	28.89	-10.0	26.63	-4.2		
		1	8.82	-3.1	4.21	-6.5	5.90	-4.9	4.30	-15.7	4.74	-10.7		
		2	7.41	4.4	6.69	-5.8	8.16	2.0	8.85	6.6	7.14	2.1		
Std.	2	3	6.61	-6.9	6.80	-4.2	7.69	-6.2	6.20	-25.3	6.09	-13.0	4.8	6.5
		4	N/A	N/A	7.13	0.4	7.73	-3.3	9.56	-8.1	8.09	-4.8		
		5	N/A	N/A	6.93	-2.4	8.24	0.5	N/A	N/A	N/A	N/A		
		GVW	22.84	-2.0	31.76	-3.5	37.72	-2.3	28.90	-10.0	26.06	-6.2		
		1	9.45	3.9	4.36	-3.1	5.39	-13.1	5.04	-1.3	5.41	2.0		
		2	7.15	0.7	6.16	-13.2	8.26	3.3	7.72	-6.9	6.54	-6.6		
Prop. <sup>h</sup>	1	3	6.50	-8.4	7.80	9.8	6.38	-22.2	8.20	-1.1	7.19	2.7	2.2	7.4
		4	N/A	N/A	6.25	-12.0	8.61	7.6	10.88	4.6	8.49	-0.2		
		5	N/A	N/A	8.15	14.8	6.80	-17.0	N/A	N/A	N/A	N/A		
		GVW	23.10	-0.8	32.72	-0.5	35.44	-8.2	31.9	-0.8	27.62	-0.7		
		1	9.26	1.8	4.14	-8.0	6.39	3.0	4.93	-3.3	5.84	10.1		
		2	7.90	11.3	6.13	-13.7	10.29	28.7	7.96	-4.1	6.92	-1.2		
Prop.	2	3	6.378	-10.3	8.03	13.1	6.24	-23.9	8.17	-1.6	7.57	8.1	2.4	10.6
		4	N/A	N/A	6.29	-11.5	9.85	23.1	10.54	1.3	8.52	0.3		
		5	N/A	N/A	9.18	29.3	6.92	-15.6	N/A	N/A	N/A	N/A		
		GVW	23.54	1.0	33.76	2.6	39.69	2.8	31.59	-1.6	28.85	3.8		

<sup>a</sup> Approach, <sup>b</sup> Lane, <sup>c</sup> Axle, <sup>d</sup> Estimate, <sup>e</sup> error, <sup>f</sup> gross-vehicle-weight, <sup>g</sup> Standard, <sup>h</sup> Proposed

\* Note: Average absolute error calculated based on all five cases for each lane and approach

### 3.5.2 Multiple-truck cases

This section shows that the proposed approach also works accurately for multiple-truck cases. According to Subsection 3.4.3, six different cases were considered (shown in Figure 3.10). Overall, considering all trucks in all six cases, the mean absolute errors were 4.50% and 11.3% for GVW and axle weight estimations. The details are provided in Table 3.5.

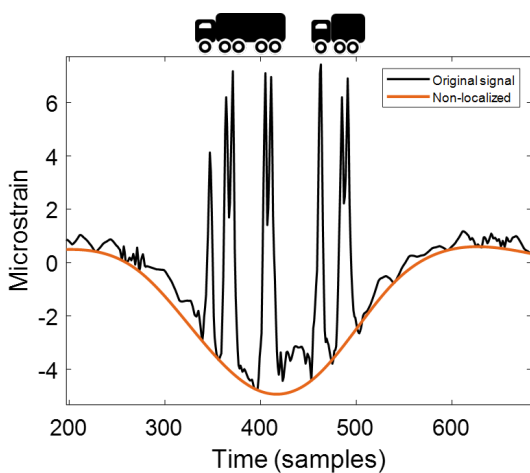
Figure 3.11 shows the results for Case 1, where two trucks, i.e., a 5-axle and a 3-axle, with a longitudinal distance of 8 m, simultaneously passed through the first lane. Figure 3.11a shows the original strain response and the fitted curve to its non-localized portion. According to this figure, when the sensors are placed where maximum localized strain occurs, the axles can be successfully captured even for closely-spaced ones. Additionally, Figure 3.11b shows the modified strain response (when the non-localized portion of the strain is removed) and the selected portions needed for weight estimation. The same procedure was conducted for Case 2, where the same trucks with the same distance passed through the second lane. The results are shown for both cases in Table 3.5. According to this table, the GVW estimation errors for Case 1 were -6.4% and -1.1% for the 3-axle and 5-axle trucks, respectively, while they were -4.6% and 1.5% for Case 2. Thus, overall, except for the 5-axle truck in Case 2, GVWs were all underestimated. Also, in both cases, the GVW estimation errors associated with the 3-axle trucks were greater than the 5-axles. Additionally, considering all axles of both 3-axle and 5-axle trucks, lane two generated greater axle weight errors than lane one (11.6% vs. 7.4%); however, in average, GVW error associated with lane one (3.8%) was greater than lane two (3.1%). Similar to the GVW errors, the axle weights errors are also greater for the 3-axle compared to the 5-axle trucks in both cases. The reason for the variability of errors was already discussed in Subsection 3.5.1

For Case 3, which is a zigzag pattern with two 3-axle trucks on the first lane and a 3-axle

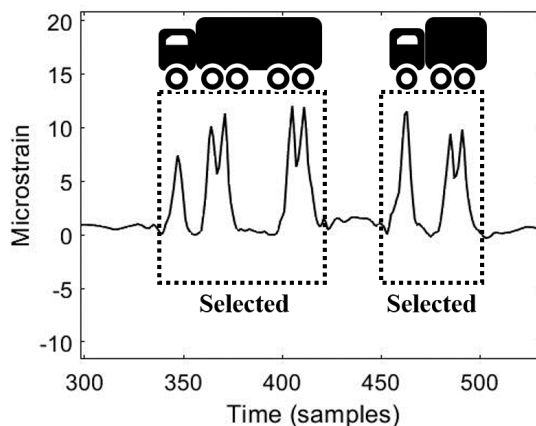
Table 3.5: The results of multiple-truck cases

Case no.	Axle no.	Truck 1		Truck 2		Truck 3	
		Est. (ton)	error (%)	Est. (ton)	error (%)	Est. (ton)	error (%)
1	1	9.21	1.2	5.80	-6.5	N/A	N/A
	2	7.38	3.9	7.99	-0.15	N/A	N/A
	3	5.23	-26.3	7.35	-10.4	N/A	N/A
	4	N/A	N/A	8.57	7.1	N/A	N/A
	5	N/A	N/A	8.49	3.6	N/A	N/A
GVW		21.82	-6.4	38.19	-1.1	N/A	N/A
2	1	8.79	-3.4	6.09	-1.8	N/A	N/A
	2	8.56	20.5	8.88	11.0	N/A	N/A
	3	4.89	-31.2	7.11	-13.3	N/A	N/A
	4	N/A	N/A	8.57	7.2	N/A	N/A
	5	N/A	N/A	8.53	4.0	N/A	N/A
GVW		22.24	-4.6	39.17	1.5	N/A	N/A
3	1	10.00	9.9	9.61	5.7	9.96	9.4
	2	8.02	12.9	8.07	13.7	7.74	9.0
	3	6.89	-2.9	6.15	-13.4	6.62	-6.8
GVW		24.91	6.9	23.83	2.3	24.32	4.4
4	1	9.52	4.7	10.18	11.9	10.19	11.9
	2	8.11	14.2	7.29	2.7	8.56	20.5
	3	6.35	-10.6	7.20	1.3	6.41	-9.7
GVW		23.98	2.9	24.67	5.9	25.16	8.0
5	1	9.19	1.0	9.65	6.1	6.57	5.9
	2	8.22	15.8	8.38	18.1	10.61	32.6
	3	5.94	-16.4	5.95	-16.2	6.38	-22.2
	4	N/A	N/A	N/A	N/A	10.60	32.5
	5	N/A	N/A	N/A	N/A	7.37	-10.2
GVW		23.35	0.2	23.99	3.0	41.51	7.6
6	1	9.68	6.3	6.77	9.3	N/A	N/A
	2	7.12	0.3	9.90	23.8	N/A	N/A
	3	4.03	-43.2	8.09	-1.3	N/A	N/A
	4	N/A	N/A	7.63	-4.6	N/A	N/A
	5	N/A	N/A	7.13	-13.0	N/A	N/A
GVW		20.83	-10.6	39.53	2.4	N/A	N/A

Note: The overall mean absolute errors, based on all six multiple-truck cases, for axle weight and GVW estimations, were 11.36% and 4.43%, respectively.



(a) The original strain-time response

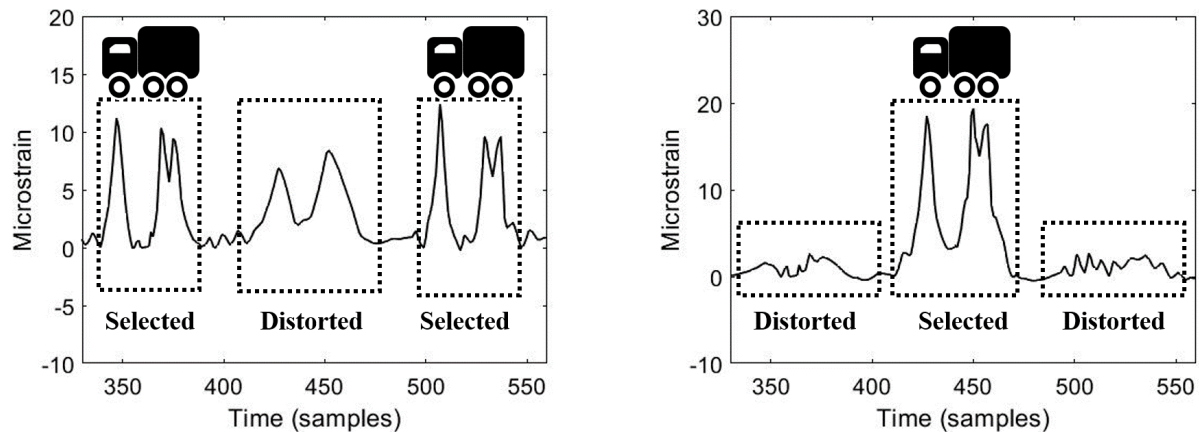


(b) The proposed approach result (selected portions)

Figure 3.11: Case 1: a 5-axle truck and a 3-axle truck on the lane one

truck on the second lane, only the modified strain response (non-localized portion removed) and the selected portion for weight estimation are shown (for conciseness). Figures 3.12a and 3.12b respectively show the modified strain responses and the selected portions for weight estimation on lanes one and two. Also, as explained earlier, when two trucks move on two adjacent lanes, the strain response will be a combination of sharp peaks due to the trucks on the same lane and distorted peaks due to the reflection of the truck on the adjacent lane. This is clearly shown in Figure 3.12. Only the portions with sharp peaks were used for weight estimation and the distorted parts were discarded. This was already explained in detail in Section 3.2. The same procedure was performed for Case 4 with a zigzag pattern with one 3-axle truck on the first lane and two 3-axle trucks on the second lane. Table 3.5 shows the results for both cases. According to this table, the GVW estimation errors for Case 3 were 6.9% (lane one), 2.3% (lane two), and 4.4% (lane one) for the left, middle, and right 3-axle trucks while they were 2.9% (lane two), 5.9% (lane one), and 8.0% (lane two) for Case 4. Thus, in average, lane two generated smaller GVW errors compared to lane one. Also, the mean absolute errors for axle weight estimation were similar values of 9.3% and 9.7% for

Cases 3 and 4, respectively (considering all axles and all trucks for each case). However, in average, lane 2 generated greater axle weight errors (11.6%) compared to lane one (7.4%), considering both Cases 3 and 4 together.



(a) The selected and discarded portions in the response from Lane 1

(b) The selected and discarded portions in the response from Lane 2

Figure 3.12: Case 3: a zigzag pattern with two 3-axle trucks on the first lane and a 3-axle truck on the second lane

Case 5 is a zigzag pattern with two 3-axle trucks on the first lane, a 5-axle truck on the second lane, and two light-weight vehicles on the third lane. Similar to Cases 3 and 4, the strain responses from lanes one and two were decomposed, and the distorted portions (adjacent truck reflection) were excluded and only the portions with sharp peaks were selected. The light-weight vehicles (total weight of 1.2 tons), due to their small weights, did not have a considerable reflection on the responses extracted from lanes one and two. According to Table 3.5, the GVW estimation errors were 0.2% (lane one), 3% (lane one), and 7.6% (lane two) for the two 3-axle trucks and the 5-axle truck, respectively. Thus, overall, the 5-axle truck and lane two generated greater GVW errors. The axle weight error for the 5-axle truck on the second lane (20.68%) was overall greater than the 3-axle trucks on the first lane (12.3%).

Case 6 is a 5-axle truck and a 3-axle truck in two adjacent lanes moving side-by-side at a longitudinal distance of 2 m. As explained in Section 3.2, for side-by-side trucks, the strain response has a combination of clear and distorted peaks, and only the clear peaks should be kept and the remaining should be removed. This was already explained in detail in Section 3.2. According to Table 3.5, the GVW estimation errors were -10.6% (lane two) and 2.4% (lane one) for the 3-axle and the 5-axle trucks, respectively. Additionally, the mean absolute error for axle weight estimation was 12.7%.

In general, different factors can contribute to the weight estimation error: 1) truck type (3-axle vs. 5-axle), 2) truck weight, 3) different lanes 4) transverse position and 5) temperature change. In this study, the first three factors were simultaneously changing, making the parametric study difficult. Here, a preliminary parametric study is conducted for the first three factors and further discussion is left for a future study where these factors change one by one. Overall, in all these six cases, the 3-axle truck (lighter) eleven times and the 5-axle truck (heavier) four times were used. According to the results, in both GVW and axle weight estimations (considering all six cases), the proposed approach was, on average, more successful on the 5-axle truck compared to the 3-axle truck. The average GVW and axle weight errors were respectively 5.0% and 11.5% for the 3-axle truck and 3.2% and 11.0% for the 5-axle truck. Also, in 4 cases (Cases 1,2,5, and 6), the 3-axle truck was directly compared with the 5-axle truck. In three out of four cases (Cases 1,2, and 6), GVW estimation was more accurate for the 5-axle truck, and in only one case (Case 5), it was more accurate for the 3-axle truck. This was the same for axle weight estimation. A similar comparison can be used to discuss the effect of truck weight (factor 2 mentioned above) since the 5-axle truck is heavier than the 3-axle truck. In this study, lanes one and two were both tested. It was observed that (for both GVW and axle weight estimations), the proposed approach was, on average, more accurate on lane one compared to lane two. The average errors for GVW and



axle weight were 4.3% and 9.3% for lane one and 5.7% and 14.0% for lane two. Also, two other important factors are temperature change and the transverse position of the trucks (factors 4 and 5). As explained earlier, the proposed BWIM method focuses on the localized strain portion. Also, the localized portion, particularly the peaks' values, can be affected by the truck transverse position and temperature change. These are out of the scope of this study but should be considered in a future study.

The main limitation for the proposed BWIM approach is going to be for a case where two side-by-side trucks with exactly the same axle configurations (axle spacing and the number of axles) crossing over the sensors at exactly the same time. In this case, the strain responses' peaks will align with each other and will not be straightforward to decompose. However, this can rarely happen as the accuracy of the data acquisition timestamp is 0.001 s. Thus, even if both trucks are exactly the same, there will most likely be some time delay between the truck positions and their peaks in the strain responses in the real situation. Overall, as mentioned earlier, the mean absolute errors, considering all trucks in all six cases, were respectively 4.5% and 11.3% for GVW and axle weight estimations. This shows that the proposed approach is capable of computing the axle and gross vehicle weights accurately, even for complex traffic load patterns with a combination of trucks and lightweight vehicles.

### 3.6 Conclusions, Discussion, and Future Study

This paper reports the results of a study on a novel bridge-weigh-in-motion (BWIM) technique to estimate the traversing trucks' gross vehicle weights (GVW) and axle weights. This approach resolves the significant shortcoming of the existing BWIMs, which is their limitation for multiple simultaneous trucks on bridges. These may present with an arbitrary number of trucks and lightweight vehicles, simultaneously crossing the bridge in any traffic

configuration. To show the applicability of the approach, a finite element model (validated against experimental data with great agreement) was used to consider single-truck events and complex multiple-truck traffic cases, including in-one-row trucks, zigzag patterns, side-by-side trucks, and a combination of several trucks with several lightweight vehicles. Based on the results, the following conclusions are made:

When the sensors are placed where maximum localized strain occurs, the axles can be successfully captured even for closely-spaced ones.

Removing the non-localized strain does not eliminate much important information when it is used for single-truck events. Compared to the standard BWIM approach, the proposed approach not only did not reduce the GVW estimation accuracy but also improved it from 4.1% error to 2.2% for lane one and from 4.8% to 2.4% for lane two. However, the mean absolute errors (MAE) of the axle weights were increased from 4.8% to 7.4% for lane one and from 6.5% to 10.6% for lane two. This increase in axle weight estimation errors can be ignored since they are still in a reasonable range, and simultaneously, the GVW estimation accuracy is improved, and multiple-truck weight estimation is enabled.

The proposed approach was tested on two in-one-row trucks (a 5-axle and a 3-axle), two zigzag-pattern events (with three 3-axle trucks), a side-by-side case (with a 5-axle and 3-axle trucks), and a complex multiple-vehicle event with three trucks and two lightweight vehicles distributed in all three lanes. Results demonstrated that the proposed approach can successfully decompose the strain responses associated with each truck. Also, it can accurately estimate the GVWs and axle weights. The overall mean absolute errors, based on all complex multiple-truck cases, were respectively 4.5% and 11.3% for GVW and axle weight estimations. According to the results, out of fifteen trucks (in all six multiple-truck events), nine GVW errors were less than 5%, five errors were between 5% and 10%, and only one GVW error was greater than 10%. Additionally, out of 53 axle weight estimations, 44

cases had an error less than 20% (28 cases had an error less than 10% and 16 cases an error greater than 10% but less than 20%) and only 9 cases with an error greater than 20%. These results are quite comparable with expensive pavement-based WIM systems and traditional BWIM technologies.

In this study, the fundamental goal was to present a proof-of-concept study to show that the proposed BWIM approach effectively works for single and multiple trucks with complex traffic patterns. Additionally, in an actual situation, it is usually very challenging to control the traffic (without lane closure) to consider desired/complex traffic load patterns with multiple trucks involved. Thus, a finite element model (validated against experimental data) was used to resolve this issue. However, in a future study, it is necessary to experimentally evaluate the proposed approach against a decent number of multiple-truck events. Factors such as transverse position and temperature change should be carefully considered.

Also, other than the techniques used in this study to remove the non-localized strain response (manual process, high-pass filter with low cut-off frequency, and envelope function), there might be other techniques which may improve the weight estimation results.

# Chapter 4

## A Novel Dual-Purpose Procedure for Bridge Health Monitoring and Weigh-In-Motion Used for Multiple-Vehicle Events

Every year, transportation agencies report a large number of aging bridges that are structurally damaged. Also, evolving traffic and particularly overloaded traffic can further threaten bridges' integrity and safety. An integrated system that can monitor the bridge integrity and over-loaded traffic is more attractive to practitioners because it brings improved performance at a lower cost. Nothing-on-road bridge-weight-in-motion (NOR-BWIM) is a system that uses the instrumented bridges (a few sensors under the road surface) as a scale to compute the trucks' weights. This addresses some of the main challenges of pavement-based WIM and traditional BWIM systems, including interruption to traveling traffic, sensitivity to daily tire impacts, etc. Additionally, previous studies have shown that BWIM systems are versatile candidates for overcoming critical challenges of structural health monitoring (SHM) such as applicability to various types of bridges. In this study, a multiple-presence dual-purpose (MPDP) SHM approach was proposed to monitor the integrity of bridges using the BWIM system existing sensors. This approach centers on the influence line (IL) change and uses

a recently developed multiple-presence IL (MP-IL) technique for SHM application for the first time in the literature. This can effectively handle the multiple presence issue of the current integrated SHM-BWIM systems to make them more practical. Also, unlike many SHM-BWIM studies, transverse position change of the trucks (defined as a false damage indicator) was included in the proposed procedure to provide a more realistic bridge health monitoring approach. To show the applicability of the approach, a long-span concrete-box-girder bridge, called Varina-Enon, was modeled. The model was validated against a set of experimental data using known large events. The model was then used to evaluate the MPDP approach under single and multiple truck events. Eleven damage scenarios were simulated, and three SHM trucks (a 3-axle, a 4-axle, and a 5-axle) were used to improve the SHM accuracy. Also, an updated sensor placement was proposed to effectively work for both BWIM and SHM applications in both single and multiple-truck events. According to the results, the MPDP SHM procedure coupled with the novel MP-IL and the proposed sensor placement could effectively detect the damage scenarios in both single and multiple-truck events. Also, it was shown that using several independent SHM trucks can make the monitoring process more effective.

## 4.1 Introduction

Factors such as aging, corrosion, and fatigue degrade the structural capacity of bridges. This, in combination with the rapid growth in traffic volume, particularly vehicle overweight enforcement on degraded bridges, increases safety concerns and maintenance challenges for transportation agencies [4]. Intelligent transportation system (ITS) and structural health monitoring (SHM) systems have the potential to save highway infrastructure managers millions in traffic control and maintenance operations, respectively. The integration of the

these two systems is more a more attractive candidate for transportation agencies since it brings improved performance and it is more cost-effective. Furthermore, ITS can make SHM estimates more accurate by providing load information, while SHM can complement ITS data to help estimate vehicle weights more confidently and overcome deficiencies in camera measurements. By fusing system information, fewer sensors are required overall. Thus, an integrated, cost-effective monitoring system can be beneficial for the transportation agencies to 1) consistently detect the overloaded vehicles without disrupting the traffic and 2) regularly monitor the bridge integrity (structural health monitoring) without imposing much additional cost. These are defined as two needs in this study.

For the first need, a proper intelligent transportation system that has the potentiality to be integrated with the SHM systems should be used. In this regard, bridge weight-in-motion (BWIM), first introduced by Moses [8], has broadly been used over the last decades [63]. This system uses the bridge as a scale and takes the bridge response to estimate the traversing trucks' information [92]. In this system, the prerequisites, e.g., speed, axle spacings, and the number of axles, should first be obtained to be later used for gross and axle weight estimation. Several BWIM types have been introduced in the literature [10–12] for prerequisite estimation. However, in a particular type of BWIM, called nothing-on-road BWIM (NOR-BWIM) [13, 18–20], only a few weighing sensors should be installed under the bridge top slab. Since nothing will be installed on the road surface, NOR-BWIM addresses some of the main challenges of pavement-based WIM and traditional BWIM systems. These include lane closure, interruption to the traveling traffic, and sensitivity to daily tire impacts and harsh weather conditions. It also provides a portable solution with a less labor-intense installation process.

The first step in vehicle information computation using BWIM is always influence line (IL) calculation using experimental data. Furthermore, suppose the stiffness of the indeterminate

bridge changes due to a damage at a certain point. In that case, the structural response and, consequently, the IL of the bridge will change due to internal force redistribution. This concept can be used for bridge integrity monitoring applications (the second need defined above). Thus, IL can be a connecting element to convert the SHM and BWIM systems to a single, multi-functional system. In fact, besides BWIM's excellent capability in weight enforcement estimation, it can also be appropriately adjusted for structural health monitoring (SHM) using the existing sensors and the bridge IL.

Bridge monitoring using IL calculation can be performed using different structural quantities to provide displacement influence line [57–59], rotation influence line [3, 60], and strain/stress influence line [7, 22, 61]. However, this study aims to integrate the BWIM and SHM systems. In most cases, the BWIM system relies on strain measurements due to applicability to different types of bridges and simplicity in measurement and prerequisites calculation.

In this regard (stress/strain IL in SHM), in some cases, IL was indirectly used for SHM (usually BWIM-informed SHM systems). For instance, a WIM-based method was proposed along with a damage index for level I damage detection [61]. Two types of WIM systems were used, pavement-based and BWIM. IL was employed for the BWIM weight estimation. The ratio of the computed weights using these two systems was used as a damage index. This was based on the fact that the truck weight computed using BWIM on the damaged bridge will be different from the weight computed on the intact bridge. In another study, called the “virtual axle” method, an additional weightless axle was assumed for the traversing vehicle to detect damage [22]. It was shown that any change in structural behavior caused by damage would lead to a non-zero estimate for the virtual axle. This was used as a damage indicator.

In a more direct application of stress IL in SHM, a regularization method was proposed for the stress influence line based on a train passing over Tsing Ma Bridge in Hong Kong [7]. Three damage indexes were introduced and tested, including the IL change and its

corresponding first-order and second-order differences, showing satisfying results.

However, these studies have two significant shortcomings. 1) They are only applicable when a single truck is on the bridge. In fact, when multiple trucks move on the bridge simultaneously, the standard IL techniques cannot decompose the strain responses associated with each truck properly. Thus, since it is not guaranteed to only have one truck on the bridge at the monitoring stage without lane closure, they are not practical for long and medium-span bridges. 2) Two challenging factors, i.e., noise and transverse positions, are ignored while these can make a false damage indicator even for the intact bridge and need to be included in the process.

To address these shortcomings, this study proposes a multiple-presence dual-purpose (MPDP) structural health monitoring (SHM) approach. This is called “multiple-presence” since it is to monitor the integrity of bridges under multiple simultaneous trucks and using the existing sensors for BWIM systems. Additionally, this procedure is called “dual-purpose” since it can be used for SHM and BWIM applications. The proposed procedure computes the change in the ILs of a bridge experimentally extracted at the monitoring stage compared to its initial ILs extracted from the intact bridges.

This procedure has three contributions to the literature: 1) for the first time in the literature, a recently developed IL extraction technique proposed by Moghadam et al. in 2022 [74], called Multiple-Presence IL (MP-IL) in this study, is applied to SHM. MP-IL can successfully remove the effect of unwanted vehicles in complex multiple-truck traffic conditions and obtain the IL [74]. This resolves the significant multiple-presence limitation of the standard BWIMs for IL extraction, weight estimation, and SHM. 2) Other important factors, such as noise and transverse position, are also considered in the proposed procedure to provide a more realistic bridge health monitoring approach. 3) An updated instrumentation plan is proposed to be effective for both the multiple-presence BWIM system and SHM in single-truck and



multiple-truck events.

This paper is organized as follows: extensive details about the proposed MPDP SHM procedure, standard IL, and the MP-IL techniques are presented in Section 4.2. Section 4.3 introduces the long-span bridge used, the validated finite element model against experimental data, and the monitoring procedure. Section 4.4 discusses about the results of single-truck and multiple-truck events as well as a parametric study performed on the truck characteristics. Lastly, the main conclusions and future works are provided in Section 4.5.

## 4.2 Methodology

### 4.2.1 The multiple-presence dual-purpose (MPDP) SHM approach

#### 4.2.1.1 Significance

The structural damage detection includes four levels of identification: level 1 is for damage presence, level 2 is damage location identification, level 3 is damage intensity quantification, and level 4 is to determine the remaining service life to failure [45]. This paper proposes a procedure (multiple-presence dual-purpose (MPDP)) to monitor the integrity of bridges (level I damage detection) in single-truck and even multiple-truck events. This is using several known trucks with known configurations and weights. The goal is to employ the existing sensors used for BWIM systems and, thus, to use the MPDP system for both BWIM and SHM applications. This makes the multi-functional system more affordable.

The proposed procedure centers on the change in the ILs of the bridges (at the time of regular monitoring) compared to their initial/reference ILs extracted from the intact bridges. This procedure is expanded using a novel technique and has three significant novelties. First,

a recently developed IL extraction technique proposed by Moghadam et al. [74], called Multiple-Presence IL (MP-IL) in this study, is used for SHM application. Moghadam et al. already showed that, unlike the standard IL extraction techniques, MP-IL could successfully decompose the desired strain response associated with the corresponding truck to extract the IL of the bridge. MP-IL can also remove the effect of the unwanted trucks simultaneously on the bridge [74]. This resolves the significant multiple-presence limitation of the standard BWIMs for IL extraction, weight estimation, and SHM. Second, other significant factors, i.e., noise and transverse position change, defined as false damage indicators, are included in the procedure to provide a more realistic and robust approach for SHM. Third, a sensor placement is proposed for the integrated system to be effectively used for both BWIM and SHM applications. It is also suggested to use several independent SHM trucks to make the process more effective and successful.

#### 4.2.1.2 Possible traffic events and suitable IL techniques

As explained above, the proposed MPDP technique computes the difference between the initial IL of the bridge and IL at the monitoring stage. To monitor the bridge, the SHM trucks with known but different axle configurations and weights need to move over the target bridge. Depending on what traffic cases exist during the truck passage, the IL extraction technique used should change. As shown in Figure 4.1, three cases may occur: 1) a single SHM truck on a long-span bridge, 2) a single SHM truck on a short-span bridge, and 3) multiple trucks (SHM truck surrounded by several unwanted trucks) on a long-span bridge. As mentioned earlier, IL change is the key to determine if any damage has occurred. Thus, for the first two cases (single-truck events), the standard IL technique should be used, but for the latter one (multiple-truck event) MP-IL [44] should be employed for IL extraction. The reasoning for using different IL estimates is as follows: unlike standards IL techniques, MP-

IL estimation requires an additional strain decomposition step. The rest of the procedures are very similar. The additional step removes certain portions of the strain to decompose the strain associated with each truck in multiple-truck cases. Thus, it is suggested to use IL computation using the standard IL (not MP-IL) for the single-truck cases since 1) for the single-truck cases, no strain decomposition is needed. Hence, using the MP-IL will impose additional analysis steps and makes the procedure time-consuming. This can be more significant for a bulk of truck analyses; 2) the additional decomposition step may cause additional errors; 3) the standard IL takes the entire strain response while MP-IL takes only a certain portion (localized strain) of it, and therefore, the standard IL technique may be able to generate more comprehensive damage indicators with larger values. Thus, MP-IL should be avoided when it is not necessary. However, the MP-IL and standard IL techniques are complementary. The standard IL cannot be used for multiple-truck events, and this is where MP-IL should be used. Standard IL and MP-IL techniques are briefly explained in Subsections 4.2.3 and 4.2.4, respectively. In both, the effects of noise and transverse position change are included. This is explained further later in this section.

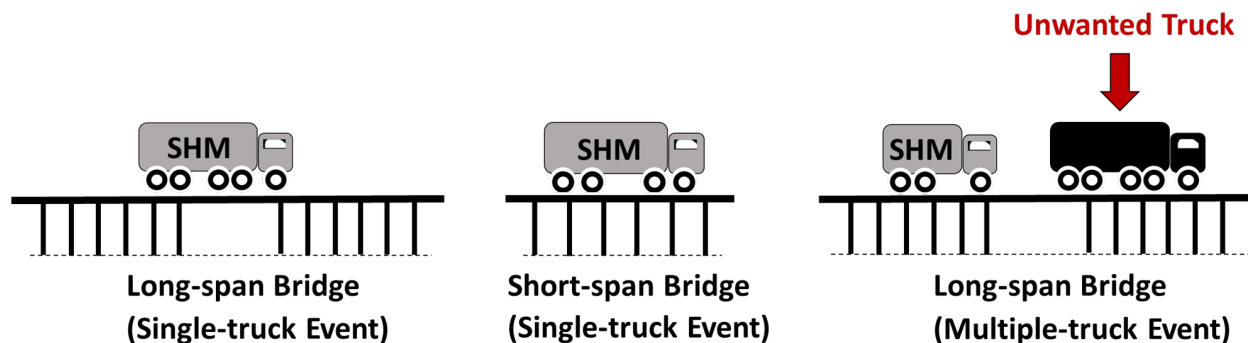


Figure 4.1: The cases occurred during bridge monitoring

### 4.2.1.3 Steps of MPDP procedure

In general, the MPDP procedure has two main steps shown in Figure 4.2. According to this figure, in the first step, i.e., “Calibration on the Intact Bridge”, each SHM truck should move through the intact bridge several times and the strain-time responses should be obtained. For each truck, several passages are needed to include the possible variation of transverse position and noise content. These factors will naturally be included since for each passage, the transverse position (depending on the driver’s accuracy) and noise can be slightly different. It should be noted that noise and transverse position change can create false changes (false damage indicator) to the IL of the intact bridge and that is why they should be taken into consideration. In this study, for transverse position change, three different variations are considered and the trucks moved through them to include the drivers’ inaccuracy. Three different noise contents were also considered to include the noise variation. The simulation process for noise and transverse position change is later explained in more detail in Subsection 4.3.3.

Once the responses are obtained, the standard IL and MP-IL techniques should be applied to the responses to extract two reference ILs for each truck type. These ILs are the references for future bridge monitoring subjected to single-truck and multiple-truck events. Any change in ILs called “Damage Indicator (DI)” can be a sign of damage as long as it is greater than certain thresholds (explained below). In this study, the DI is computed as the mean-square-error (MSE) of the reference IL and the IL at the monitoring stage.

Once the reference ILs are extracted, for each SHM truck, two DI thresholds, one for single-truck cases and the other for multiple-truck cases (called thresholds 1 and 2, respectively), should be computed. The DI threshold is upper 95% confidence bound of the DIs calculated using the ILs extracted from intact bridge and for multiple truck passages (different trans-

verse positions with different noise contents). In other words, the MSE (DI) of the reference IL and each IL from the intact bridge, under a certain truck (3-axle, 4-axle, etc.) and event (single/multiple-truck) with multiple passages for each should be calculated. Then, a 95% confidence analysis should be performed on the computed DIs. The upper bound is going to be a threshold for a certain truck and event (called threshold 1 for single-truck events and threshold 2 for multiple-truck events). For this particular study, since there are three transverse positions considered and three noise levels, a total number of nine DIs should be computed for each truck-event. This process is shown in Figure 4.3 for more clarity. These thresholds are to find a reliable range that can necessarily be related to a damage occurrence. If the DI value (at the monitoring stage) comes up to be greater than the thresholds, it can be concluded that damage has occurred with 95% confidence. If DI is smaller than that, we cannot necessarily conclude that damage has occurred even for a non-zero DI value.

The second step of the MPDP procedure, shown in Figure 4.2, is called “Integrity Monitoring of the Bridge”. According to this figure, the same trucks with the same axle configurations and weights should again be used at the monitoring stage (every two years, for instance) to obtain the strain responses. Similar to the first step (Calibration on the Intact Bridge), for single-truck events and multiple-truck events, standard IL and MP-IL should respectively be used to obtain the monitoring stage ILs. Then, the DI will be the MSE of the new IL and the reference ILs (for single-event, IL1, and for multiple-truck events, IL2). In fact, the monitoring process is more like a “recalibration” using the same truck but at the monitoring stage. As explained earlier, if the DI is greater than the DI thresholds, the bridge is damaged with 95% confidence. Otherwise, there is not enough evidence to decide about the integrity of the bridge.

In this study, it is suggested to use the same truck at the calibration stage (reference IL extraction) and the monitoring stage. This is because it is expected to get exactly the same

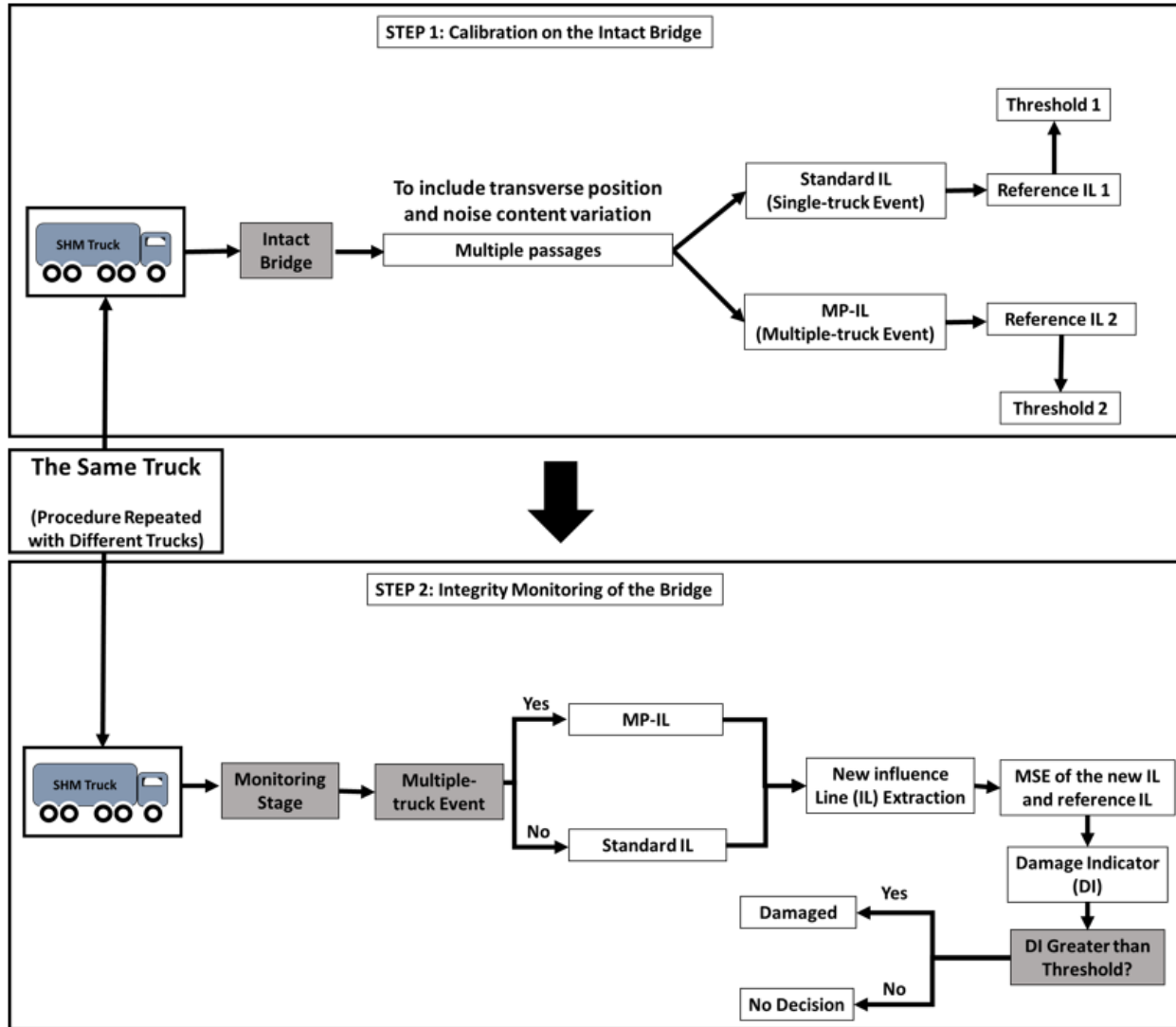


Figure 4.2: The MPDP SHM procedure

ILs ( $DI=0$ ) when no damage has occurred and when the truck is the same for both stages (with no transverse position change and noise). However, when the truck at the monitoring stage is different than the calibration stage, for the same test (no damage, no noise, and same transverse position), the DI value will be non-zero (false damage indicator). This is because any change in the truck characteristics can slightly change the IL when the truck type at the calibration stage is different than the monitoring stage even if no damage has occurred. This variation happens due to a change in the strain response content. In fact,

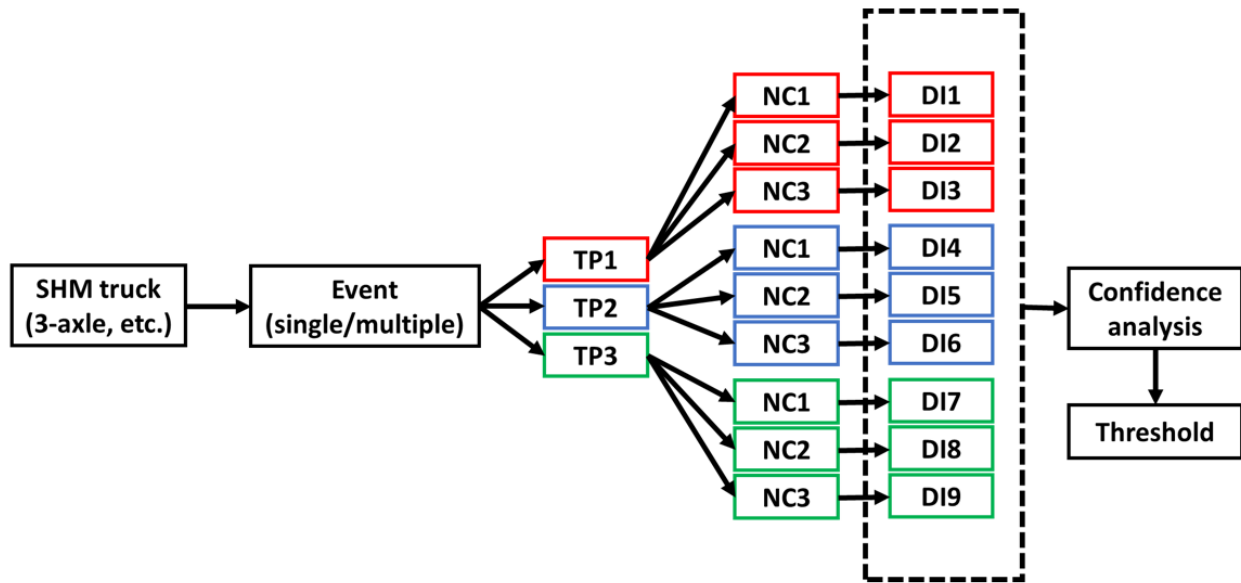


Figure 4.3: The threshold computation procedure (TP=transverse position, NC=noise content, DI=damage indicator)

since the IL extraction techniques take the strain response and generate the IL, any change in the strain response may change the IL. Although these IL techniques mostly remove these effects as later shown in Figure 4.12, some variation still exist. The IL change due to truck characteristic change was already acknowledged by previously published studies in the BWIM area. For instance, this is clearly mentioned on the first page of the paper published on MLE method developed by Ieng in 2015 [34]. According to this study, the MLE method takes multiple trucks with multiple passages into account to include the variability of the effects of the calibration vehicles on the bridge. This was later agreed by other researchers in this area as well [35].

Also, for a similar reason, it is recommended in this study to use an independent reference IL for each truck and not a single reference IL for all trucks together. This is because when one chooses to compute a single reference IL considering all trucks together, a future IL at the monitoring stage (using a 3-axle truck, or etc.) will definitely generate a non-zero DI

even for an intact bridge with no transverse position change and noise. In fact, the reference IL computed using all trucks cannot be exactly the same as the reference ILs computed for each individual trucks when no damage exists.

### 4.2.2 Prerequisites' estimation approach

Prerequisites, i.e., the number of axles, axle spacings, and speed, should usually be obtained prior to influence line calculation. For concrete box girder bridges, if the sensors, usually strain gauges, are installed properly where maximum localized strain under the tire path usually happens, the strain response will consist of clear peaks equal to the number of traversing axles. A common practice is to record the strain responses of 3-4 successive strain gauges and to measure/compute three parameters: 1) the time delay between the peaks within a strain response from a specific strain gauge, 2) the time delay between the peaks in strain responses from successive strain gauges, and 3) the physical distance between the successive strain gauges. These should then be used for prerequisites estimation, assuming that the truck speed is constant when passing over the sensors. Once the prerequisites are properly computed, they can be used for IL calculation using a proper method.

In this study, it is assumed that the prerequisites are already obtained appropriately. For more details on prerequisite estimation, see two studies conducted by He et al. [18] and Deng et al. [20].

### 4.2.3 Standard influence line approach

Previously published studies have proposed methods to experimentally compute the IL of a bridge [28–30, 34]. However, Carraro et al. showed that among all, maximum likelihood estimation (MLE) [34] provides the most accurate results [35]. Thus, the MLE method is



selected as the standard IL approach used in this study. MLE method suggests to include multiple trucks (1-2 trucks) with independent passages to compute a single IL. This is to consider the effects of the calibration vehicle variability, noise, etc., on the bridge.

Equation (4.1) summarizes this method in a mathematical format and more details are provided in the original paper by Ieng [34].

$$\sum_{j=1}^N A_j^T A_j I = \sum_{j=1}^N A_j^T M_j^T. \quad (4.1)$$

In Equation (2.9),  $M$  is the measured strain response and  $I$  is the influence line vector consisting of the influence line ordinates. Also,  $A$  is a matrix consisting of the axles weights shifted vertically in Toeplitz-matrix from.

However, standard IL methods (including MLE) are unable to decompose the strain responses associated with each truck in a multiple-truck event, and another technique (MP-IL) recently published [74] is needed to handle multiple trucks simultaneously on the bridge. This technique was already used only in the BWIM area and in this study, it is now extended for SHM application.

#### 4.2.4 Multiple-presence influence line (MP-IL) approach

Moghadam et al. recently published a novel influence line approach (MP-IL) to handle multiple-truck events with a combination of light-weight vehicles and heavy trucks on the bridge simultaneously [74]. The strain response under a truck path consists of two main components that are superposed together: 1) the non-localized strain response of the entire bridge acting as a beam and 2) additional strain, called localized strain response, due to the plate behavior of the top slab. The localized and non-localized strains are shown in Figures

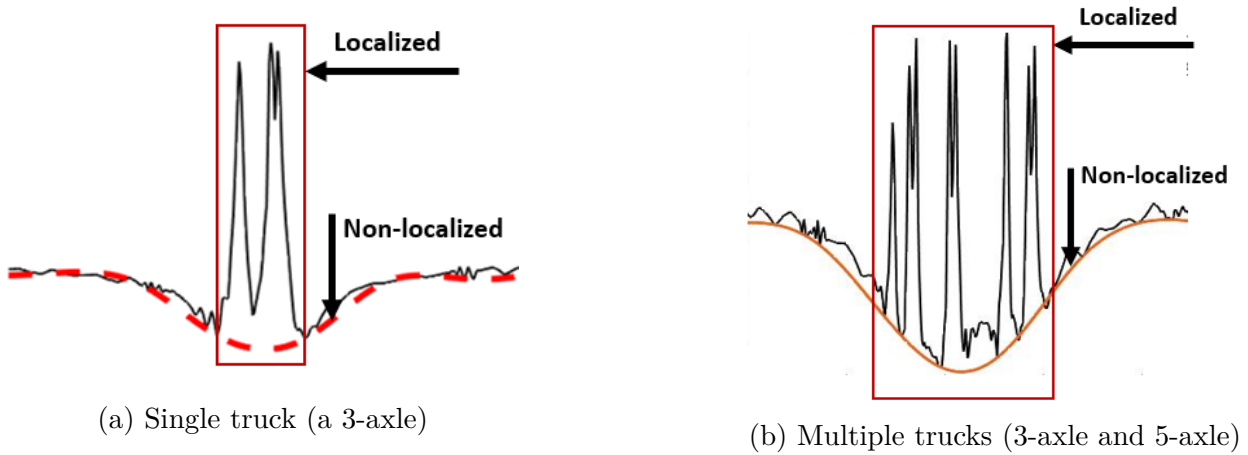


Figure 4.4: MP-IL procedure

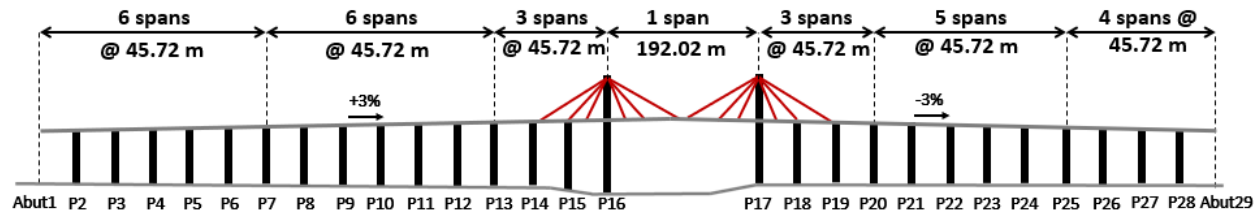
4.4a and 4.4b for single and multiple-truck events, respectively.

As shown in Figure 4.4a, MP-IL first filters out the non-localized strain portion (sensitive to nearby loads) and only keeps the localized portion. To do this, a curve fitted to the non-localized strain (dash line) will be subtracted from the original strain response. Then, the strain response corresponding to each truck should be properly extracted and fed into the standard IL approach such as MLE. More details are provided in the original paper [74].

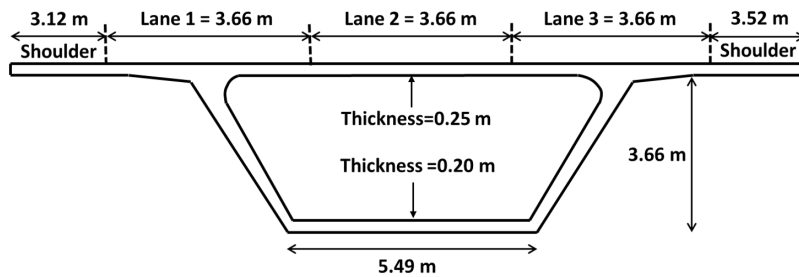
## 4.3 Analysis

### 4.3.1 Bridge description

In this study, the Varina-Enon bridge (VEB) shown in Figure 4.5a was selected. VEB is a cable-stayed, concrete-box-girder bridge over the James River in Virginia, with a total length of 1426.5 m and twenty-eight spans. This bridge has a total of seven approach units (shown in 4.5a) with various number of spans. All spans are 45.72m, except for the longest one, which is about 192 m. The middle part, shown in Figure 4.5a, is cable-stayed, consisting of 3



(a) The bridge schematic side-view



(b) The bridge elevation

Figure 4.5: The Varina-Enon bridge [74]

approach units with seven spans (spans 13 to 19). Each span of the bridge is post-tensioned with eight external tendons with nineteen 0.6-in-diameter strands in each tendon.

Figure 4.5b shows a typical elevation of all spans, including span 6 (the focus of this study) and the trapezoidal-shape concrete box. According to this figure, the total width of the top slab is 17.62 m, including three 3.66-m lanes and the two shoulders with various widths.

### 4.3.2 Validated finite element model

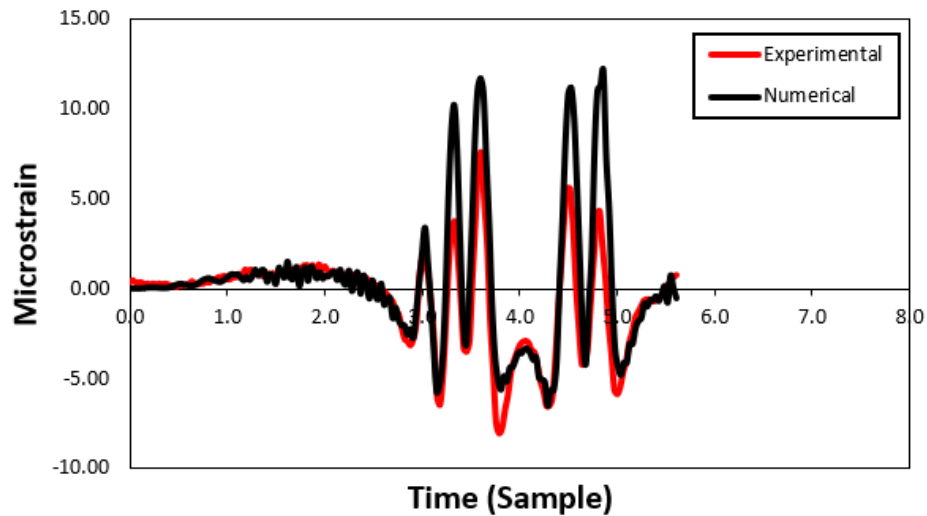
In this study, a similar 3-D finite element (FE) model (validated against experimental data) to the model developed by Moghadam et al. [74] was used with some minor modifications. Unlike the previous study, only two spans (spans 5 and 6) of the VE bridge were modeled as shown in Figure 4.8a. This is because there is an expansion joint at Pier 7 and Spans 6 and 7 are not connected to each other and they only share a pier. Eight external tendons with nineteen 0.6-in strands for each were simulated. The cable stays were ignored since spans

5 and 6 were significantly far from the middle approach units of the bridge. The bearings were also assigned between the superstructure and the piers with three elastic springs in three directions with stiffness values of 5456605 KN/m, 5010 KN/m, and 185776 KN.m/m. Appendix A shows the computation details.

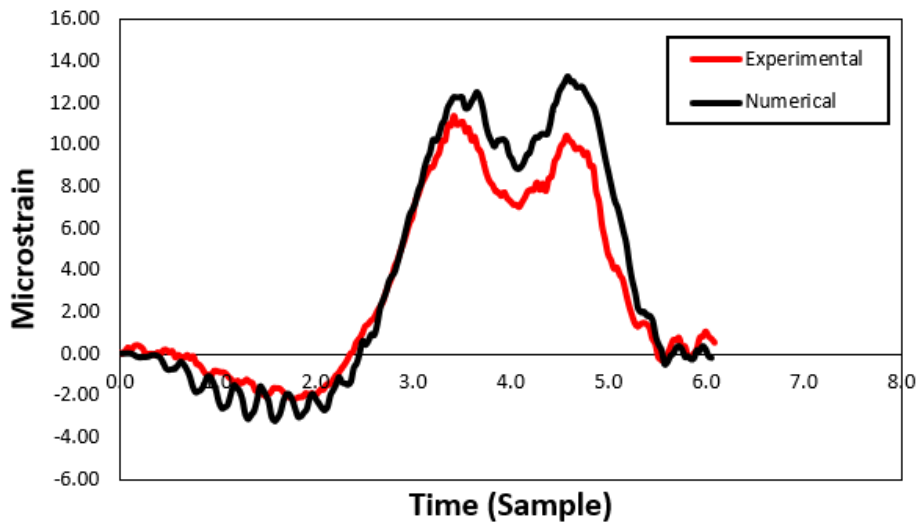
The isometric-view and top-view of the bridge are provided in Figures 4.8a and 4.8b. The model was created using eight-node solid elements. A mesh size of maximum 2.9 X 1.2 X 0.1 m was assigned to the entire slab, but it was refined around the strain measurement points (discussed below) to a maximum of 0.4 X 0.2 X 0.1 m. These mesh sizes were selected through a mesh sensitivity analysis.

Two measurements were conducted, one for the model validation against experimental data and the other for SHM application. Figures 4.9a and 4.9b show these two measurement types. For model validation, two points were selected in 18.3 m from Pier 7, at the bottom of the top slab and on top of the bottom slab. A time-history analysis with a sampling rate of 33 Hz was then performed to obtain the strain responses of the bridge subjected to two large events. The responses were then compared to those obtained from a set of experimental tests conducted on the VEB in 2020. The results are shown in Figures 4.6 and 4.7. The results showed that similar to the experimental data, the numerical model can capture the localized strain responses showing a great agreement for the general shape of the responses and magnitudes. More details are provided in the original paper [74]. It should be noted that the experimental data was only used to validate the FE model and for the rest of the process (SHM), the model is used to generate data.

It should be clarified that for the rest of this study, different measurement points were used for the SHM application. As already discussed, this study aims to provide a multiple-presence dual-purpose (MPDP) procedure to integrate the BWIM and SHM systems using the novel MP-IL technique for multiple-presence events. Thus, the same measurement points



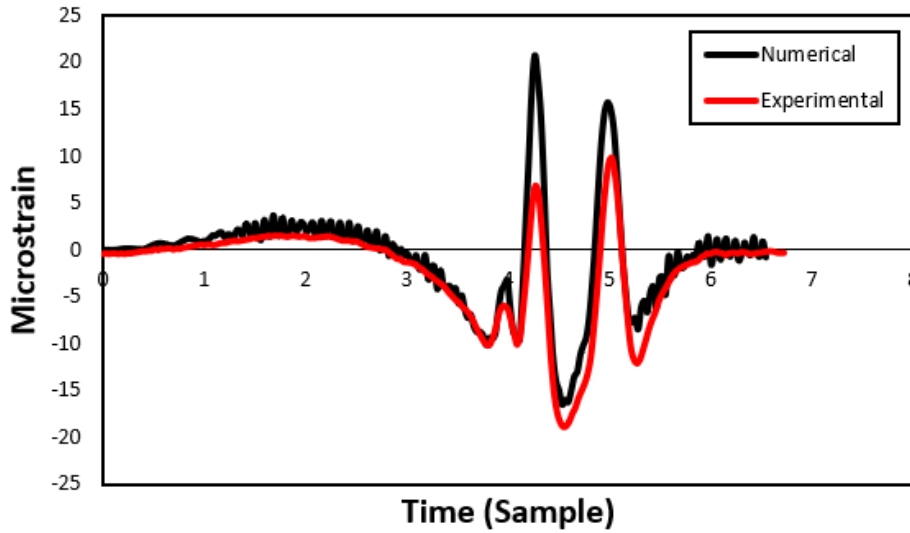
(a) Special permit on the top slab



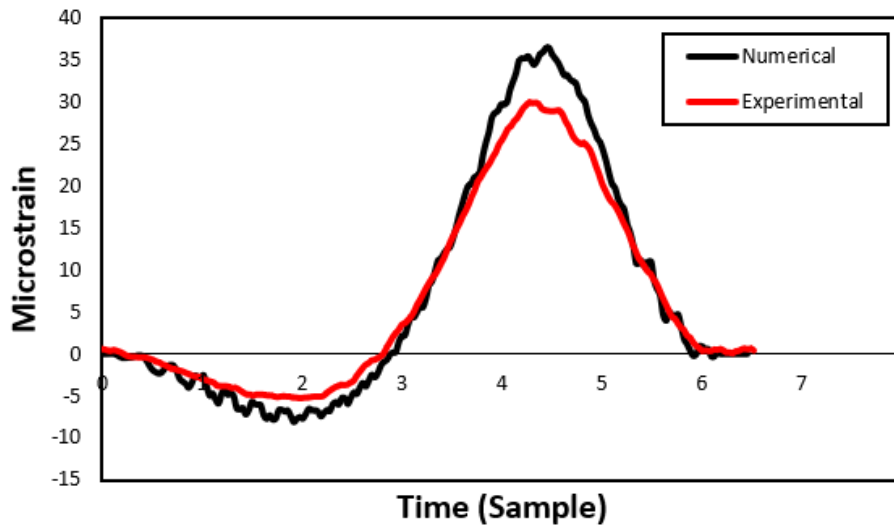
(b) Special permit on the bottom slab

Figure 4.6: The FE model validation results (Special permit)

recommended in the original paper [74] were used. The measurement points were selected at mid-span (span 6) and in a transverse position of 57cm from the pavement markings. This transverse position improves the accuracy of the results for prerequisite estimation [74] and needs to be kept the same for SHM application. This is clearly shown in Figure 4.9b. Also, unlike the validation part, the sampling rate was 100 Hz.



(a) Superload on the top slab



(b) Superload on the bottom slab

Figure 4.7: The FE model validation results (Superload)

### 4.3.3 Experimental procedure

This section describes the initial sensor placement, the region of interest (ROI), damage scenarios, trucks used, sampling rate, transverse position and noise inclusion approach, and how the tests are performed for SHM application.

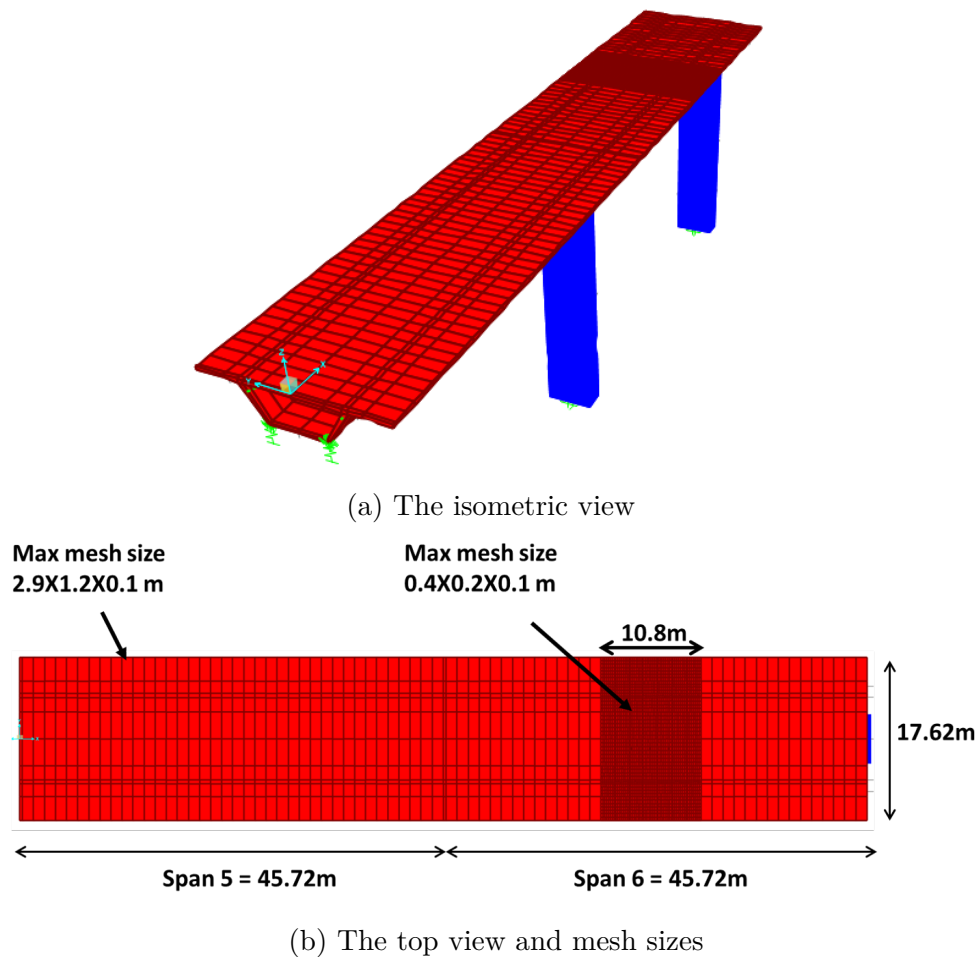


Figure 4.8: Finite element model overview and the mesh sizes

#### 4.3.3.1 Initial sensor placement

One of the goals of this study is to propose a sensor placement that effectively works for both the BWIM and SHM applications. A common practice for BWIM systems is to use at least three sensors (such as strain gauges) to obtain the prerequisites (i.e., speed, number of axles, and axle spacing) to be later used for weight estimation. As shown in Figure 4.10b, the distance between the successive strain gauges is suggested to be 1.6 m in this study, which is in good agreement with the papers published in the BWIM area [18, 20]. This should later be updated per the MPDP SHM results.

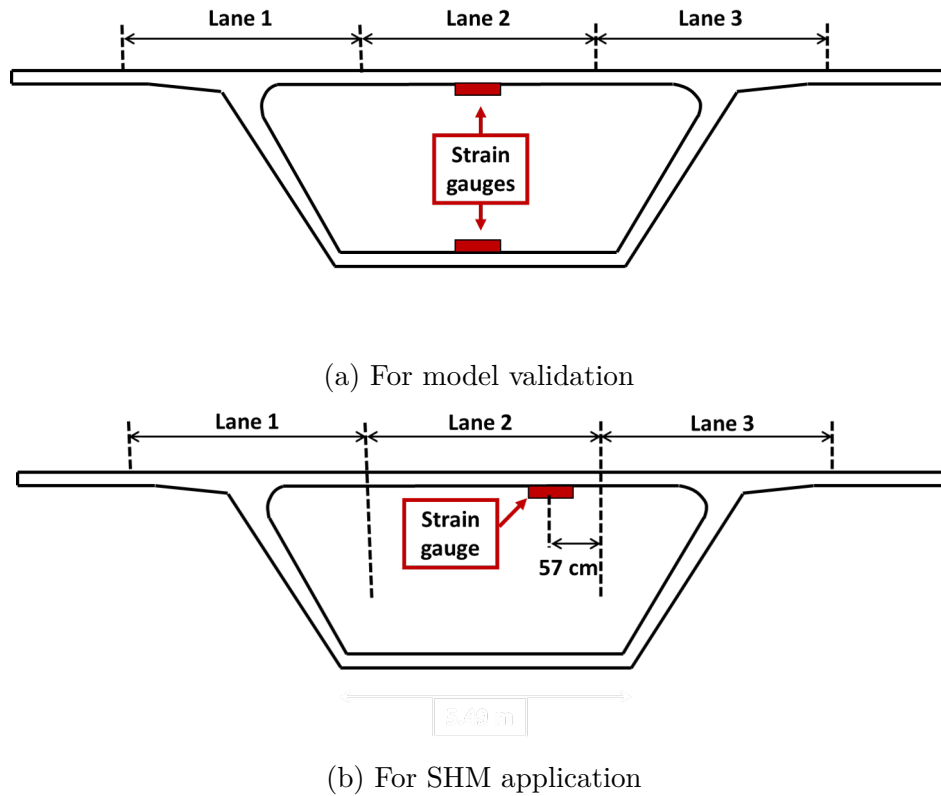


Figure 4.9: Measurement points

#### 4.3.3.2 Region of interest (ROI)

The goal is to monitor the integrity of the concrete-box top slab and the area where maximum local (under tires) and global deflections (maximum tension in concrete) usually happen (shown in Figure 4.10a). Due to symmetry, only the top right quadrant of the second measurement point is evaluated, and the results will be extended to other quadrants around the measurement point. This is called “Region of Interest (ROI)” shown in Figure 4.10b. This study results from more than 90 truck passages in CSI Bridge software with more than 110 hours of effective analysis time (more than 70 minutes each). Considering the ROI and extending the results reduced the analysis time significantly.

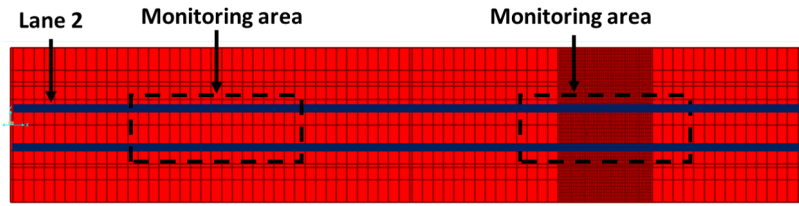


#### 4.3.3.3 Damage scenarios

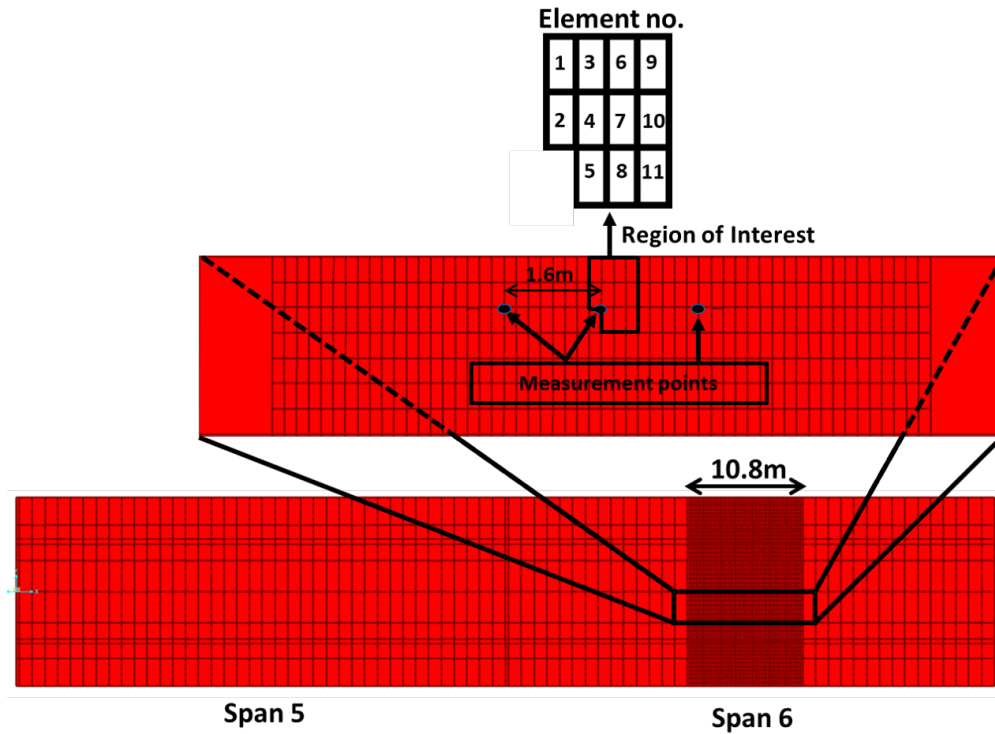
To test the MPDP SHM procedure on the ROI, several damage scenarios should properly be introduced. This is to understand how sensitive the monitoring system and the proposed MPDP approach are to different damage locations. Later, depending on the monitoring system's effectiveness in the damage locations, the sensor placement and their distances are updated to more effectively monitor the top slab and to be still suitable for the BWIM application. Eleven different elements (in the ROI) shown in Figure 4.10b were removed one by one, and separate analyses were performed (each analysis with only one removed element). These are called damage scenarios 1 through 11. It should be noted that top slab monitoring is only an example to show the capability of the integrated system and can be extended to other damage scenarios as well. This is left for future studies. In this study, the analyses were conducted using three SHM trucks (a 3-axle, a 4-axle, and a 5-axle) with different axle configurations and weights. These are shown in Figure 4.11. Also, the sampling rate was selected to be 100 Hz, suggested by other studies [74]

#### 4.3.3.4 Strain response vs. IL

As discussed in Subsection 4.2.1, the key computation for bridge health monitoring using the MPDP procedure is the change occurred in the ILs of the bridges at the monitoring stage compared to the reference ILs (IL1 and IL2). As a proof of concept, it is important to show why IL is selected for SHM and not strain response. For this, the strain response of the intact bridge and its corresponding IL under the 3-axle truck are plotted against the strain response and IL under the same 3-axle truck but with doubled axle weights. This is shown in Figure 4.12. According to this figure, the strain responses (both localized and non-localized) are significantly different; however, the IL still remained unique for this bridge.



(a) The Monitoring area



(b) The region of interest

Figure 4.10: Region of interest and measurement points

#### 4.3.3.5 Transverse position and noise

As explained in Subsection 4.2.1, it is first necessary to compute the reference ILs. It was also discussed that factors such as noise and the transverse position may change the IL of the bridge and can create false non-zero DIs even for the intact bridge. This subsection explains how the transverse position variation and noise inclusion were performed.

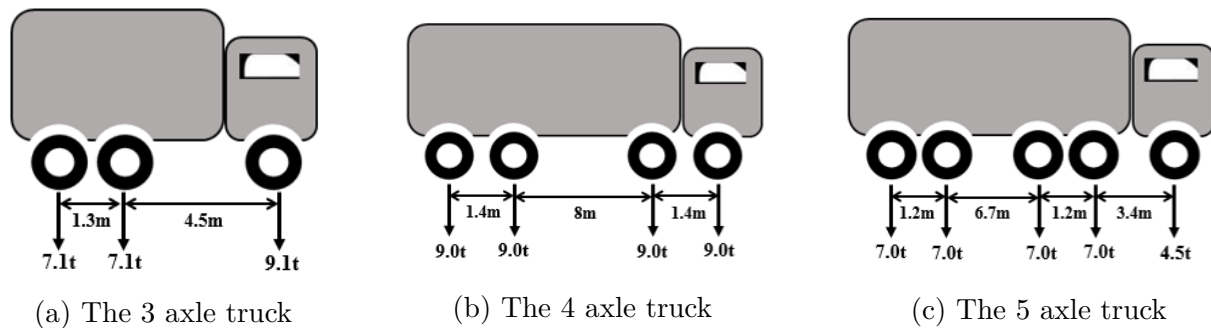


Figure 4.11: SHM trucks

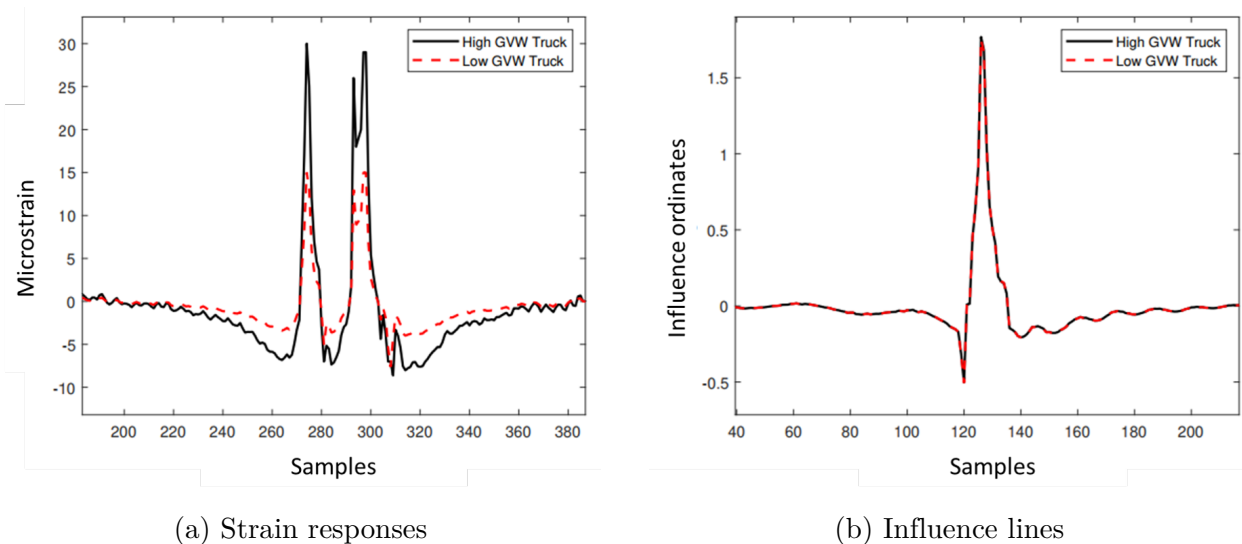


Figure 4.12: Comparison of the strain responses and ILs for the same trucks but with significantly different GVWs

The first step in considering the transverse position was to compute a reasonable range for its variability. According to a survey [90], the mean width of heavy trucks is 2.52 m, with approximately 90% from 2.5 to 2.6 m. Also, the maximum width of commercial trucks is 2.6 m [91]. Thus, the trucks' transverse position variability is a maximum of 57 cm for a standard lane width of 3.66 m (12 ft). Also, the bridge monitoring is usually an under-control evaluation process, and the SHM truck drivers can be requested to possibly drive on the center of the lanes. Thus, it is reasonable to consider a smaller value than 57cm for the transverse position change. In this study, a maximum of  $\pm 30$  cm was considered only to

include the drivers' accuracy in the procedure.

To include the effects of noise, white noise was added to the strain-time responses from all variations of the trucks' transverse positions (three for each truck and a total of nine responses). In this study, the "randn" function in MATLAB was used to generate signals with normally distributed random numbers that were then added to the original strain responses.

#### 4.3.3.6 Tests

This subsection defines how the tests were performed on each damage scenario. The goal is to understand if the proposed MPDP procedure is sensitive enough to different damage scenarios under single and multiple events. Also, it is aimed to understand in what distance from the measurement point, the procedure can still provide reliable results for this particular damage intensity.

For this, per Subsection 4.2.1, the reference ILs were computed for each truck considering all responses from difference transverse positions and with different noise contents. These were then used for future monitoring. Then, for each truck shown in Figure 4.11, two DI thresholds, one for single-truck events and the other for multiple-truck events (called thresholds 1 and 2, respectively), were computed. Extensive details were already provided in Subsection 4.2.1 and Figure 4.3.

At the monitoring stage, the same trucks introduced in Figure 4.11 were again used on the damaged bridge. For each damage scenario and truck, a separate analysis was performed and the strain response was obtained (33 responses overall). For single-truck events and multiple-truck events, the ILs of the damaged cases were obtained. The DIs were then computed and compared with the DI thresholds to see if they are greater than the thresholds. Based on

these results, the sensor placement should be updated if any of the damage scenarios are not covered by the system. A damage scenario with a DI value of smaller than threshold is called unsuccessful in this study. This is because one cannot ensure that the non-zero DI is necessarily due to a damage.

#### 4.3.3.7 Parametric study approach

As mentioned earlier, the proposed MPDP procedure should be repeated with different trucks with different configurations and weights. It is later shown in Section 4.4 that this can improve the bridge integrity monitoring results. To understand the reason why this improvement happens, a parametric study was performed to consider the effect of different factors on DI values.

When the type of truck is changed (from a 3-axle to a 5-axle, for instance), three factors may change: 1) gross vehicle weight, 2) axle weights 3) axle spacings. Thus, the 3-axle truck shown in Figure 4.11a was used as a reference, and its characteristics were changed one by one, and the DI values were compared with the reference 3-axle truck. Table 4.1 shows three different cases to consider the effect of the trucks' characteristics on the DI value. In Case 1, the gross vehicle weights (GVW) were changed compared to the reference 3-axle truck, but the axle weight ratios and axle spacings were the same. In Case 2, the GVWs and axle weight ratios were the same, and only the first axle spacings were altered, while in Case 3, only the axle weight ratios were changed, and the other two factors remained constant.

Table 4.1: Different configurations of the 3axle truck used for parametric study

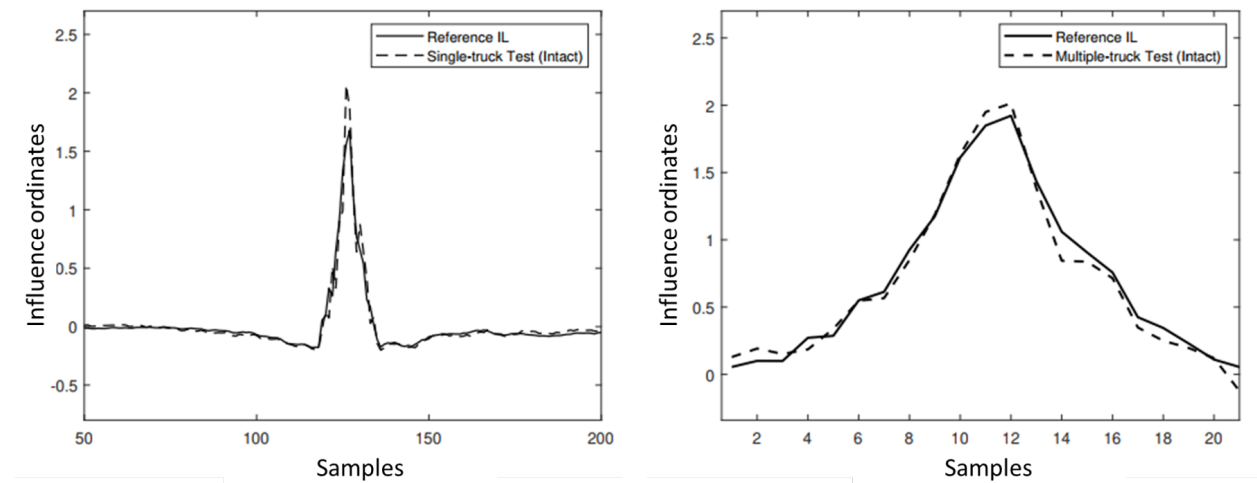
Case no.	Truck no.	Axle weight (ton)			GVW (ton)	Axle spacing (m)	
		$AW_1^a$	$AW_2$	$AW_3$		$AS_1^b$	$AS_2$
1	1	18.20	14.20	14.20	46.6	4.5	1.3
	2	13.65	10.65	10.65	34.95	4.5	1.3
	3	6.07	4.73	4.73	15.53	4.5	1.3
	4	4.55	3.55	3.55	11.65	4.5	1.3
2	5	9.10	7.10	7.10	23.30	6.0	1.3
	6	9.10	7.10	7.10	23.30	3.0	1.3
3	7	11.10	6.10	6.10	23.30	4.5	1.3
	8	13.10	5.10	5.10	23.30	4.5	1.3
	9	7.10	8.10	8.10	23.30	4.5	1.3
	10	7.77	7.77	7.77	23.30	4.5	1.3
	11	16.10	3.60	3.60	23.30	4.5	1.3

<sup>a</sup>AW=Axle weight, <sup>b</sup>AS=Axle spacing

## 4.4 Discussion of Results

### 4.4.1 Reference ILs and thresholds

As discussed earlier in Subsection 4.2.1, the first step for bridge health monitoring using the proposed MPDP approach is to compute two reference ILs (IL1 for the single-truck event and IL2 for the multiple-truck event) for each SHM truck (shown in Figure 4.11), including the effect of noise and transverse position. Figures 4.13a and 4.13b compare the reference IL1 and 2, respectively, against the ILs extracted from a single 5-axle and two 5-axle trucks on the intact bridge. This helps to make sense of how these reference ILs may look like compared to the future ILs at the monitoring stage. The shape of the reference ILs (Figures a and b) are obviously different since IL1 is obtained using the entire strain response while IL2 is obtained only using the localized portions. Figure 4.13a shows that the reference IL1 is



(a) Reference IL1 vs. the IL of a single-truck event (a 5-axle truck) (b) Reference IL2 vs. the IL of a multiple-truck event (Two 5-axle trucks)

Figure 4.13: Reference IL vs. IL of the intact bridge subjected to test trucks

overall in good agreement with IL at the monitoring stage at most points. A larger difference is appeared at the peak point that is caused by transverse position change included in the reference IL. Figure 4.13b shows a great agreement between the IL under a multiple-truck event versus the reference IL. This shows how successful the MP-IL has decomposed the strain response associated with each truck.

In the next step, the DI values and thresholds were computed for each truck-event and per Subsection 4.2.1 and Figure 4.3. Table 4.2 shows the computed DI values for each truck-event and in different transverse positions and noise contents (nine for each truck-event and fifty-four for all). According to Table 4.2, overall, the noise and transverse position factors can make a maximum DI variation of 0.068 and 0.4 for the single-truck and multiple-truck events, respectively. This table also shows the computed thresholds for each SHM truck (single and multiple-vehicle cases), based on nine runs for each combination. As an example, the confidence interval (95% confidence) for the single 5-axle truck is  $0.039 \pm 0.008$ , with an upper limit (threshold) of 0.047.

Table 4.2: Thresholds and the DI values for different trucks on the intact bridge in different transverse positions and with different noise contents

Truck Type	Event Type	Transverse Position 1			Transverse Position 2			Transverse Position 3			Threshold (UL <sup>b</sup> )
		NC1 <sup>a</sup>	NC2	NC3	NC1	NC2	NC3	NC1	NC2	NC3	
3-axle		0.066	0.084	0.073	0.020	0.016	0.023	0.038	0.071	0.049	0.066
4-axle	Single	0.044	0.056	0.050	0.018	0.009	0.013	0.034	0.038	0.050	0.046
5-axle		0.042	0.045	0.060	0.039	0.026	0.019	0.046	0.031	0.039	0.047
3-axle		0.130	0.115	0.163	0.229	0.195	0.199	0.307	0.389	0.315	0.287
4-axle	Mult.	0.244	0.317	0.220	0.351	0.306	0.401	0.620	0.452	0.540	0.471
5-axle		0.210	0.286	0.288	0.271	0.269	0.220	0.176	0.296	0.193	0.275

<sup>a</sup>NC=Noise content, <sup>b</sup>UL=Upper limit with 95% confidence

#### 4.4.2 Single-truck and multiple-truck events

Now that the reference ILs and the thresholds were obtained, eleven different damage scenarios shown in Figure 4.10b were tested to understand if the proposed MPDP SHM procedure can be used when any of the damage scenarios occur. Thus, each truck moved once for each damage scenario (a total of eleven for each truck and thirty-three for all trucks) in a single-truck event, and the new ILs and accordingly, the DI values were obtained. Figure 4.14 shows the DI values for each truck and each damage scenario. Colored elements in Figure 4.14 mean that the DI values are greater than the DI thresholds specified in Table 4.2. In other words, for these damage scenarios with colored elements, one can conclude that the damage has occurred with 95% confidence.

The purpose of using several trucks was to improve the bridge monitoring accuracy. In fact, the SHM outcome will be the summation of all covered elements for each truck type. However, Figure 4.14 shows that for single-truck events, any one of the SHM trucks could be enough to realize if any damage has occurred in the region of interest (shown in Figure 4.10b). This is because, for all damage scenarios and truck types, the DI values were significantly



greater than the thresholds. Figure 4.15a shows an example to reveal how the damaged IL looks like compared to the reference IL1 for damage scenario 2.

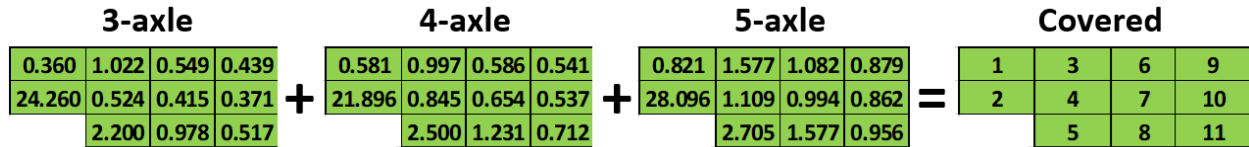
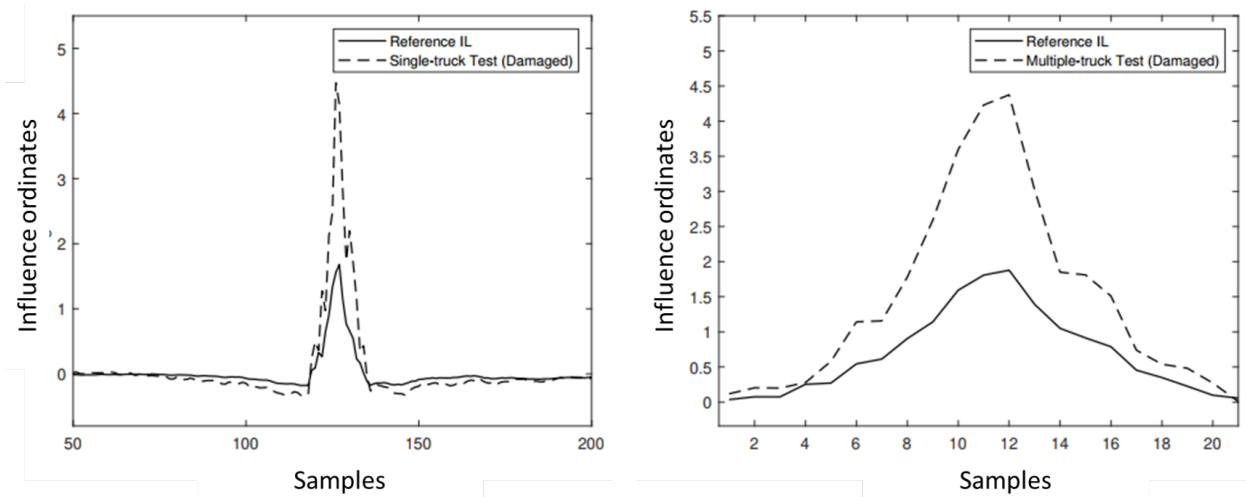


Figure 4.14: The DI values for the damaged bridge under a single truck and the corresponding damage positions

However, as mentioned in Subsection 4.2.1, sometimes, multiple trucks will be simultaneously on the bridge at the monitoring stage that should be handled with the new IL extraction technique (MP-IL). To evaluate the capability of the MP-IL technique, thirty-three multiple-truck analyses were conducted using each truck (i.e., two in-one-row 3-axle trucks, etc.) and for each damage scenario. The DI values are shown in Figure 4.16 for each multiple-truck event. According to Figure 4.16, damage scenarios 2, 3, 4, 5, 7, 8 are covered using all trucks. However, some other damage scenarios are only covered by a certain truck type (1, 6, 11), and some (9, 10) are not covered at all. Considering all truck types, only two damage scenarios are not covered. This shows that the MPDP procedure can work effectively even for multiple-truck events, and also, the idea of incorporating different types of trucks could improve the accuracy. Figure 4.15b shows an example to compare the damaged IL with the reference IL2 for damage scenario 2.

According to the results for single-truck and multiple-truck events, it can be concluded that the single-truck events can more easily identify the damage, and only one truck can be enough. This is because, in the standard IL technique used for single-truck events, the entire strain will be used while MP-IL first removes the non-localized portion to decompose the strain responses associated with each truck. Thus, the single-truck events are more likely to generate a higher value than the threshold and capture the damage. However, the standard



(a) Single 5-axle truck (DI=28.096)

(b) Multiple 5-axle trucks (DI=24.640)

Figure 4.15: Reference IL vs. the IL of the damaged bridge with damage scenario 2

IL and MP-IL are complementary, and both are needed for the dual-purpose SHM procedure since it is not guaranteed to only have one truck on the bridge during the bridge monitoring process.

Now that it is shown the damage scenarios in the region of interest (shown in Figure 4.10b) in the top-right quadrant can be effectively covered, it can be extended to other quadrants around each sensor, assuming a similar structural behavior in those regions. This assumption was made due to symmetry and to reduce the required analysis time since each analysis in CSI Bridge software takes 70 minutes. These results are the outcome of a minimum of 110 hours of effective analysis time.

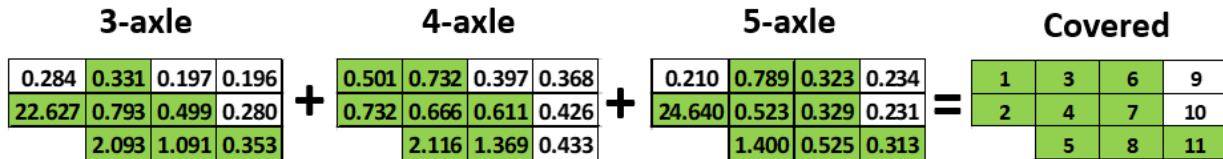


Figure 4.16: The DI values for the damaged bridge under multiple trucks and the covered damage positions

### 4.4.3 Updated sensor placement

Lastly, the instrumentation plan should be updated to effectively work for both BWIM and SHM to cover all damage scenarios for the damage intensity considered. It was mentioned in Subsection 4.3 that the initial distance between the successive sensors was selected to be 1.6m per previously published BWIM studies. It was observed that all damage scenarios were covered in single-truck and multiple-truck events except for scenarios 9 and 10 in the latter event. Thus, the successive distance between the sensors should be updated to 0.8 to 1 m (0.4-0.5 m from each sensor) for maximum effectiveness.

### 4.4.4 Parametric study

In this subsection, a parametric study is provided to answer what factors may change when the SHM truck type is changed and how these factors may affect the DI values and the SHM approach effectiveness. It was already explained in Subsection 4.2.1 that changing the truck characteristics can change the DI values slightly. Here, we are going to quantify these variations. So far, it was explained that the same truck should be used at the calibration and monitoring stages. But, now, it is also aimed to explain whether one is allowed to change the GVW or axle weights ratios even if the same truck is used. Additionally, this parametric study is to show how axle spacing change can affect the DI values in a case that a similar truck with the same number of axles and weight is available but the axle spacings are slightly different.

Different factors may change when a different truck is used. These include gross vehicle weight (GVW), axle weights' ratios, and axle spacings. To consider the effect of these factors (GVW, axle weights' ratios, and axle spacings), three cases (all 3-axles) with different characteristics (introduced in Table 4.1) were considered and compared with the original 3-

axle truck as a reference (shown in Figure 4.11a). According to this table, in each case (1,2, and 3), only one parameter is changed. For instance, in Case 1, only GVW is changed and other factors (axle spacings, etc) are constant for all trucks. To ensure that the trucks at the monitoring and calibration stages are exactly the same except for the target parameter, a reference IL was computed for each truck in Table 4.1. The same truck was then used on the damaged bridge with damage scenario 8. Also, noise and transverse positions were not included to ensure that the target parameter is the solely changing factor.

In Case 1, all trucks had the same axle weights' ratios and axle spacings, but their GVWs differed. According to the results shown in Figure 4.17, the DI values for Trucks 1 through 4 were all similar numbers ( $0.576 < DI < 0.600$ ) compared to the original 3-axle truck ( $DI=0.599$ ). In Case 2, the second axle spacing changed from 4.5m to 6m (Truck 5) and 3m (Truck 6), while the GVWs and axle weights' ratios were constant. The DI variation was slightly higher than Case 1 (0.655 for Truck 5 and 0.535 for Truck 6). In Case 3, only the axle weights' ratios changed, and the other two factors remained constant. According to the results, the DI values varied from 0.526 for Truck 7 to 0.646 for Truck 10.

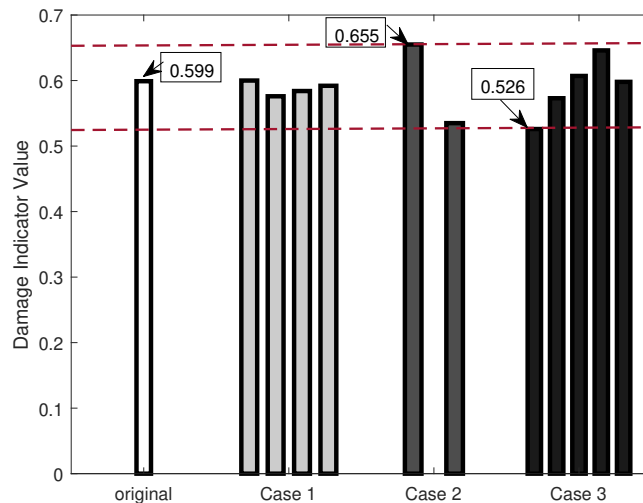


Figure 4.17: DI values for the cases specified in Table 4.1

According to the results, as expected, all parameters (GVW, axle weights' ratios, and axle spacings) can slightly change the IL and subsequently DI values. Thus, it is ideal to hold all truck characteristics at the monitoring stage to be exactly the same as the calibration stage. This can happen by using the same truck with the same axle configurations and with empty containers. This can also happen if one use the same block loads (e.g., concrete blocks) at certain places inside the trucks' containers. Among all, GVW change made the smallest variation on the DI values (variation range=0.024) while other two factors had a same variation of 0.12. Thus, it can be concluded that GVW variation does not make a huge inaccuracy as long as other two factors remain the same.

Overall, it seems that the DI value range is in good agreement to the original DI related to the reference 3-axle truck. Also, variation due to changing parameters is within the range of variation due to transverse position and noise shown in Table 4.2. This shows that the IL extraction technique can successfully remove the effect of the truck characteristics and make it unique for a particular bridge, but still, some variations exist. However, this variation was shown earlier in Figure 4.16 to be a positive factor for this study. In fact, it can be acceptable and even positive as long as we use separate reference ILs and DI thresholds for each truck (Table 4.2).

## 4.5 Conclusions and Future Study

In this study, a multiple-presence dual-purpose (MPDP) structural health monitoring (SHM) approach is proposed to monitor the integrity of bridges (level I damage detection) using the BWIM system existing sensors. This procedure uses a novel multiple presence IL (MP-IL) technique for SHM application that can effectively handle the multiple presence issue. The proposed SHM procedure makes the application of the integrated BWIM and SHM systems

more realistic and practical. Also, other factors such as noise and transverse position (defined as false damage indicators) are also considered in the proposed procedure to provide a more realistic bridge health monitoring approach. The following conclusions were made:

As observed, the noise and transverse position factors had a significant effect on the damage indicator (DI) values. It was explained that this can make a false damage indicator. However, it was shown that the DI thresholds computed based on the DI variation caused by noise and transverse position, can improve the accuracy of the bridge monitoring compared to other studies even in highly noisy environment and when transverse position change exists. This is called “improvement” because when the DI is greater than the thresholds, one can say (with 95% confidence) that a damage has occurred. However, when the threshold is not included in the process, any non-zero DI value can be a sign of damage while this value can be due to transverse position change or noise, and not necessarily damage.

In this study, eleven damage scenarios were considered and three SHM trucks (a 3-axle, a 4-axle, and a 5-axle) were used to improve the SHM accuracy. However, it was shown that using multiple SHM trucks is not needed for the single-truck events, and for the considered damage intensity, using each of these trucks can easily detect all damage scenarios. However, in multiple-truck events, some damage scenarios were only detected using a certain truck and incorporating different trucks overall improved the accuracy. Thus, it can be concluded that the single-truck events can more easily identify damage. This is because for the single-truck events, the standard IL technique has been used. This takes the entire strain. However, in multiple-truck events, MP-IL should be used. This first removes the non-localized strain response to decompose the strain responses associated with each truck. Thus, the single-truck events are more likely to generate a larger value than the threshold and generate a reliable sign for the damage. However, the standard IL and MP-IL are complementary, and both are needed for the MPDP SHM procedure since it is not guaranteed to only have one truck

on the bridge during the bridge monitoring process. Also, as shown, for the multiple-truck events, overall, all damage scenarios were detected except for only two of them. This shows that the MPDP procedure can work effectively even for multiple-truck events, particularly when different types of trucks were incorporated.

To make the sensor placement even more effective for both the BWIM and SHM in multiple-truck events, an updated instrumentation plan was proposed. According to the monitoring results, the successive distance between the strain gauges should be decreased to 0.8-1 m. This was selected based on the distance of the damage scenarios that did not generate DIs greater than the thresholds.

Several cases were considered to study the effect of the truck characteristics. In Case 1, all trucks had the same axle weights' ratios and axle spacings, but their GVWs changed. The DI values for Trucks 1 through 4 were all similar numbers with a variation range of 0.024. Thus, it can be concluded that GVW variation does not make a huge inaccuracy as long as other two factors remain the same. In Case 2, the second axle spacing changed and the axle weights' ratios and GVWs were constant. The DI variation was 0.12 which was slightly higher than Case 1. In Case 3, only the axle weights' ratios changed, and the other two factors remained constant, and a similar variation range to Case 2 was resulted. However, it was concluded that the DI values were all in good agreement to the DI value of the reference truck. This slight variation can be a positive factor for SHM application, as long as separate reference IIs and DI thresholds are used for each truck. This makes it a reasonable practice for a real-world application since one is able to use the same trucks for both calibration and monitoring stages. This is called a "positive factor" since, according to the results, for each truck type (3-axle, 4-axle, and 5-axle), only some damage scenarios were covered that were not covered by others. Thus, superposing all damage detection results by different truck types helped to improve the monitoring results.

In this study, the capability of the MPDP SHM procedure for single and multiple-truck events was numerically shown. However, as a future study, experimental evaluation on multiple bridges with different structures is needed. It is necessary to carefully include the factors considered in this study (such as transverse position and noise) and not considered (such as temperature change).



# Chapter 5

## Discussion and Future Work

This dissertation reports the results of a three-phase study. The motivation for this study was to effectively integrate the BWIM and SHM systems and to provide a single system that can be used for traffic monitoring and SHM applications on the long-span bridges. In this study, a novel BWIM technique was proposed that can make the integrated systems more practical for commercial applications. This can handle the multiple-presence events on long-span bridges. Incorporating the novel BWIM, a dual-purpose SHM procedure was then proposed for monitoring of bridges under multiple-presence events. An updated, cost-effective sensor placement is also proposed to make the system even more effective for SHM and BWIM purposes. The results of this study are summarized below:

### 5.1 Phase 1: NOR-BWIM Used for Long-span Bridges

The first phase was an experimental case study on the Smart Road (SR) bridge to evaluate the accuracy of NOR-BWIM systems and the static weight estimation techniques on the long-span concrete box girder bridges. This was to understand if long-span concrete box girder bridges with thicker top slabs can still provide sharp peaks for prerequisite estimation depending on construction and sensor placement. Also, it was aimed to see if the level of error due to dynamic effects is still in a reasonable range, and one can actually still use the long-spans for NOR-BWIM. This phase did not still deal with multiple presence issue

in weight estimation and SHM applications, but considered the multiple presence events in prerequisite estimation. Also, an effective sensor placement was proposed to be used for the prerequisite estimation (the truck speed, number of axles, axle spacing), weight, and truck lane position.

- The results demonstrated that when the strain gauges are placed where maximum strains due to maximum local deflections occur, clear peaks will appear in the strain response. This was as close as possible to the wheel path. Dealing with the closely-spaced axles has usually been a challenging issue in the literature. However, the proposed sensor placement illustrated a great success in this regard such that no error was observed for the number of axles. According to the results, the mean absolute error (MAE) for speed was 2.56% with a variation between 1.42% to 3.7% with 95% confidence. Furthermore, the mean-absolute-error for axle spacings 1, 2, 3, and 4 were 2.00%, 4.30%, 0.73%, and 1.15%, with an upper limit of 2.79%, 6.12%, 1.25%, and 1.93%, respectively. Thus, the NOR-BWIM system can still work accurately for prerequisite estimation in single-truck events. This was shown that it can also work effectively for prerequisite estimation in multiple-truck events as well.
- Like the single-truck events, quite clear peaks resulted for each truck in in-one-row events. According to the results, in both runs and for both trucks, the axle spacing estimation errors for the 5-axle truck were all less than 2.5%. Similarly, the speed estimation errors for both runs and trucks were also low (less than 2.1%). This shows that the NOR-BWIM system works accurately on the long-span, concrete-box-girder bridge even if multiple trucks are concurrently on the bridge.
- According to the results, the proposed sensor placement was also capable of detecting the truck lane position. Only two strain gauges, one under the right lane and one

under the left lane, were enough.

- This was also demonstrated that the MAE of the GVW estimation came out to be 4.60% with an upper limit of 6.66% with 95% confidence. According to the results, in 11 out of 14 cases, the error was less than 5.5%, and only one case had an error greater than 10%. Also, the dynamics effects were in a reasonable range and did not make huge errors; thus, MLE can still be used for long-span bridges with similar characteristics to the SR bridge.
- It was already discussed that various types of construction could have different load-transfer mechanisms from the slab to other components. A concrete-box-girder bridge was considered in this study, and other construction methods should be addressed in a future study. Additionally, only a single experimental test on long-span bridges cannot be enough for a solid conclusion about the accuracy of the NOR BWIM system. More experimental tests on other long-span bridges should be conducted as a future study. Also, due to some restrictions, the axle weights were not measured, and therefore, the focus was only on the GVW estimation. However, in the BWIM area, axle weight estimation is usually more challenging. Other factors such as temperature change should also be considered carefully. In this study a simple (not necessarily accurate) method was used to remove the effect of temperature (please see the MATLAB codes). However, it is suggested to place some thermocouples on the concrete surface where the strains will be measured (in the future experimental studies). This helps to more accurately remove the effect of the temperature from the strain response. When temperature change is included, it is suggested to perform a parametric study on speed change to see how the results will be affected by.

## 5.2 Phase 2: Novel BWIM for Multiple-vehicles Events

Now that the first shortcoming of the literature was addressed, it was needed to resolve the second issue associated with the current BWIM studies, before using it for SHM. Thus, the second phase reports the results of a study on a novel bridge-weigh-in-motion (BWIM) technique, called multiple-presence (MP) NOR BWIM, addressing the significant shortcoming of the existing BWIMs (multiple-truck events). The proposed technique dealt with an arbitrary number of trucks and lightweight vehicles simultaneously crossing the bridge in any traffic configuration. This includes in-one-row and zigzag patterns, side-by-side trucks, and a combination of heavy trucks with lightweight vehicles. A detailed FE model was simulated and validated against the experimental data to evaluate the performance of the MP NOR BWIM technique in single and multiple-truck events. On an actual bridge, it is almost impossible to make the complex multiple-truck events without lane closure, and the FE model was to resolve this issue. Since it was validated against experimental data, realistic outcomes were expected.

- The proof-of-concept step was to ensure that removing the non-localized strain does not eliminate much important information. The results demonstrated that the proposed approach improves the GVW estimation accuracy by about 1.9% (from 4.1% error to 2.2%) for lane one and about 2.4% (from 4.8% to 2.4%) for lane two. However, a slight increase was observed in the axle weights. This increase in axle weight estimation errors can be ignored since they were still in a reasonable range. Simultaneously, the GVW estimation accuracy was improved, and multiple-truck weight estimation was enabled.
- The proposed approach was tested on six multiple-truck events, including two in-one-row events, two zigzag-pattern events, a side-by-side case, and a complex multiple-

vehicle event with three trucks and two lightweight vehicles distributed in all three lanes. According to the results, the proposed approach successfully decomposed the strain responses associated with each truck and accurately estimated the GVWs and axle weights. The MAE of GVW and axle weights were 4.5% and 11.3%, respectively. These results are quite comparable with expensive pavement-based WIM systems and traditional BWIM technologies.

- In this phase, three techniques were used to remove the non-localized strain response. These include a manual process, a high-pass filter with low cut-off frequency, and envelope function. Furthermore, the most accurate one was suggested (envelope function). Other possible techniques might improve the results. This is left for a future study. Also, it is true that a validated model against experimental data was used to provide realistic results. However, the proposed approach should be evaluated experimentally under multiple-truck events and on bridges with different structures and span lengths. Other challenging factors such as temperature change and transverse positions should be considered.

Additionally, a parametric study should be performed to consider the effect of trucks' distances in multiple-truck events to see if the proposed NOR-BWIM approach still works accurately. Also, in this study, the trucks' speeds were all constant and it is suggested to change the truck's speeds in future studies to see if the results will be affected.

## 5.3 Phase 3: Novel SHM-BWIM for Multiple-vehicle Events

Now that it was shown that the NOR-BWIM system can still be effective on long-span concrete box girder bridges and the multiple-presence issue was also addressed, it can be used for SHM application. Thus, in the last phase of this study, a multiple-presence dual-purpose (MPDP) structural health monitoring (SHM) approach was proposed. In this procedure, the proposed BWIM system in the second phase dealt with multiple-truck events. The proposed SHM procedure makes the application of the integrated BWIM and SHM systems more realistic and practical. Also, noise and transverse position were included in the procedure to further address the current studies' shortcomings and provide a more realistic SHM approach.

- As expected, the noise and transverse position factors significantly affected the damage indicator (DI) values. It was explained that this could make a false damage indicator. However, it was also shown that the DI thresholds computed based on the DI variation caused by noise and transverse position can improve the bridge monitoring accuracy even in a highly noisy environment and when transverse position change exists. This is called “improvement” because when the DI is greater than the thresholds, one can say (with 95% confidence) that a damage has occurred. However, when the threshold is not included in the process, any non-zero DI value can be a sign of damage while this value can be due to transverse position change or noise, and not necessarily a damage.
- In this phase, eleven damage scenarios were considered, and three SHM trucks (a 3-axle, a 4-axle, and a 5-axle) were used to improve the SHM accuracy. However, it was shown that multiple SHM trucks are not needed for single-truck events. For the damage intensity considered, using each of these trucks can be enough to easily

detect all damage scenarios. However, in multiple-truck events, some damage scenarios were only detected using a particular truck, and incorporating different trucks overall improved the accuracy. Thus, it can be concluded that the single-truck events can more easily identify the damage. However, the standard IL and MP-IL are complementary. Both are needed for the MPDP SHM procedure since it is not guaranteed to only have one truck on the bridge during the bridge monitoring process. Also, as shown, for the multiple-truck events, overall, all damage scenarios were detected except for only two of them. This shows that the SHM procedure can work effectively even for multiple-truck events, particularly when different types of trucks are incorporated.

- To make the sensor placement even more effective for both the BWIM and SHM in multiple-truck events, an updated instrumentation plan was proposed. According to the results, the successive distance between the strain gauges should be decreased to 0.8 m. This was selected based on the distance of the damage scenarios that did not generate DIs greater than the thresholds to the measurement points.
- A parametric study was conducted, and several cases were considered and compared with a reference truck to consider the effect of the truck type. Three cases were considered, and each time, only a single parameter was changed. These parameters were axle weight ratio, axle spacing, and GVW. The results showed that the DI values were all in good agreement compared to the DI value of the reference truck. This shows that the MP-IL technique can provide a relatively unique IL even when the truck type is changed. However, still, a slight variation was observed. However, it was shown that this variation is a positive factor for SHM application, as long as separate reference ILs and DI thresholds are computed for each truck. This is called a “positive factor” since according to the results, for each truck type (3-axle, 4-axle, and 5-axle), only some damage scenarios were covered that were not covered by others. Thus, superposing

all damage detections using different truck types helped to improve the monitoring results.

- In this study, the capability of the MPDP SHM procedure for single and multiple-truck events was numerically shown. However, as a future study, experimental evaluation on multiple bridges with different structures is needed. It is necessary to include the factors considered in this study (such as transverse position and noise) and not considered (such as temperature change). Also, the effects of long-term variation in material properties (e.g. modulus of elasticity) should be included. The goal will be to realize how to distinguish between the change made in the IL due to material properties change and damage.

Also, as explained, the damage was simulated by removing an element from the top slab as a proof-of-concept. However, more realistic damage scenarios should also be simulated in the future studies such as bearing seizure, differential settlement, great prestress loss, and corrosion.



# Appendices

# Appendix A

## Bridge Bearings Stiffness Values

In this section, the stiffness values of the bearings in three directions, i.e., horizontal, vertical, and rotational, are computed. The stiffness expressions for the elastomeric bearings can be derived using solid mechanics. Three different deformations should be considered (axial, shear, and rotational), and the corresponding stiffness values should then be computed. A stiffness value is a required force that makes a unit deflection in a particular direction. However, due to the nonlinear behavior of the rubber, some empirical relations should still be included for a more accurate bridge analysis. International codes usually have design methods that include these nonlinear factors. In this study, part 4 (bearings and deck joints) of the Australian Standard [93] is used. This Standard (clause 12.7) explicitly provides the expressions for the elastomeric bearing stiffnesses in all directions. All equations provided below are for rectangular bearings and are extracted from the Australian Standard. The required section can be downloaded in this link: [http://files.engineering.com/getfile.aspx?folder=d01afd12-9fc6-4910-a548-5013e78c7341&file=Elastomeric\\_Bearings.pdf](http://files.engineering.com/getfile.aspx?folder=d01afd12-9fc6-4910-a548-5013e78c7341&file=Elastomeric_Bearings.pdf).

The bearings' dimensions were already provided in Table 3.1 in Chapter 3. Also, two more parameters are needed for the following computations, shear modulus (G) and bulk modulus (B). These parameters should usually be provided by the bearing producer. However, since there was no information about them, they were assumed to be 0.69 and 2000 MPa, respectively.

## A.1 Compressive stiffness

The compressive stiffness should be computed per Equation (A.1)

$$K_c = \frac{1}{\sum \frac{1}{K_{cn}}}, \quad (\text{A.1})$$

where  $K_{cn}$  is the compressive stiffness of layer n and should be computed using Equation (A.2):

$$K_{cn} = \frac{E_c A_b}{t_n}, \quad (\text{A.2})$$

in which:

$t_n$  = the thickness of each elastomer layer = two 0.635-cm and eight 1.27-cm layers

$A_b$  = the bonded surface area = 0.83 m<sup>2</sup>

$E_c$  = the effective compression modulus of elastomer and should be computed using Equation (A.3):

$$E_c = 4G \left[ 1 - \left( \frac{q}{1+q^2} \right)^2 \right] + \left[ \frac{C_1 G S^2}{1 + \frac{C_1 G S^2}{0.75B}} \right], \quad (\text{A.3})$$

where:

q = minimum value of the side-to-side elastomer ratios, i.e., min (a/b, b/a),

$C_1$  = a constant dependent on the bearing shape and should be computed using Equation (A.4):

$$C_1 = 4 + q(6 - 3.3q). \quad (\text{A.4})$$

Since the bearings are square,  $q$  is going to be 1 and accordingly,  $C_1$  will be 6.7.

Additionally,  $S$  is the elastomer shape factor for each layer. This is equal to the plan area divided by the lateral area of a layer. This comes up to be 18 for this bearing considered in this study.

According to Equation (A.3), parameters computed above, and shear and bulk modulus values introduced earlier in this section,  $E_c=751.4$  MPa. Then, using Equation (A.2), for the 1.27-cm layers,  $K_{cn} = 491.1 \times 10^5$   $KN/m$  and for the 0.635-cm layers,  $K_{cn} = 982.1 \times 10^5$   $KN/m$ . Lastly, according to Equation (A.1) and knowing that we have eight 1.27-cm and two 0.635-cm layers, the compressive stiffness comes up to be  $K_c = 5456605$   $KN/m$ .

## A.2 Shear stiffness

The shear stiffness should be computed per Equation (A.5)

$$K_c = \frac{A_r G}{t}, \quad (\text{A.5})$$

where  $A_r$  is the average rubber layer plan ( $0.83$   $m^2$ ) and  $t$  is the total thickness of the rubber and for this particular bearing is 11.43 cm. According to Equation (A.5),  $K_s = 5010.5$   $KN/m$ .

### A.3 Rotational stiffness

The rotational stiffness should be computed per Equation (A.6)

$$K_c = \frac{1}{\sum \frac{1}{K_{rn}}}, \quad (\text{A.6})$$

where  $K_{rn}$  is the rotational stiffness of layer n and should be computed using Equation (A.7):

$$K_{cn} = \frac{E_r I}{t_n}, \quad (\text{A.7})$$

in which:

$I$ = moment of inertia about the axis of rotation=0.057  $m^4$ ,

$E_r$ = the effective rotational modulus of elastomer and should be computed using Equation (A.8):

$$E_r = 4G \left[ 1 - \left( \frac{m}{1 + m^2} \right)^2 \right] + \left[ \frac{C_2 G S^2}{1 + \frac{C_2 G S^2}{0.75B}} \right], \quad (\text{A.8})$$

where:

$m$ = ratio of the sides of a rectangular laminated elastomeric bearing (a/b)

For a square elastomer, this will be 1. Also,

$C_2$ = a constant dependent on the bearing shape and should be computed using Equation (A.9):

$$C_2 = 4 - \frac{32}{10 + m(4 + 3m + m^2)}, \quad (\text{A.9})$$

According to Equation (A.9),  $C_2$  is going to be 2.2 for this particular bearing. Also, according to Equation (A.8),  $E_r=372.5$  MPa. Then, using Equation (A.7), for the 1.27-cm layers,  $K_{cn} = 1672 \times 10^3$  *KN.m/m* and for the 0.635-cm layers,  $K_{cn} = 3343.7 \times 10^3$  *KN.m/m*. Lastly, according to Equation (A.6) and knowing that we have eight 1.27-cm and two 0.635-cm layers, the rotational stiffness comes up to be  $K_r = 185776$  *KN.m/m*.

# Bibliography

- [1] C. Wang, H. Zhang, Q. Li, Reliability assessment of aging structures subjected to gradual and shock deteriorations, *Reliability Engineering & System Safety* 161 (2017) , pp. 78–86.
- [2] W. Han, J. Wu, C. Cai, S. Chen, Characteristics and dynamic impact of overloaded extra heavy trucks on typical highway bridges, *Journal of Bridge Engineering* 20 (2015) 05014011.
- [3] F. Huseynov, C. Kim, E. OBrien, J. Brownjohn, D. Hester, K. Chang, Bridge damage detection using rotation measurements—experimental validation, *Mechanical Systems and Signal Processing* 135 (2020) 106380.
- [4] B. Heitner, F. Schoefs, E. J. OBrien, A. Žnidarič, T. Yalamas, Using the unit influence line of a bridge to track changes in its condition, *Journal of Civil Structural Health Monitoring* 10 (2020) 667–678.
- [5] S. M. Khan, S. Atamturktur, M. Chowdhury, M. Rahman, Integration of structural health monitoring and intelligent transportation systems for bridge condition assessment: current status and future direction, *IEEE Transactions on Intelligent Transportation Systems* 17 (2016) 2107–2122.
- [6] T. Bao, S. K. Babanajad, T. Taylor, F. Ansari, Generalized method and monitoring technique for shear-strain-based bridge weigh-in-motion, *Journal of Bridge Engineering* 21 (2016) 04015029.

- [7] Z.-W. Chen, S. Zhu, Y.-L. Xu, Q. Li, Q.-L. Cai, Damage detection in long suspension bridges using stress influence lines, *Journal of Bridge Engineering* 20 (2015) 05014013.
- [8] F. Moses, Weigh-in-motion system using instrumented bridges, *Journal of Transportation Engineering* 105 (1979).
- [9] F. Moses, Instrumentation for weighing truck-in-motion for highway bridge loads, Technical Report, 1983.
- [10] M. Lydon, S. E. Taylor, D. Robinson, A. Mufti, E. Brien, Recent developments in bridge weigh in motion (b-wim), *Journal of Civil Structural Health Monitoring* 6 (2016) 69–81.
- [11] T. Ojio, C. Carey, E. J. OBrien, C. Doherty, S. E. Taylor, Contactless bridge weigh-in-motion, *Journal of Bridge Engineering* 21 (2016) 04016032.
- [12] J. Lee, K.-C. Lee, S. Jeong, Y.-J. Lee, S.-H. Sim, Long-term displacement measurement of full-scale bridges using camera ego-motion compensation, *Mechanical Systems and Signal Processing* 140 (2020) 106651.
- [13] E. O'Brien, D. Hajializadeh, N. Uddin, D. Robinson, R. Opitz, Strategies for axle detection in bridge weigh-in-motion systems, in: *Proceedings of the international conference on weigh-in-motion (ICWIM 6)*, 2012, pp. 79–88.
- [14] M. Lydon, D. Robinson, S. Taylor, G. Amato, E. Brien, N. Uddin, Improved axle detection for bridge weigh-in-motion systems using fiber optic sensors, *Journal of Civil Structural Health Monitoring* 7 (2017) 325–332.
- [15] H. Kalhori, M. M. Alamdari, X. Zhu, B. Samali, S. Mustapha, Non-intrusive schemes for speed and axle identification in bridge-weigh-in-motion systems, *Measurement Science and Technology* 28 (2017) 025102.



- [16] E. J. O'Brien, A. Žnidarič, W. Baumgärtner, A. González, P. McNulty, Weighing-in-motion of axles and vehicles for europe (wave), Report of work package 1 (2001).
- [17] J. Kalin, A. Žnidarič, I. Lavrič, Practical implementation of nothing-on-the-road bridge weigh-in-motion system, in: International symposium on heavy vehicle weights and dimensions, 2006.
- [18] W. He, L. Deng, H. Shi, C. Cai, Y. Yu, Novel virtual simply supported beam method for detecting the speed and axles of moving vehicles on bridges, *Journal of Bridge Engineering* 22 (2017) 04016141.
- [19] Y. Yu, C. Cai, L. Deng, Vehicle axle identification using wavelet analysis of bridge global responses, *Journal of Vibration and Control* 23 (2017) 2830–2840.
- [20] L. Deng, W. He, Y. Yu, C. Cai, Equivalent shear force method for detecting the speed and axles of moving vehicles on bridges, *Journal of Bridge Engineering* 23 (2018) 04018057.
- [21] W. He, T. Ling, E. J. OBrien, L. Deng, Virtual axle method for bridge weigh-in-motion systems requiring no axle detector, *Journal of Bridge Engineering* 24 (2019) 04019086.
- [22] D. Cantero, R. Karoumi, A. González, The virtual axle concept for detection of localised damage using bridge weigh-in-motion data, *Engineering Structures* 89 (2015) 26–36.
- [23] H. Wang, T. Nagayama, B. Zhao, D. Su, Identification of moving vehicle parameters using bridge responses and estimated bridge pavement roughness, *Engineering Structures* 153 (2017) 57–70.
- [24] Y. Wang, W.-L. Qu, Moving train loads identification on a continuous steel truss girder by using dynamic displacement influence line method, *International Journal of Steel Structures* 11 (2011) 109–115.

- [25] J. Dowling, E. J. OBrien, A. González, Adaptation of cross entropy optimisation to a dynamic bridge wim calibration problem, *Engineering Structures* 44 (2012) 13–22.
- [26] L. Deng, C. Cai, Identification of dynamic vehicular axle loads: theory and simulations, *Journal of Vibration and Control* 16 (2010) 2167–2194.
- [27] N.-B. Wang, L.-X. He, W.-X. Ren, T.-L. Huang, Extraction of influence line through a fitting method from bridge dynamic response induced by a passing vehicle, *Engineering Structures* 151 (2017) 648–664.
- [28] E. J. OBrien, M. Quilligan, R. Karoumi, Calculating an influence line from direct measurements, in: *Proceedings of the Institution of Civil Engineers-Bridge Engineering*, volume 159, Thomas Telford Ltd, 2006, pp. 31–34.
- [29] E. J. OBrien, C. W. Rowley, A. Gonzalez, M. F. Green, A regularised solution to the bridge weigh-in-motion equations, *International Journal of Heavy Vehicle Systems* 16 (2009) 310–327.
- [30] E. J. OBrien, L. Zhang, H. Zhao, D. Hajializadeh, Probabilistic bridge weigh-in-motion, *Canadian Journal of Civil Engineering* 45 (2018) 667–675.
- [31] H. Zhao, N. Uddin, E. J. O'Brien, X. Shao, P. Zhu, Identification of vehicular axle weights with a bridge weigh-in-motion system considering transverse distribution of wheel loads, *Journal of Bridge Engineering* 19 (2014) 04013008.
- [32] J. Richardson, S. Jones, A. Brown, E. O'Brien, D. Hajializadeh, On the use of bridge weigh-in-motion for overweight truck enforcement, *International Journal of Heavy Vehicle Systems* 21 (2014) 83–104.
- [33] X. Zheng, D.-H. Yang, T.-H. Yi, H.-N. Li, Development of bridge influence line iden-

- tification methods based on direct measurement data: A comprehensive review and comparison, *Engineering Structures* 198 (2019) 109539.
- [34] S.-S. Ieng, Bridge influence line estimation for bridge weigh-in-motion system, *Journal of Computing in Civil Engineering* 29 (2015) 06014006.
- [35] F. Carraro, M. S. Gonçalves, R. H. Lopez, L. F. F. Miguel, A. M. Valente, Weight estimation on static b-wim algorithms: A comparative study, *Engineering Structures* 198 (2019) 109463.
- [36] A. Moghadam, A signal-processing-based approach for damage detection of steel structures, Ph.D. thesis, Kansas State University, 2019.
- [37] L. Qiao, A. Esmaily, H. G. Melhem, Structural damage detection using signal pattern-recognition, in: *Key Engineering Materials*, volume 400, Trans Tech Publ, 2009, pp. 465–470.
- [38] P. Doyle, C. Scala, Crack depth measurement by ultrasonics: a review, *Ultrasonics* 16 (1978) 164–170.
- [39] P. C. Chang, S. C. Liu, Recent research in nondestructive evaluation of civil infrastructures, *Journal of materials in civil engineering* 15 (2003) 298–304.
- [40] M. Shariati, N. H. Ramli-Sulong, M. M. Arabnejad, P. Shafigh, H. Sinaei, Assessing the strength of reinforced concrete structures through ultrasonic pulse velocity and schmidt rebound hammer tests, *scientific research and essays* 6 (2011) 213–220.
- [41] F. J. Koch, L. C. Vandervalk, D. J. Beamish, High resolution ultrasonic coating thickness gauge, 1998. US Patent 5,723,791.

- [42] X. Xu, T. Xia, A. Venkatachalam, D. Huston, Development of high-speed ultrawideband ground-penetrating radar for rebar detection, *Journal of Engineering Mechanics* 139 (2013) 272–285.
- [43] R. Sarlo, P. A. Tarazaga, M. E. Kasarda, High resolution operational modal analysis on a five-story smart building under wind and human induced excitation, *Engineering Structures* 176 (2018) 279–292.
- [44] A. Moghadam, H. G. Melhem, A. Esmaily, A proof-of-concept study on a proposed ambient-vibration-based approach to extract pseudo-free-vibration response, *Engineering Structures* 212 (2020) 110517.
- [45] S. W. Doebling, C. R. Farrar, M. B. Prime, D. W. Shevitz, Damage identification and health monitoring of structural and mechanical systems from changes in their vibration characteristics: a literature review (1996).
- [46] G. Hearn, R. B. Testa, Modal analysis for damage detection in structures, *Journal of structural engineering* 117 (1991) 3042–3063.
- [47] J. Loya, L. Rubio, J. Fernández-Sáez, Natural frequencies for bending vibrations of timoshenko cracked beams, *Journal of sound and vibration* 290 (2006) 640–653.
- [48] J. Fernandez-Saez, L. Rubio, C. Navarro, Approximate calculation of the fundamental frequency for bending vibrations of cracked beams, *Journal of sound and vibration* 225 (1999) 345–352.
- [49] M. SoleimaniBabakamali, A. Moghadam, R. Sarlo, M. Hebdon, P. Harvey, Mast arm monitoring via traffic camera footage: a pixel-based modal analysis approach, *Experimental Techniques* 45 (2021) 329–343.

- [50] W. Heylen, S. Lammens, P. Sas, Modal analysis theory and testing, dept. of mech, Engrg., Katholieke Univ. Leuven, Heverlee, Belgium (1995).
- [51] N. Maia, J. Silva, E. Almas, R. Sampaio, Damage detection in structures: from mode shape to frequency response function methods, *Mechanical systems and signal processing* 17 (2003) 489–498.
- [52] Z. Shi, S. Law, L. Zhang, Structural damage localization from modal strain energy change, *Journal of sound and vibration* 218 (1998) 825–844.
- [53] T.-J. Huang, Z. Liang, G. C. Lee, Structural damage detection using energy transfer ratios(etr), in: *International Modal Analysis Conference(IMAC)*, 14 th, Dearborn, MI, 1996, pp. 126–132.
- [54] I. Kang, M. J. Schulz, J. H. Kim, V. Shanov, D. Shi, A carbon nanotube strain sensor for structural health monitoring, *Smart materials and structures* 15 (2006) 737.
- [55] A. Cardini, J. T. DeWolf, Long-term structural health monitoring of a multi-girder steel composite bridge using strain data, *Structural Health Monitoring* 8 (2009) 47–58.
- [56] J. J. Lee, Y. Fukuda, M. Shinozuka, S. Cho, C.-B. Yun, Development and application of a vision-based displacement measurement system for structural health monitoring of civil structures, *Smart Structures and Systems* 3 (2007) 373–384.
- [57] M. Breccolotti, M. Natalicchi, Bridge damage detection through combined quasi-static influence lines and weigh-in-motion devices, *International Journal of Civil Engineering* 20 (2022) 487–500.
- [58] Y. Zeinali, B. A. Story, Impairment localization and quantification using noisy static deformation influence lines and iterative multi-parameter tikhonov regularization, *Mechanical Systems and Signal Processing* 109 (2018) 399–419.

- [59] S. Zhang, Y. Liu, Damage detection in beam bridges using quasi-static displacement influence lines, *Applied Sciences* 9 (2019) 1805.
- [60] M. M. Alamdari, K. Kildashti, B. Samali, H. V. Goudarzi, Damage diagnosis in bridge structures using rotation influence line: Validation on a cable-stayed bridge, *Engineering Structures* 185 (2019) 1–14.
- [61] D. Cantero, A. González, Bridge damage detection using weigh-in-motion technology, *Journal of Bridge Engineering* 20 (2015) 04014078.
- [62] H. Kalhori, M. Makki Alamdari, X. Zhu, B. Samali, Nothing-on-road axle detection strategies in bridge-weigh-in-motion for a cable-stayed bridge: case study, *Journal of Bridge Engineering* 23 (2018) 05018006.
- [63] Y. Yu, C. Cai, L. Deng, State-of-the-art review on bridge weigh-in-motion technology, *Advances in Structural Engineering* 19 (2016) 1514–1530.
- [64] D. Dounsuvanh, P. Pheinsusom, Y. Sato, Thai truck loading monitoring using bwim system, *ASEAN Engineering Journal* 3 (2014) 55–67.
- [65] F. C. MS, A. VALENTE, R. LOPEZ, L. MIGUEL, R. PINTO, Effectiveness of the correlation approach for determination of vehicle velocity on real world nor-bwim data, *ICWIM8* (2019) 61.
- [66] K. Helmi, B. Bakht, A. Mufti, Accurate measurements of gross vehicle weight through bridge weigh-in-motion: a case study, *Journal of Civil Structural Health Monitoring* 4 (2014) 195–208.
- [67] A. Gonzalez, *Development of a Bridge Weigh-In-Motion System: A technology to convert the bridge response to the passage of traffic into data on vehicle configurations, speeds, times of travel and weights*, LAP Lambert Academic Publishing, 2010.

- [68] A. GONZALEZ, Development of Accurate Methods of Weighting Trucks in Motion, Ph.D. Thesis, Department of Civil Engineering, Trinity College, Dublin, Ireland, 2001.
- [69] L. Zhang, H. Zhao, E. J. OBrien, X. Shao, Virtual monitoring of orthotropic steel deck using bridge weigh-in-motion algorithm: Case study, *Structural Health Monitoring* 18 (2019) 610–620.
- [70] H. Wang, A. Li, J. Niu, Z. Zong, J. Li, Long-term monitoring of wind characteristics at sutong bridge site, *Journal of Wind Engineering and Industrial Aerodynamics* 115 (2013) 39–47.
- [71] M. Quilligan, R. Karoumi, E. J. O'Brien, Development and testing of a 2-dimensional multi-vehicle bridge-wim algorithm, in: 3rd International Conference on Weigh-in-Motion (ICWIM3), 2002, pp. 199–208. URL: <https://trid.trb.org/view/723285>.
- [72] S.-Z. Chen, G. Wu, D.-C. Feng, Development of a bridge weigh-in-motion method considering the presence of multiple vehicles, *Engineering Structures*, 191 (2019), pp. 724–739. doi:10.1016/j.engstruct.2019.04.095.
- [73] A. Žnidarič, I. Lavrič, J. Kalin, M. Kreslin, Using strips to mitigate the multiple-presence problem of bwim systems, in: 6th International Conference on Weigh-In-Motion (ICWIM 6) International Society for Weigh-In-Motion Institut Francais des Sciences et Technologies des Transports, de l'Aménagement et des Réseaux (IFSTARR) International Transport Forum Forum of European National Highway Research Laboratories (FEHRL) Transportation Research Board Federal Highway Administration, 2012. URL: <https://trid.trb.org/view/1265751>.
- [74] A. Moghadam, M. AlHamaydeh, R. Sarlo, Bridge-weigh-in-motion approach for simultaneous multiple vehicles on concrete-box-girder bridges, *Automation in Construction* 137 (2022) 104179.

- [75] E. J. OBrien, D. Cantero, B. Enright, A. González, Characteristic dynamic increment for extreme traffic loading events on short and medium span highway bridges, *Engineering Structures* 32 (2010) 3827–3835.
- [76] M. Ilbeigi, M. Ebrahimi Meimand, Statistical forecasting of bridge deterioration conditions, *Journal of Performance of Constructed Facilities* 34 (2020) 04019104.
- [77] H. Sekiya, K. Kubota, C. Miki, Simplified portable bridge weigh-in-motion system using accelerometers, *Journal of Bridge Engineering* 23 (2018) 04017124.
- [78] A. González, A. T. Papagiannakis, E. J. O’Brien, Evaluation of an artificial neural network technique applied to multiple-sensor weigh-in-motion systems, *Transportation research record* 1855 (2003) 151–159.
- [79] J. Wang, M. Wu, An overview of research on weigh-in-motion system, in: *Fifth World Congress on Intelligent Control and Automation (IEEE Cat. No. 04EX788)*, volume 6, IEEE, 2004, pp. 5241–5244.
- [80] M. Maguire, C. Roberts-Wollmann, T. Cousins, Live-load testing and long-term monitoring of the varina-enon bridge: Investigating thermal distress, *Journal of Bridge Engineering* 23 (2018) 04018003.
- [81] B. Jacob, V. Feypell-de La Beaumelle, Improving truck safety: Potential of weigh-in-motion technology, *IATSS research* 34 (2010) 9–15.
- [82] N. Zolghadri, M. W. Halling, N. Johnson, P. J. Barr, Field verification of simplified bridge weigh-in-motion techniques, *Journal of Bridge Engineering*, 21 (2016), p. 04016063. doi:[10.1061/\(ASCE\)BE.1943-5592.0000930](https://doi.org/10.1061/(ASCE)BE.1943-5592.0000930).
- [83] P. Burnos, J. Gajda, Thermal property analysis of axle load sensors for weighing vehicles in weigh-in-motion system, *Sensors* 16 (2016) 2143.



- [84] B. Kafle, L. Zhang, P. Mendis, N. Herath, M. Maizuar, C. Duffield, R. G. Thompson, Monitoring the dynamic behavior of the merlynston creek bridge using interferometric radar sensors and finite element modeling, *International journal of applied mechanics*, 9 (2017), p. 1750003. doi:[10.1142/S175882511750003X](https://doi.org/10.1142/S175882511750003X).
- [85] X. Zheng, D.-H. Yang, T.-H. Yi, H.-N. Li, Z.-W. Chen, Bridge influence line identification based on regularized least-squares qr decomposition method, *Journal of Bridge Engineering*, 24 (2019), p. 06019004. doi:[10.1061/\(ASCE\)BE.1943-5592.0001458](https://doi.org/10.1061/(ASCE)BE.1943-5592.0001458).
- [86] Y. Yu, C. Cai, L. Deng, Nothing-on-road bridge weigh-in-motion considering the transverse position of the vehicle, *Structure and Infrastructure Engineering*, 14 (2018), pp. 1108–1122. doi:[10.1080/15732479.2017.1401095](https://doi.org/10.1080/15732479.2017.1401095).
- [87] X. Zheng, D.-H. Yang, T.-H. Yi, H.-N. Li, Bridge influence surface identification method considering the spatial effect of vehicle load, *Structural Control and Health Monitoring*, 28 (2021), Article e2769. . doi:[10.1002/stc.2769](https://doi.org/10.1002/stc.2769).
- [88] C. R. Johnson Jr, W. A. Sethares, A. G. Klein, Software receiver design: build your own digital communication system in five easy steps, Cambridge University Press, 2011, ISBN: 9781139501453. URL: [https://scholar.google.com/scholar?hl=en&as\\_sdt=0%2C47&q=Software+receiver+design%3A+build+your+own+digital+communication&btnG=](https://scholar.google.com/scholar?hl=en&as_sdt=0%2C47&q=Software+receiver+design%3A+build+your+own+digital+communication&btnG=).
- [89] M. D. Fontaine, L. E. Dougald, C. S. Bhamidipati, et al., Evaluation of Truck Lane Restrictions in Virginia: Phase II, Technical Report, Virginia Transportation Research Council, 2009. URL: <https://rosap.ntl.bts.gov/view/dot/38170#tabs-2>.
- [90] R. Berard, A. Bourion, Truck widths and paths, *Transportation research circular*, (1998), pp. 14–1. URL: [https://www.safetylit.org/citations/index.php?fuseaction=citations.viewdetails&citationIds\[\]=citjournalarticle\\_181294\\_19](https://www.safetylit.org/citations/index.php?fuseaction=citations.viewdetails&citationIds[]=citjournalarticle_181294_19).

- [91] R. O. DECISION, Federal highway administration, US Department of Transportation, Washington, DC (2015). URL: [https://scholar.google.com/scholar?hl=en&as\\_sdt=0%2C47&q=Federal+highway+administration+US+Department+of+Transportation&btnG=](https://scholar.google.com/scholar?hl=en&as_sdt=0%2C47&q=Federal+highway+administration+US+Department+of+Transportation&btnG=).
- [92] S. Ham Ph D, S.-H. Chao, K. R. Ryu, Y. C. Yu, D. S. Kumar David, Study on hybrid model combining super learner and physics-based models for shm in bridges using low-cost bwim (2021).
- [93] AS 5100, Bridge design, part 4: Bearings and deck joints, Australian Standard, 2017. URL: [https://infostore.saiglobal.com/preview/825802792907.pdf?sku=99573\\_SAIG\\_AS\\_AS\\_209331](https://infostore.saiglobal.com/preview/825802792907.pdf?sku=99573_SAIG_AS_AS_209331).